UCLA-ENG-7627
MARCH 1976

SEPARATION OF BODY AND SURFACE WAVES IN STRONG GROUND MOTION RECORDS

George Ching-Chi Liang

Principal Investigator: C.M. Duke
A.K. Mal

Prepared for the
National Science Foundation
Under Grant No. GI 44056

School of Engineering and Applied Science
University of California
Los Angeles, California

1.a

50272-101

REPORT DOCUMENTATION PAGE	1. REPORT NO. NSF/RA-761694	2.	3. Recipient's Accession No. PB298975

4. Title and Subtitle
Separation of Body and Surface Waves in Strong Ground Motion Records

5. Report Date
March 1976

6.

7. Author(s)
G.C. Liang, C.M. Duke, A.K. Mal

8. Performing Organization Rept. No.
UCLA-ENG-7627

9. Performing Organization Name and Address
University of California at Los Angeles
School of Engineering and Applied Science
Los Angeles, California 90024

10. Project/Task/Work Unit No.

11. Contract(C) or Grant(G) No.
(C)
(G) GI44056

12. Sponsoring Organization Name and Address
Engineering and Applied Science (EAS)
National Science Foundation
1800 G Street, N.W.
Washington, D.C. 20550

13. Type of Report & Period Covered

14.

15. Supplementary Notes

16. Abstract (Limit: 200 words)

A method to separate body and surface waves in strong motion accelerograms is devised based on a linear system model. Described is the development and application of the model, and subsequent changes in design. The mathematics of linear system analysis, source functions, directionality and travel path effects, and local site properties are included. Mainshock records from the 1971 San Fernando Earthquake are used to test the method. The existence of large unrealistic peaks in the separated body and surface wave spectra indicating false data led to the introduction of various methods to eliminate these peaks from the spectrum. Several of these methods, described here, prove to be effective in different ways. The corrected body and surface wave spectra show expected characteristics. It is suggested that further development in the system model is needed to improve the surface wave transfer functions.

17. Document Analysis a. Descriptors

Earthquakes
Seismic waves
Soil dynamics
Waveforms
Shock spectra
Surface wave tests
Computer programs
Mathematical models

b. Identifiers/Open-Ended Terms

Body waves
San Fernando Earthquake 1971

c. COSATI Field/Group

18. Availability Statement	19. Security Class (This Report)	21. No. of Pages
NTIS		168
	20. Security Class (This Page)	22. Price A08-A01

(See ANSI-Z39.18) See Instructions on Reverse

OPTIONAL FORM 272 (4-77)
(Formerly NTIS-35)
Department of Commerce

CAPITAL SYSTEMS GROUP, INC
5410 EXECUTIVE BOULEVARD
SUITE 250
ROCKVILLE, MARYLAND 20852

ABSTRACT

A linear system model which accounts for the behavior of both body and surface waves has been recently developed. A method to separate body and surface waves in strong motion accelerograms was devised based on this model. Preliminary development of the surface wave transfer functions was undertaken so that the method of wave separation could be tested using this new system model. Mainshock records from the 1971 San Fernando earthquake were used to test the method.

A problem with spurious peaks was encountered in the calculation. Tests showed that these large unrealistic peaks were indeed false information. Their existence in the separated body and surface wave spectra had made the spectra useless. Various methods were introduced to eliminate these large peaks from the spectrum. These methods all proved to be effective, in different ways. The corrected body and surface wave spectra showed the expected characteristics.

Only preliminary studies were done in this thesis. Further development on the system model is needed. In particular, the surface wave transfer functions should be improved. Methods should be developed to evaluate the accuracy of the separated body and surface wave spectra.

Preceding page blank

TABLE OF CONTENTS

		Page
CHAPTER 1	INTRODUCTION	1
1.1	Previous Work	1
1.2	Mathematics of the Linear System Analysis	2
1.3	A Complete System Model for Earthquakes	7
1.4	A Simplified Body Wave Model	8
1.5	A Simplified Body and Surface Wave Model	10
1.6	Source Functions	10
1.7	Directionality Effect	14
1.8	The Effects of the Travel Path	17
1.9	Local Site Properties	19
CHAPTER 2	SEPARATION OF BODY AND SURFACE WAVES	23
2.1	Methods to Separate Wave Contents in an Accelerogram	23
2.2	Separation Using Linear System Analysis	29
CHAPTER 3	APPLICATION OF LINEAR SYSTEM MODEL	34
3.1	The System Functions	36
3.2	The Problem in Computing Separated Waves	44
CHAPTER 4	A DEMONSTRATION OF THE CAUSE OF THE SPURIOUS PEAKS PROBLEM	60
4.1	Preparation of Test Data	61
4.2	Testing the Separation Equations	63
4.3	Parametric Studies	67

Preceding page blank

Page

CHAPTER 5 COMPUTATIONAL PROCEDURE..... 90

5.1 Method A: A Rough Treatment..... 90

5.2 Method B: Smoothing..... 91

5.3 Method C: Interpolation..... 100

5.4 Method D: Multiple-Station Procedure..... 107

5.5 Discussion..... 113

CHAPTER 6 CONCLUSION..... 114

BIBLIOGRAPHY..... 117

APPENDIX A..... 122

APPENDIX B..... 128

LIST OF FIGURES

		Page
1.1	Convolution.....	5
1.2a	Cascade Filtering in Time Domain.....	6
1.2b	Cascade Filtering in Frequency Domain....	6
1.3	A Complete Linear System.....	9
1.4	Simplified Body Wave Model.....	11
1.5	Simplified Body and Surface Wave Model...	12
1.6	Shear Wave Radiation Pattern Due to A Double Couple Point Source.....	15
1.7a	Coordinate System for A Fault Motion in the ξ_1 Direction and 1-2 Plane.....	16
1.7b	Rotated Coordinate System for Describing Radiation Pattern on the Ground Surface..	16
1.8	Properties of The Transfer Functions W_b and W_s.....	20
2.1	Comparison between Typical Far Field Records for their Contrast in Distinguishability of Various Wave Contents.....	24
2.2	Identification of Body and Surface Waves from Strong Motion Records at Various Distances.....	26
2.3	Linear System with Two Stations.....	31
3.1	Stations used in the Analyses.....	35
3.2	Double Couple Source Model for the San Fernando Mainshock.....	37
3.3	Radiation Patterns for the San Fernando Mainshock for a Double Couple Point Source.....	38
3.4a	Typical Body Wave Path Transfer Function.	39
3.4b	Typical Surface Wave Path Transfer Function.....	39

		Page
3.5	Site Amplification Spectra For Vertically Traveling S-Waves.....	41
3.6	Travel Paths used to Calculate the Differences in Arrival Times.....	43
3.7	Separation of Body and Surface Waves, Orion and CPE Pair.....	47
3.8	Separation of Body and Surface Waves Orion and Ventura Pair.....	53
3.9	Effect of Large Peaks in the Fourier Spectrum of the Inverse Transformed Time History.....	59
4.1	One Layer Site Amplification Model.....	64
4.2	The Ground Motion and Its Exact Surface and Body Wave Contents.....	65
4.3	The Denominator and The Resulting Surface and Body Waves with The Epicentral Distance of Station #2 Increased by 2 Units.....	70
4.4	The Denominator and The Resulting Surface and Body Waves with The Epicentral Distance of Station #2 Decreased by 2 Units.....	72
4.5	The Denominator and The Resulting Surface and Body Waves with The Arrival Time Differences for Both Types of Waves Increased by 0.001 Unit.....	74
4.6	The Denominator and The Resulting Surface and Body Waves with The Arrival Time Differences for Both Types of Waves Increased by 0.01 Unit.....	76
4.7	The Denominator and The Resulting Surface and Body Waves with The Arrival Time Differences for Both Types of Waves Increased by 0.1 Unit.....	78

Page

4.8 Artificial Source Functions Used for the Third Study..... 80

4.9 Parametric Studies with Source Function E_1..... 81

4.10 Parametric Studies with Source Function E_2..... 84

4.11 Parametric Studies with Source Function E_3..... 87

5.1 Surface Waves at Orion, Orion and Ventura Pair, Using Method of Smoothing..... 92

5.2 Body Waves at Orion, Orion and Ventura Pair, Using Method of Smoothing..... 94

5.3 Surface Waves at Ventura, Orion and Ventura Pair, Using Method of Smoothing.. 96

5.4 Body Waves at Ventura, Orion and Ventura Pair, Using Method of Smoothing..... 98

5.5 Interpolation Procedure..... 102

5.6 Surface Wave Spectrum at Orion after Interpolation, Orion and Ventura Pair.... 103

5.7 Body Wave Spectrum at Orion after Interpolation, Orion and Ventura Pair.... 104

5.8 Surface Wave Spectrum at Ventura after Interpolation, Orion and Ventura Pair.... 105

5.9 Body Wave Spectrum at Ventura after Interpolation, Orion and Ventura Pair.... 106

5.10 The Denominators are used as Weighting Factors for Multiple-Station Procedure... 109

5.11 The Two Independently Calculated Spectra for Surface Wave at Orion and The Combined Spectrum..... 110

Page

5.12 The Two Independently Calculated Spectra for Body Wave at Orion and The Combined Spectra..... 111

5.13 Inverse Transform of the Combined Spectra of Surface Wave and Body Wave Components at Orion..... 112

LIST OF TABLES

Page

4.1 Values of the Parameters Used in Designing W_b and W_s 62

5.1 Frequency Ranges For Which the Amplitudes were Interpolated 101

CHAPTER 1

INTRODUCTION

1.1 PREVIOUS WORK

In order to provide reliable design earthquake procedures, various properties of the earthquake mechanism must be understood. The behaviors of the earthquake source, the travel path and the local site conditions are all important factors in the prediction of earthquake motions.

A complete system model was first proposed by Kanai (1957) in his work on the prediction of ground motions. This model incorporated all the properties of an earthquake from the source to the site. Since then, many researches have been carried out based on this concept. References of the various early researches on this subject can be found in the works of Lastrico (1970), and Johnsen (1972). At the UCLA Earthquake Laboratory, a linear system model has been developed based on the same concept. This model describes the body wave behaviors from source to site (Lastrico 1970). Numerous applications of this model were made using data from the 1971 San Fernando earthquake. These researches included the works done by Johnsen (1972), Engman (1973), and Duke and Hradilek (1973). However, this model was found inadequate in some of the research. In particular,

the work done by Duke and Hradilek (1973) pointed out that this model lacked the necessary surface wave characteristics.

A new model has since been developed (Duke and Mal 1975), in which the behaviours of both body and surface waves are taken into account. Reconciliation of the new model with strong motion data requires the separation of body and surface wave motions in ground motion records. In this thesis, a method for the separation of body and surface waves in accelerograms is tested against measurements for the first time. This study will serve the dual purpose of testing the new system model and of examining the feasibility of separating body and surface wave components in strong motion accelerograms. Detailed discussions of the theory of linear systems and the concept of the models of system components are presented in the following sections. The subsequent chapters apply a method of separation of body and surface waves using the new system model.

1.2 MATHEMATICS OF THE LINEAR SYSTEM ANALYSIS

According to the definition given by Bendat and Piersol (1971), a linear system is a system which has constant parameters between two clearly defined points of input and output. These parameters must be invariant with respect to time. They must be additive such that

the output of a sum of inputs is equal to the sum of the outputs produced by each input individually. They must also be homogeneous such that constants remain as constants in the system.

Two of the most frequently encountered operations in the linear system theory are convolution and Fourier transform. Convolution is used to determine the output of a system due to some specified input. The equation is given as follows,

$$y(t)=\int_{-\infty}^{+\infty} h(\tau)x(t-\tau)d\tau \qquad \text{(Eq. 1.1)}$$

where

$x(t)$ = the input,

$h(t)$ = the impulse response of the system,

$y(t)$ = the output.

Fourier transformation is used to examine the frequency content of a time dependent function. The transform pair are

$$F(\omega)=\int_{-\infty}^{+\infty} f(t)e^{-i\omega t}dt$$

$$f(t)= \frac{1}{2\pi}\int_{-\infty}^{+\infty} F(\omega)e^{+i\omega t}d \qquad \text{(Eq. 1.2)}$$

where

$F(\omega)$ is the complex Fourier spectrum,

$f(t)$ is the real time history.

Although convolution is the basic tool used in linear system analysis, the integration shown in Eq. 1.1 is computationally costly and thus avoided where feasible. Instead, a simpler method for solving it is used. This method takes the Fourier transform on both sides of Eq. 1.1, thus replacing the convolution operation in the time domain with a multiplication operation in the frequency domain. Eq. 1.1 then becomes

$$Y(\omega)=H(\omega)X(\omega) \qquad \text{(Eq. 1.3)}$$

where

$X(\omega)$ is the input spectrum,

$Y(\omega)$ is the output spectrum,

$H(\omega)$ is the transfer function (or the filter*) of the system.

For a large cascade system, see Fig. 1.2, it is then possible to arrange various properties of the system as the product of a chain of transfer functions. the response can then be calculated in the following manner,

$$Y(\omega)=X(\omega)H_1(\omega)H_2(\omega).....H_n(\omega) \qquad \text{(Eq. 1.4)}$$

This approach not only avoids the tedious integrations

---

*In the theory of system analysis, "transfer function" and "filter" are synonymous.

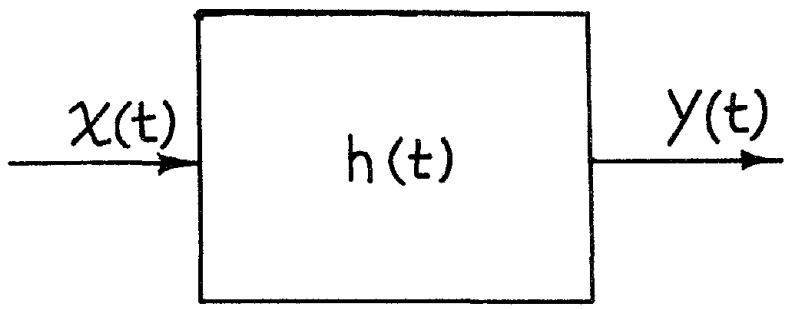

Fig. 1.1 Convolution

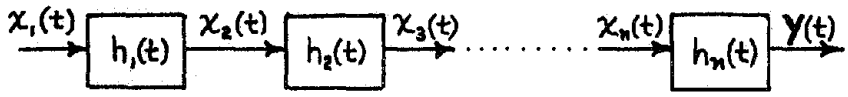

$$y(t)=\int_{-\infty}^{+\infty}\left[\int_{-\infty}^{+\infty}\left[\cdots\cdots\left[\int_{-\infty}^{+\infty}x_1(\tau_1)\,h_1(t-\tau_1)\,d\tau_1\right]\cdots\cdots\right]h_{n-1}(t-\tau_{n-1})\,d\tau_{n-1}\right]h_n(t-\tau_n)\,d\tau_n$$

Fig. 1.2a Cascade Filtering in Time Domain

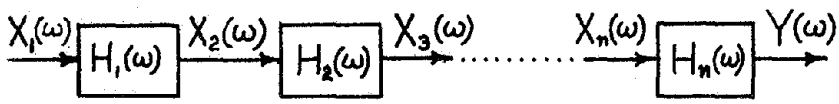

$$Y(\omega) = X_1(\omega)\,H_1(\omega)\,H_2(\omega)\cdots\cdots H_{n-1}(\omega)\,H_n(\omega)$$

Fig. 1.2b Cascade Filtering in Frequency Domain

which the convolutions require in the time domain, it also establishes the foundation for developing the linear system analysis used in this thesis.

1.3 A COMPLETE SYSTEM MODEL FOR EARTHQUAKES

The cascade filtering system can be used to model earthquake effects. Two independent linear equations can be written as shown below to describe the process of surface and body wave propagation (Båth 1974).

$$G_b(\omega,r)=S(\omega)C_b(\omega)R_b(\theta,\phi,r)M(\omega,r)W_b(\omega)X_b(\omega)I(\omega)$$
$$G_s(\omega,r)=S(\omega)C_s(\omega)R_s(\theta,\phi,r)W_s(\omega)X_s(\omega)I(\omega) \qquad \text{(Eq. 1.5)}$$

where

$G_b(\omega,r)$, $G_s(\omega,r)$ are the body and surface wave portions of the ground motion, respectively,

$S(\omega)$ describes the motion of the fault slippage,

$C_b(\omega)$ describes the processes near the source for waves propagating away from the source to the basement complex,

$C_s(\omega)$ describes the processes near the source for waves propagating from the source up to the surface.

$R_b(\theta,\phi,r)$, $R_s(\theta,\phi,r)$ are the directionality effects, or otherwise hnown as the radiation pattern.

$M(\omega,r)$ describes the effects of mantle on the waves propagating in the basement complex above it.

$W_b(\omega)$, $W_s(\omega)$ describe the attenuations and geometrical spreadings along the travel paths.

$X_b(\omega)$, $X_s(\omega)$ describe the amplifications of waves due to the local site properties.

$I(\omega)$ is the correction factor for the errors in the instrumental response.

1.4 A SIMPLIFIED MODEL USING BODY WAVES ONLY

For the analysis of strong ground motions due to a local shallow* earthquake, a simplified model has been adopted in the literature (Lastrico 1070, Johnsen 1972, Engman 1973). This model ignores surface waves and and assumes that all the energy is carried by the body waves. Eq. 1.5 is then reduced to a single equation

$$G(\omega)=E(\omega)W(\omega)X(\omega) \qquad \text{(Eq. 1.6)}$$

where

$E(\omega)$ is a lumped source function which includes both the body and the surface wave parts of $S(\omega)$, $C(\omega)$, $R(\theta,\phi,r)$.

---

*The depth of the earthquake source is considered shallow if it is relatively close to the surface compared to the depth to the mantle.

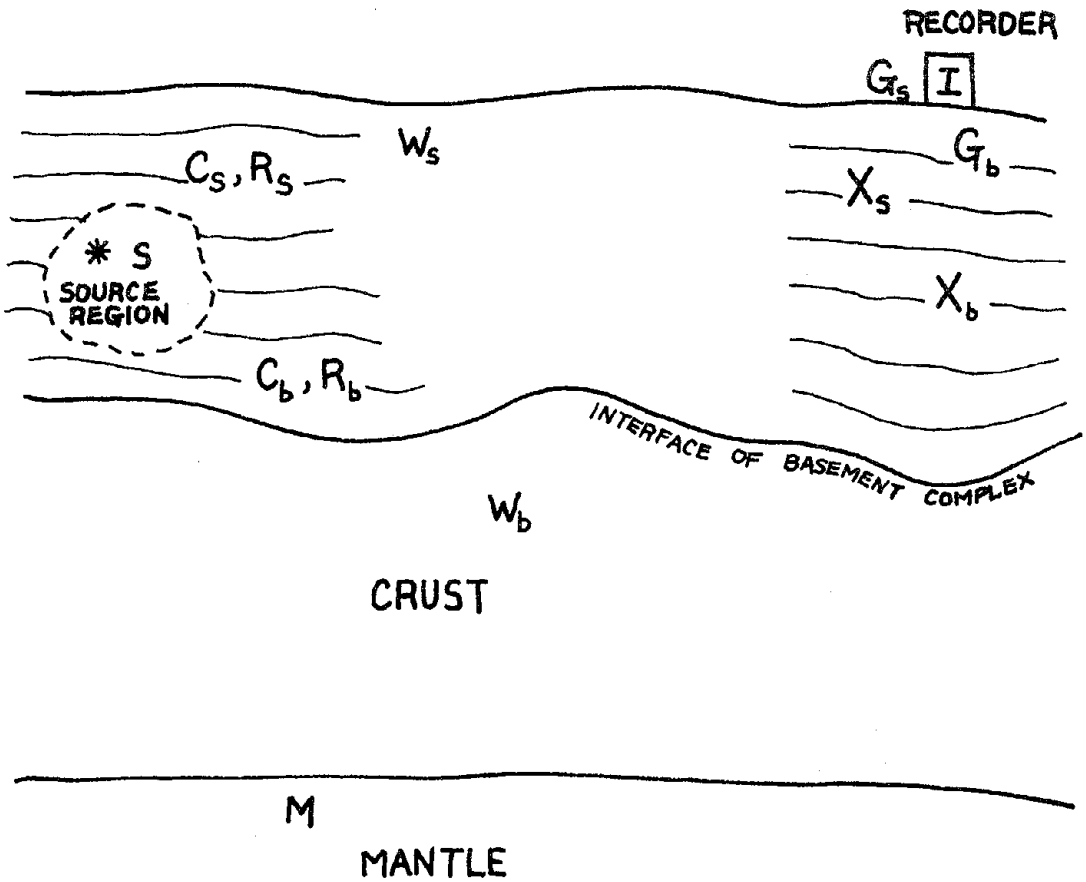

Fig. 1.3 A Complete Linear System

$W(\omega)$ is the lumped transfer function for the transmission path.

$X(\omega)$ is the lumped transfer function for the local site amplification.

However, this model was found to be inadequate for obtaining satisfactory results in analyses (Duke and Hradilek 1973).

1.5 A SIMPLIFIED BODY AND SURFACE WAVE MODEL

A better model is therefore proposed in an effort to improve the results of various analyses. This model considers body and surface waves to be equally important. The following two independent linear equations are considered simultaneously:

$$G_s(\omega)=E_s(\omega)R_s(\theta,\phi,r)W_s(\omega)X_s(\omega)$$
$$G_b(\omega)=E_b(\omega)R_b(\theta,\phi,r)W_b(\omega)X_b(\omega) \qquad \text{(Eq. 1.7)}$$

where $E_s(\omega)$ and $E_b(\omega)$ are the lumped source functions with $R_s(\theta,\phi,r)$ and $R_b(\theta,\phi,r)$ separated from them.

The subsequent sections of this Chapter describe Eq. 1.7 for the purpose of this thesis.

1.6 SOURCE FUNCTIONS

The source functions, E_b and E_s, are really the products of various properties and effects of the source mechanism. Approximate representations used for the linear system analysis allow E_b and E_s to be written as

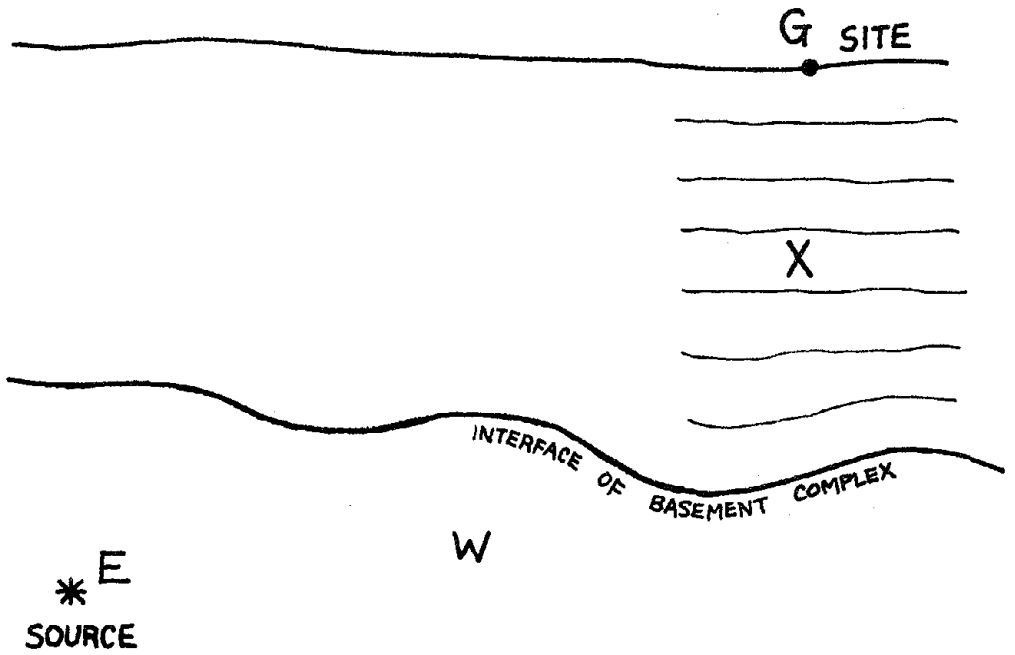

Fig. 1.4 Simplified Body Wave Model

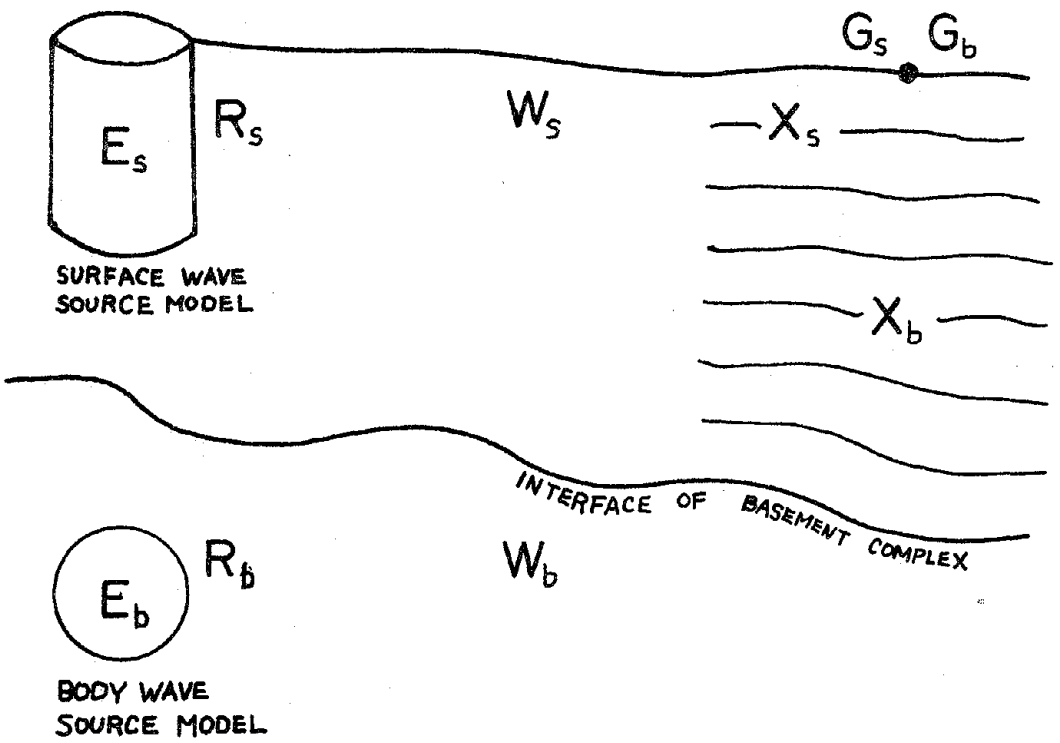

Fig. 1.5 Simplified Body and Surface Wave Model

the product of two different source properties as shown below.

$$E_s(\omega)=S(\omega)C_s(\omega)$$
$$E_b(\omega)=S(\omega)C_b(\omega) \qquad \text{(Eq. 1.8)}$$

$S(\omega)$ is the Fourier transform of the time dependent equivalent double couples due to the propagation of rupture along the fault surface. It depents on the fault parameters, such as rupture speed, fault geometry, effective stress release, and seismic moment. $C_b(\omega)$ and $C_s(\omega)$ are crustal effects near the source. They can be estimated using the Haskell-Thomson model (Thomson 1950, Haskell 1953, 1960, 1962, Matthiesen 1964, Carriveau 1970). $C_b(\omega)$ can be modeled as P and S waves propagating away from the source to the basement complex, and $C_s(\omega)$ can be modeled as the free vibration of the layers in the near field.

This thesis will not contain any detailed analysis on the modeling of the source functions. One reason is the lack of sufficient research at the present time for constructing such models. Also, for the method used in the present analysis, most elements of the source functions cancel out in the equations.

1.7 DIRECTIONALITY EFFECT

The directionality effect is also known as the radiation pattern of the source. The amount of source energy received is different for any two stations at equal distances but at different azimuthal directions from the source. Fig. 1.6 shows a typical example of the radiation pattern. The lobes represent the relative size of amplitudes in various directions. Note that for this example, the amplitudes are zero at 45°, 135°, 225°, and 315°; and the maxima are at 0°, 90°, 180°, and 270°.

For simplicity, the radiation pattern due to a double couple point source is modeled for the present study. The derivations are presented in Appendix A. The resulting transfer functions $R_s(\omega,r)$ and $R_b(\omega,r)$ are the sums of the vector components given in Eq. A.7, which is reproduced below.

$$R_{si}(\theta,\phi,r)=A(\delta_{i1}\gamma_3+\delta_{i3}\gamma_1-2\gamma_i\gamma_1\gamma_3)$$
$$R_{bi}(\theta,\phi,r)=B(\delta_{i1}\gamma_3+\delta_{i3}\gamma_1-2\gamma_i\gamma_1\gamma_3) \qquad \text{(Eq. 1.9)}$$

where

R_{si}, R_{bi} denote the ith components of the displacement vector.

1, 2, 3 are the coordinates as shown in Fig. 1.7a.

γ_1, γ_2, γ_3 are the directional cosines of the station in the above coordinate system.

δ_{ij} is the Kronecker delta.

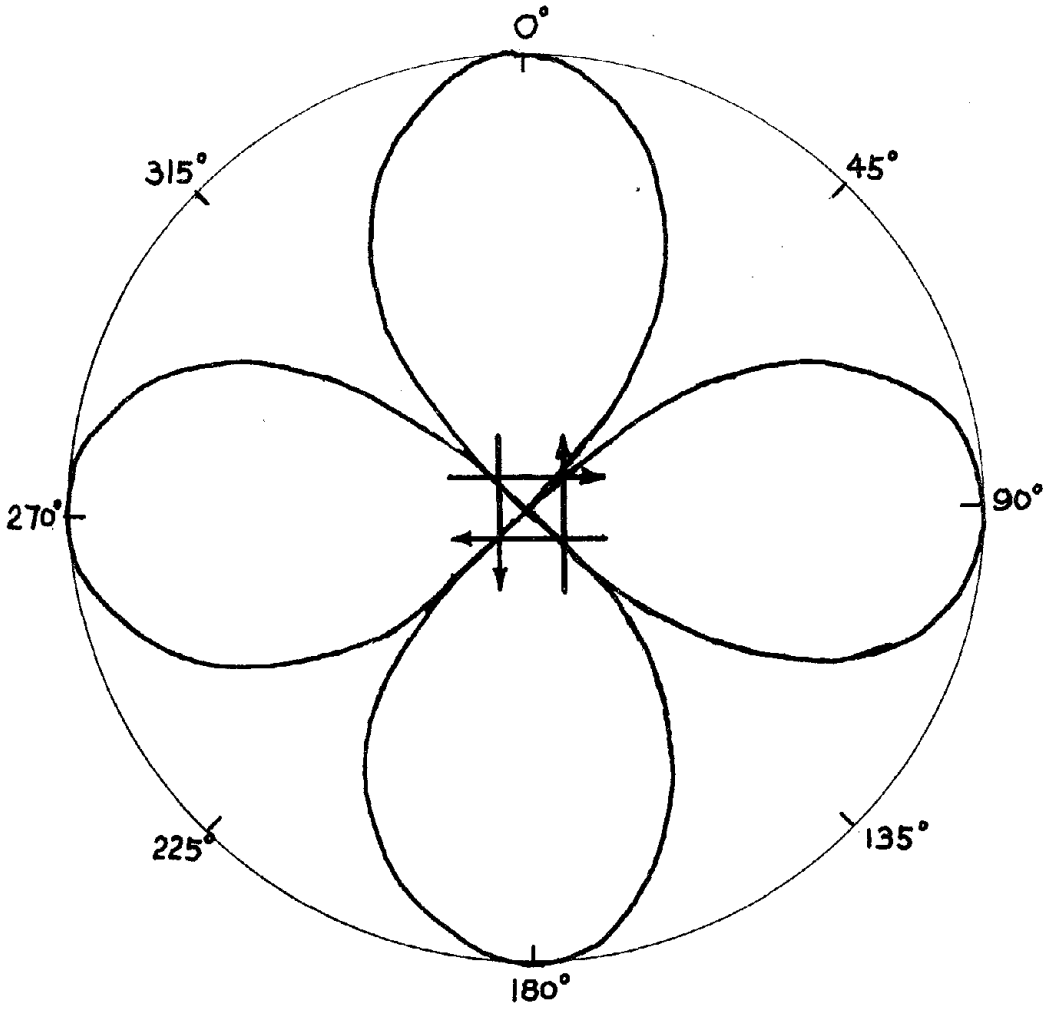

Fig. 1.6 Shear Wave Radiation Pattern Due to A Double Couple Point Source

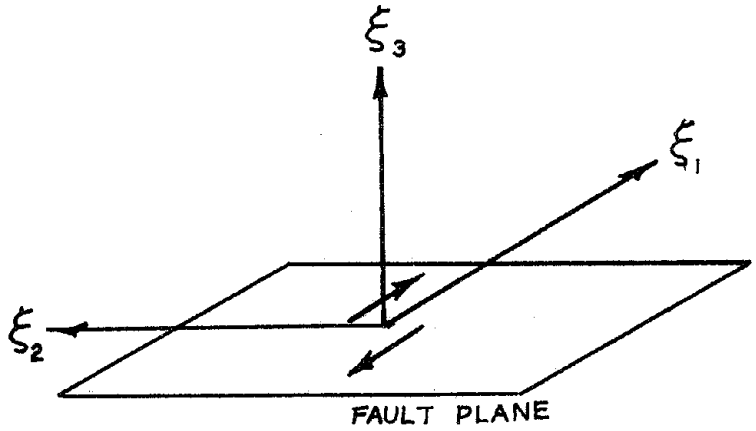

Fig. 1.7a Coordinate System for A Fault Motion in the ξ_1 Direction and 1-2 Plane

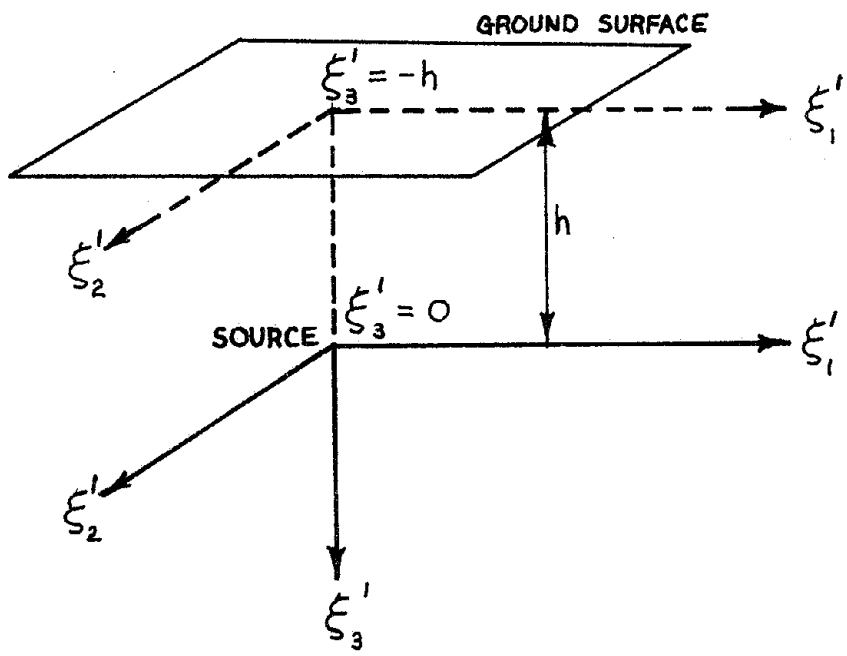

Fig. 1.7b Rotated Coordinate System for Describing Radiation Pattern on the Ground Surface

A and B are the amplitude normalization factors.

The above equations give radiation patterns on the coordinate system based on the orientation of the fault plane, which is illustrated in Fig. 1.7a. However in order to establish radiation patterns in the plane parallel to the ground surface, this coordinate system should be rotated to the orientation shown in Fig. 1.7b using the usual equations for coordinate transformation shown below.

$$\begin{aligned} x' &= a_{x'x}x + a_{x'y}y + a_{x'z}z \\ y' &= a_{y'x}x + a_{y'y}y + a_{y'z}z \\ z' &= a_{z'x}x + a_{z'y}y + a_{z'z}z \end{aligned} \qquad \text{(Eq. 1.10)}$$

where $a_{i'j}$ are the directional cosines, and x, y, z, and x', y', z' are two sets of coordinate systems.

1.8 THE EFFECTS OF THE TRAVEL PATH

It is a very difficult task to describe the earthquake waves along their path from source to site. The complex and irregular configuration of the earth's crustal structure hampers the feasibility of such a rigorous analysis. As an alternative, estimations based on simple analyses coupled with information from experimental data is used to estimate this effect.

From these studies, it was found that a wave propagating in a homogeneous medium can be described in the form $R^{-n}e^{-\alpha R}$, where R^{-n} is the geometrical spreading factor and $e^{-\alpha R}$ is the attenuation factor. Ewing and others (1957) have shown that the geometrical spreading factor for Love and Rayleigh waves should be $1/\sqrt{R}$; and for compressional and shear waves, it should be $1/R$. For the attenuation, Båth (1974), White (1965), and Lastrico (1970) have all indicated that α should take the form of $\omega/(2QV)$ where ω is the angular frequency, Q is the factor for damping (Båth 1974), which measures the rate of attenuation in the medium, and V is the propagation velocity of the waves.

To implement the above into the path dependent transfer functions, $W_b(\omega)$, $W_s(\omega)$, the appropriate equations, in their simplest forms, are

$$W_b(\omega) = \frac{1}{r_b} e^{-\frac{|\omega| r_b}{2Q_b V_b}}$$

$$W_s(\omega) = \frac{1}{\sqrt{r_s}} e^{-\frac{|\omega| r_s}{2Q_s V_s}} \qquad \text{(Eq. 1.11)}$$

The subscripts, b and s, denote the body wave and the surface wave properties of the particular arguments, respectively. V_b is the average propagation velocity of the shear waves in the bedrock. V_s is the average propagation velocity of either Love waves or Rayleigh waves, depending on whether the vibrational direction of interest is tangential motion or radial and vertical motion, respectively. Fig. 1.8 describes the various properties pictorially. The absolute values of ω's are taken in Eq. 1.13 in order to insure that the inverse transforms of W_b and W_s are real functions of time*.

1.9 LOCAL SITE PROPERTIES

In the study of strong earthquakes, it is believed by many researchers that the local geological structure has important effects on ground motions. Various types of studies on actual earthquake records have supported this statement. A study by Seed (1970) indicated that the matching of natural frequencies of the building and the local soil correlates strongly with the building damages in the Caracas Earthquake of July 29, 1967. Using spectral analysis technique,

---

*The inverse Fourier transform of an even function is real, and of an odd function is imaginary (Brigham 1974, McGillem 1974)

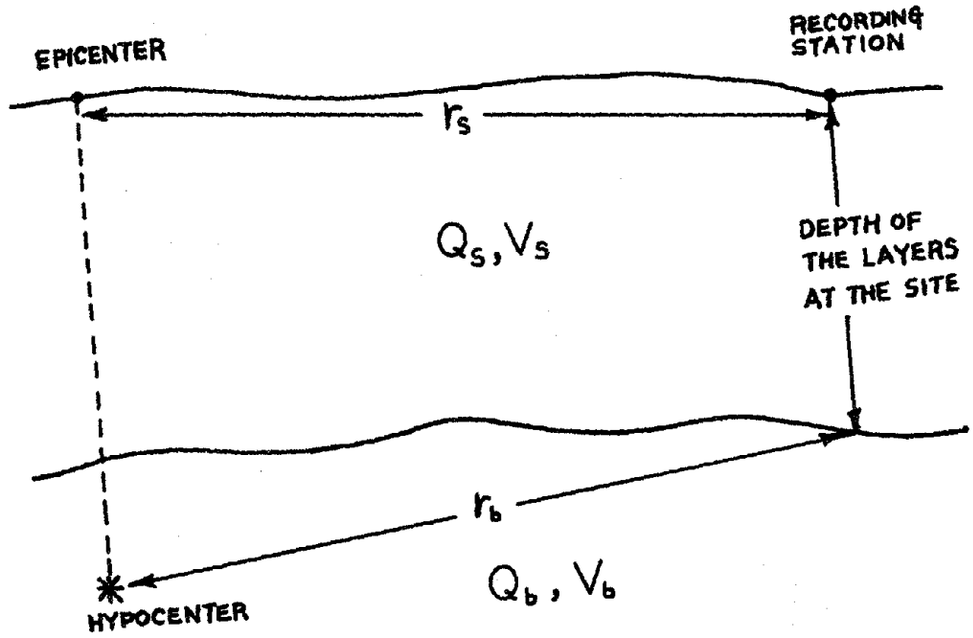

Fig. 1.8 Properties of The Transfer Functions W_b and W_s

Schnabel and others (1971) were able to match the recorded spectra with predicted spectra at the various test sites in their study by considering the effect of site conditions only. In the study by Whitman and others on the damage of the TOFAS factory in Turkey (1974), it was found that the local soil amplification was the main cause of the collapse of the buildings.

For the body wave part of the analysis pursued here, a model for the local site amplification effect, X_b, is available and has been used in the UCLA Earthquake Laboratory (Matthiesen, et. al. 1964, Lastrico 1970, Johnsen 1972, Engman 1973). Based on the Haskell-Thomson procedure (Thomson 1950, Haskell 1960, 1962), this model was developed to calculate the amplification of damped vertical shear waves traveling through uniform horizontal layers. Detailed derivation of this model can be found in the work by Lastrico (1970) and Carriveau (1970). Typical illustrations of the amplification spectra calculated from this model can be found in Chapter 3 and in the works by Johnsen (1972) and Engman (1973).

The development of a local site amplification model for surface waves is still under research. Since local surface waves are assumed to travel horizontally, instead of vertically like the local shear waves, there are difficulties in defining the boundary at

which the "local" surface wave effects begin to take place. In work done by Murphy and others (1970), the site related amplification of surface waves was shown to take place over a horizontal distance of several kilometers. This seems to contradict the concept of "local" site effects due to surface waves. For this reason, the transfer function X_s will be temporarily assumed unity for the work in this thesis.

It should be mentioned that although the site effects are generally believed to be important by many researchers, there are some who think otherwise. Hudson (1974) compared the ground motion spectra from the San Fernando Earthquake at several pairs of sites and found no direct indication of significance of the local site effects. The statistical studies done by Trifunac (1975) have also showed no significant differences in the compared indices among the 3 types of soil conditions considered.

CHAPTER 2

SEPARATION OF BODY AND SURFACE WAVES

2.1 METHODS TO SEPARATE WAVE CONTENTS IN AN ACCELEROGRAM

The separation of body and surface waves in a near field strong motion accelerogram is not an easy task. Due to the closeness of the recording stations to the epicenter, the deviations among arrival times for the various types of seismic waves are very small. Therefore, unlike far field seismograms, the various types of waves can not easily be distinguished in an accelerogram. Fig. 2.1 presents an illustration of this.

In order to use the body and surface wave contents of the accelerograms in analyses, a scheme to separate the wave contents must be devised. In the following paragraphs, two crude methods and two analytical methods are introduced. Of the two crude methods, one simply cuts the accelerograms into two parts, and the other cuts the frequency spectrum, so these can only give very rough approximations of the body and surface wave contents, and their usages are quite limited. Of the two analytical methods, one incorporates the theory of wave mechanics and the other makes use of the linear system theory. These are more reliable in obtaining separated body and surface waves.

CUTTING ACCELEROGRAMS As illustrated in Fig. 2.1, for

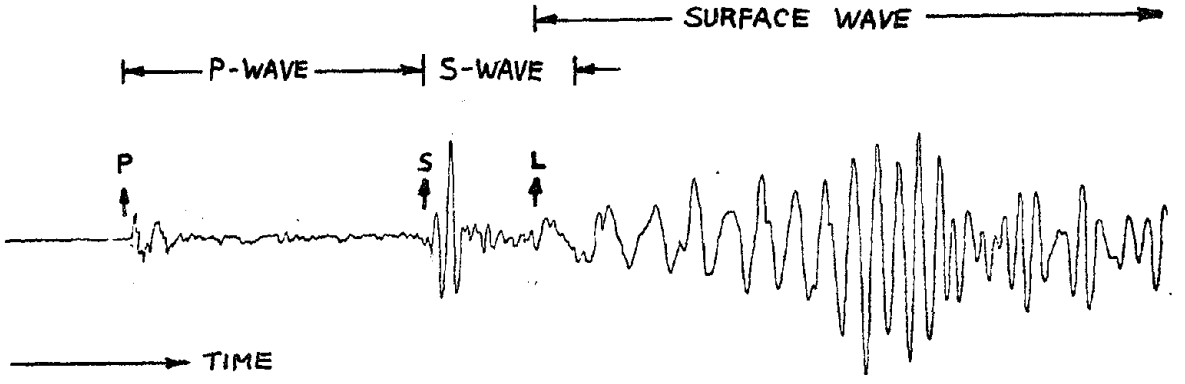

FAR FIELD SEISMOGRAM

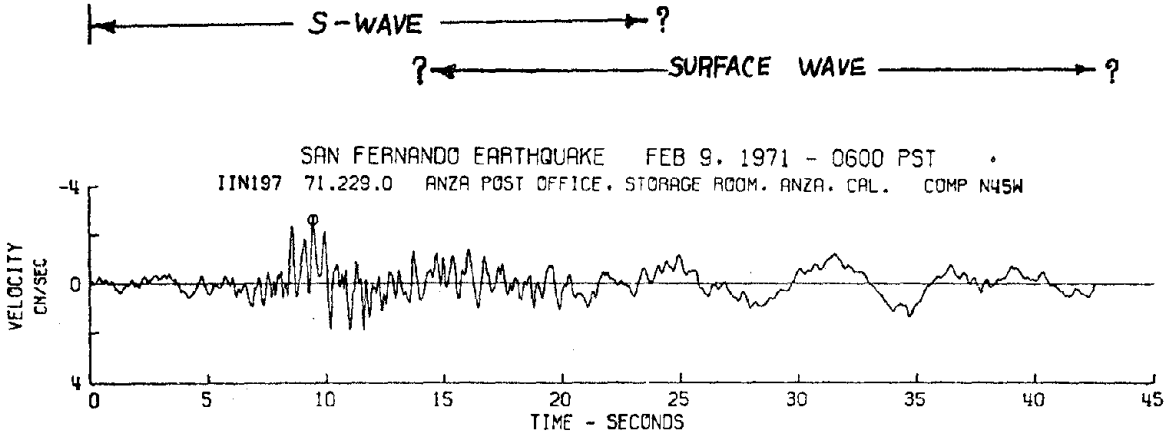

STRONG MOTION VELOCITY RECORD

Fig. 2.1 Comparison between Typical Far Field Records for their Contrast in Distinguishability of Various Wave Contents

most seismograms the various wave contents can be separated out and analyzed individually. This approach used on an accelerogram can only give crude approximations to the body and surface wave contents in the seismogram. A few velocity time histories* from the 1971 San Fernando earthquake are presented in Fig. 2.2 for illustration.

The identification of the two types of waves can be approached in the following manner. From the concept of surface wave dispersion (Båth 1974), the first long wave appearing in the velocity time history is identified as the first arrival of surface waves. The end of the body waves is identified by locating the point where the high frequency content becomes negligible in the record. This corresponds to the fact that the nondispersive body waves have more high frequency contents than do the dispersive surface waves. From this method, the approximate regions where the two types of wave exist simultaneously are identified in Fig. 2.2. If an arbitrary point can be selected in the range of the overlaps to separate each of these time histories, a set of estimated body and surface wave contents can be obtained. However, because of the apparent large overlaps between the waves, this method of wave separation can only give crude approximations.

---

*The velocity time histories are obtained by integration of the accelerograms. It is easier to distinguish between the various wave types in the velocity records than in the accelerations.

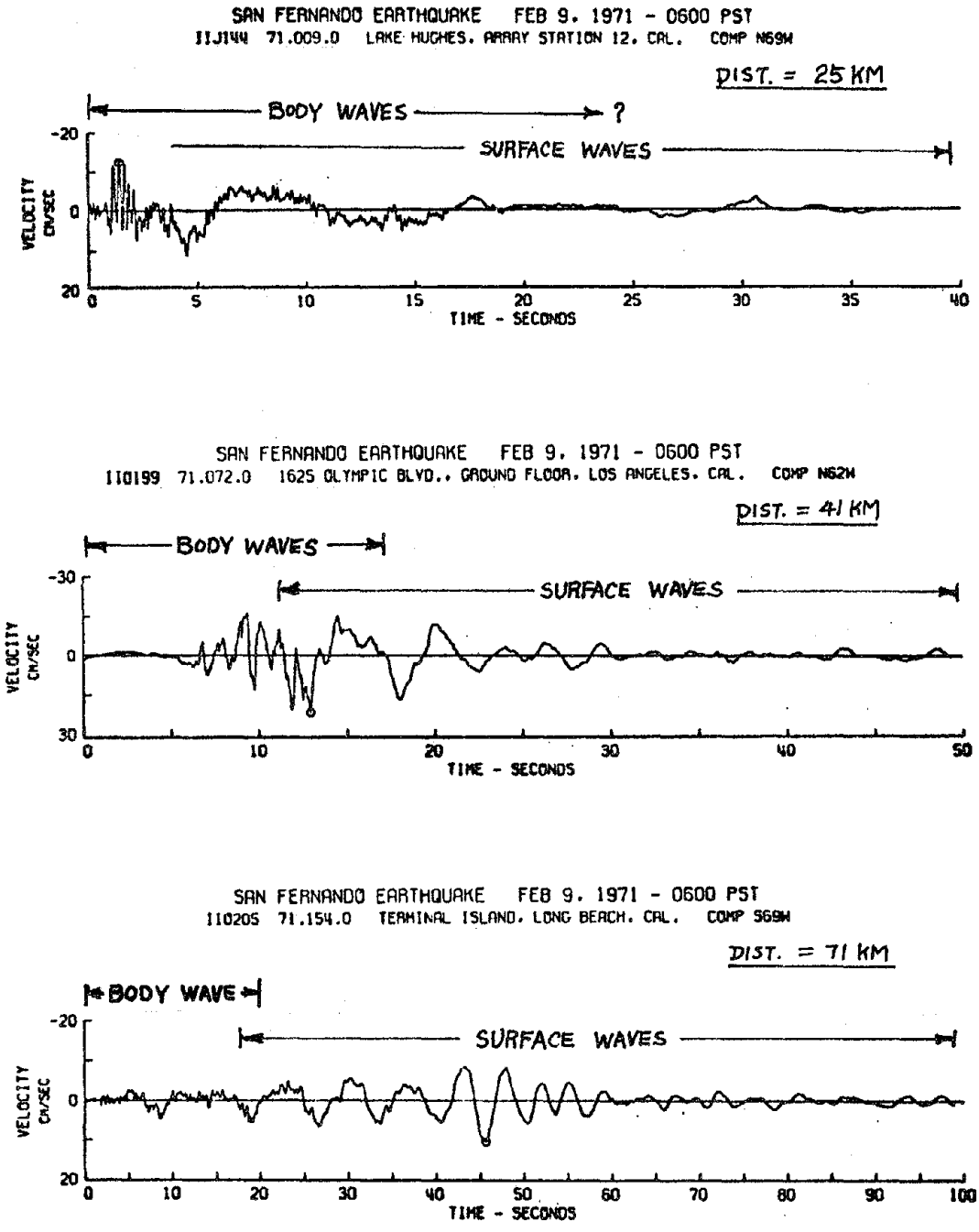

Fig. 2.2 Identification of Body and Surface Waves from Strong Motion Records at Various Distances

CUTTING SPECTRA An alternative crude approach on the cutting scheme is to break the frequency spectrum into two parts. It is generally understood that surface waves have less high frequency contents than body waves (see Fig. 2.1). Therefore, it is possible to separate the spectrum into two parts, with the higher frequency parts taken to represent body wave contents, and with the lower frequency parts taken to represent surface wave contents. The only question that needs to be answered is where should one cut the spectrum.

In an applications of this method by Murphy and others (1964), their response spectra were arbitrarily cut at 1 Hz. The portion below this value was assumed as the surface wave spectrum, and the portion above was assumed as the body wave spectrum.

APPLICATION OF ENGINEERING SEISMOLOGY One of the analytical methods for obtaining separated body and surface waves is to use the theory of wave mechanics. Rigorous mathematical model for the earth can be constructed for the analysis. From the model, the separated body waves

and surface waves can then be obtained with an accuracy as good as the model itself. In principle, the exact result can be obtained from this theory provided that the earth can be modeled in an exact way. However, in order for the computation to be simple and economical, simplifications on the model of the earth and the source mechanism are necessary. Assumptions of linearity and homogeneity of the layered earth are also needed in order to simplify the application of the theory. The ability to obtain accurate results becomes limited by the tediousness of the computation. Illustrations of the application of this theory can be found in the works of Carraveau (1973), Mal (1972) and Drake (1972).

APPLICATION OF LINEAR SYSTEM THEORY Another analytical method is to use the linear system theory, where Fourier transforms are incorporated in the analysis. Like the theory of wave mechanics, simplified model is also desirable for this analysis. However, since the transfer functions are "black boxed" mathematical models, the computation is not as tedious. For this reason, the linear system theory has been selected for the analyses on wave separations in this thesis.

2.2 SEPARATION USING LINEAR SYSTEM ANALYSIS

A linear system model suitable for the application to the separation problem was presented in Sec. 1.4. Using this model, one can separate the body and surface wave contents in the ground motion records in two ways.

The first approach involves one earthquake event and one recording station. Using the equations below

$$
\begin{aligned}
G_b(\omega) &= E_b(\omega)R_b(\theta, r_b)W_b(\omega)X_b(\omega) \\
G_s(\omega) &= E_s(\omega)R_s(\theta, r_s)W_s(\omega)X_s(\omega) \qquad \text{(Eq. 2.1)} \\
G(\omega) &= G_b(\omega) + G_s(\omega)
\end{aligned}
$$

a theoretical Fourier spectrum of the ground motion, G, can be synthesized from the predicted ground motion spectra for body and surface waves, G_b and G_s, by establishing appropriate models for E_b, E_s, R_b, R_s, W_b, W_s, X_b, and X_s. By adjusting the parameters in the model of the transfer functions using successive iteration, the contents of body and surface waves can be obtained by trying to match the predicted G with the actual recorded ground spectrum. A simpler version of the method which involved only body waves can be found in the work by Johnson (1975). In his work, theoretical

ground motion spectra in "envelope" form were compared with actual records.

However, the method presented above requires the knowledge of separate source functions for both body and surface waves. But, at the present time, such models can not be applied with confidence due to the lack of sufficient research on this subject matter. Therefore the application of the above method is avoided in the present work.

An alternative method which makes use of two stations and one earthquake event is prefered in this thesis. By means of ratios, this method bypasses the need of source functions, E_s and E_b. Based on the system model presented in Eq. 1.8 and Fig. 2.3, a set of system equations can be written for the two stations.

$$\begin{aligned} G_{s1}(\omega) &= E_s(\omega)R_{s1}(\theta,r_{s1})W_{s1}(\omega)X_{s1}(\omega) \\ G_{b1}(\omega) &= E_b(\omega)R_{b1}(\theta,r_{b1})W_{b1}(\omega)X_{b1}(\omega) \\ G_{s2}(\omega) &= E_s(\omega)R_{s2}(\theta,r_{s2})W_{s2}(\omega)X_{s2}(\omega) \\ G_{b2}(\omega) &= E_b(\omega)R_{b2}(\theta,r_{b2})W_{b2}(\omega)X_{b2}(\omega) \end{aligned} \qquad \text{(Eq. 2.2)}$$

to avoid the use of E_s and E_b, the following two ratios are used to eliminate them from the analysis.

$$\begin{aligned} \frac{G_{s1}(\omega)}{G_{s2}(\omega)} &= \frac{E_s(\omega)R_{s1}(\theta,r_{s1})W_{s1}(\omega)X_{s1}(\omega)}{E_s(\omega)R_{s2}(\theta,r_{s2})W_{s2}(\omega)X_{s2}(\omega)} \\ \frac{G_{b1}(\omega)}{G_{b2}(\omega)} &= \frac{E_b(\omega)R_{b1}(\theta,r_{b1})W_{b1}(\omega)X_{b1}(\omega)}{E_b(\omega)R_{b2}(\theta,r_{b2})W_{b2}(\omega)X_{b2}(\omega)} \end{aligned} \qquad \text{(Eq. 2.3)}$$

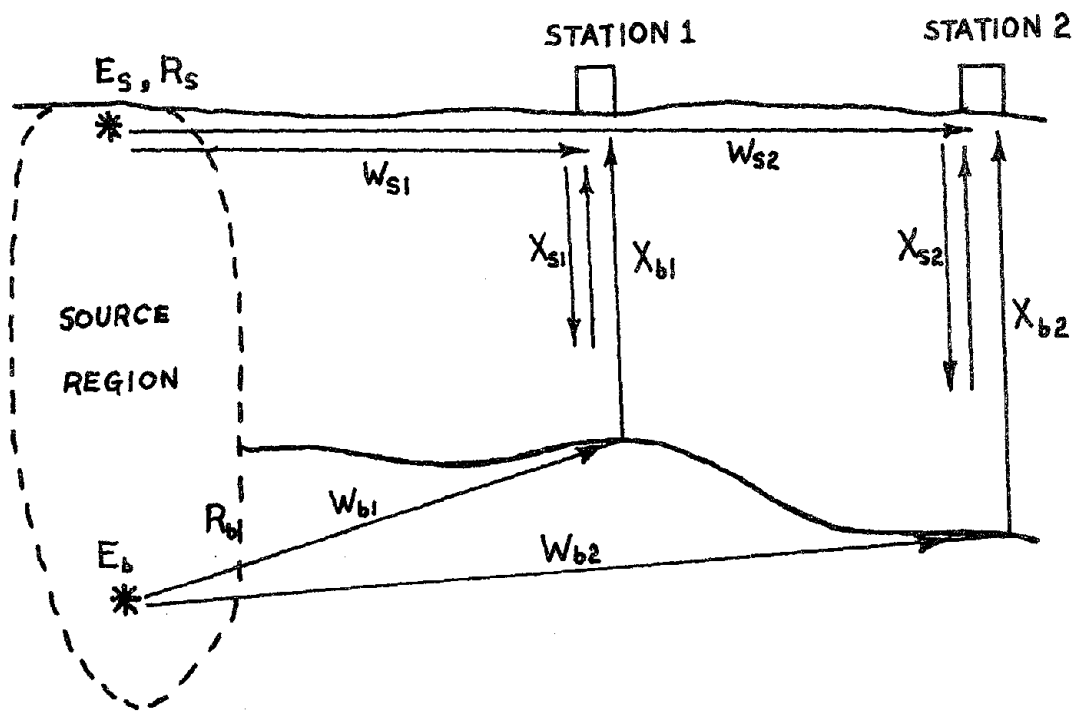

Fig. 2.3 Linear System with Two Stations

let

$$M(\omega) = \frac{G_{s1}(\omega)}{G_{s2}(\omega)}$$

$$N(\omega) = \frac{G_{b1}(\omega)}{G_{b2}(\omega)} \qquad \text{(Eq. 2.4)}$$

where $M(\omega)$ and $N(\omega)$ represent the ratio of the known surface wave transfer functions, R_s, W_s, X_s and body wave transfer functions, R_b, W_b, X_b, respectively. A set of linear equations can then be written as shown below.

$$G_{s1}(\omega)+G_{b1}(\omega)=G_1(\omega)$$
$$G_{s2}(\omega)+G_{b2}(\omega)=G_2(\omega)$$
$$G_{s1}(\omega)/G_{s2}(\omega)=M(\omega) \qquad \text{(Eq. 2.5)}$$
$$G_{b1}(\omega)/G_{b2}(\omega)=N(\omega)$$

where $G_1(\omega)$ and $G_2(\omega)$ are the Fourier spectra of the recorded ground motions at the two stations, and $M(\omega)$ and $N(\omega)$ are ratios of transfer functions shown Eq. 2.4. Solving the four equations simultaneously for the unknowns G_{s1}, G_{b1}, G_{s2}, and G_{b2}, the following solutions can be obtained.

$$G_{s2} = \frac{NG_2-G_1}{N-M} \quad ; \quad G_{s1} = \frac{M(NG_2-G_1)}{N-M}$$

$$G_{b2} = \frac{G_1-MG_2}{N-M} \quad ; \quad G_{b1} = \frac{N(G_1-MG_2)}{N-M} \qquad \text{(Eq. 2.6)}$$

where the four unknowns are now functions of the ratios

of transfer functions and the two station records, which are essentially known quantities.

The subsequent chapters will examine in detail the feasibility of using this method.

CHAPTER 3

APPLICATION OF LINEAR SYSTEM MODEL

Records from the 1971 San Fernando earthquake are selected to test the method of analysis prescribed in the preceeding section. Mainshock records at the ground levels of 8244 Orion Ave., 15250 Ventura Blvd. and 1800 Century Park East are used. Detailed description of the earthquake can be found in the publication by the USGS and the NOAA (1971). And the description on the source of the pre-processed raw records can be found in the work by Johnsen (1972). Digitized accelerograms from three stations were selected to test the method prescribed. These records were first rotated based on the epicentral location obtained by Hanks (1974), only the tangential components of them are used in this analysis. Fig. 3.1 presents a general description of the three stations of interest.

In this thesis, only a preliminary exploration will be attempted on the proposed method of wave separation. No rigorous treatment will be attempted. The reason is because many of the transfer functions required for the newly proposed model have not yet been well estalished. Therefore, instead of rigorous analysis on the separation of body and surface waves, this thesis will serve only as a preliminary examination on the wave

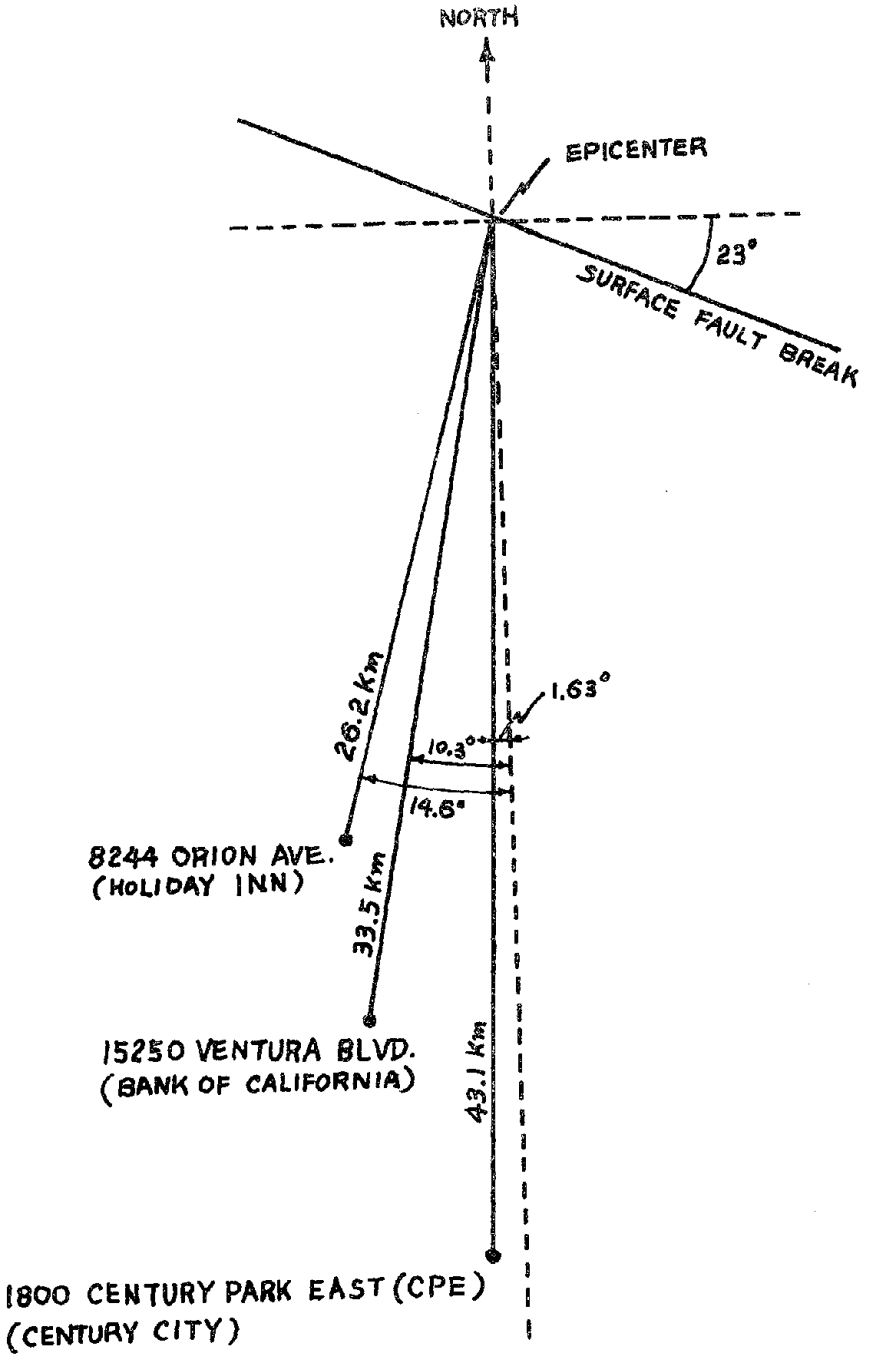

Fig. 3.1 Stations used in the Analyses

separation scheme and the newly proposed system model.

3.1 THE SYSTEM FUNCTIONS

Based on the theories discussed in Chapter 1, the required functions, the R's, W's and X's are developed below for the 3 stations used.

RADIATION PATTERN, R_b AND R_s A double couple point source on a 52° dip slip fault plane is used to calculate the directionality effect. Fig. 3.2 illustrates the orientation of this double couple. Although the double couple source function does not come close to resembling the actual source mechanism, it is, nevertheless, sufficient for the purpose of the present exploratory analysis. Using Eq. 1.11 and Eq. 1.12, the resulting radiation patterns can be obtained. Fig. 3.3 illustrates some typical results calculated from the model shown in Fig. 3.2. This solution will be assumed to be applicable for both R_b and R_s in this analysis as it is stated in Appendix A.

TRAVEL PATH EFFECTS FOR BODY WAVES The W_b function is calculated using Eq. 1.13a. The values for the parameters Q_b and V_b are selected based on the work by Lastrico (1970) and Duke et. al. (1971). For Q_b, a value of 200 is used to express the damping in the crystalline rock in the San Fernando Valley region. For V_b, a value of 3.4 Km/sec is used as the shear wave

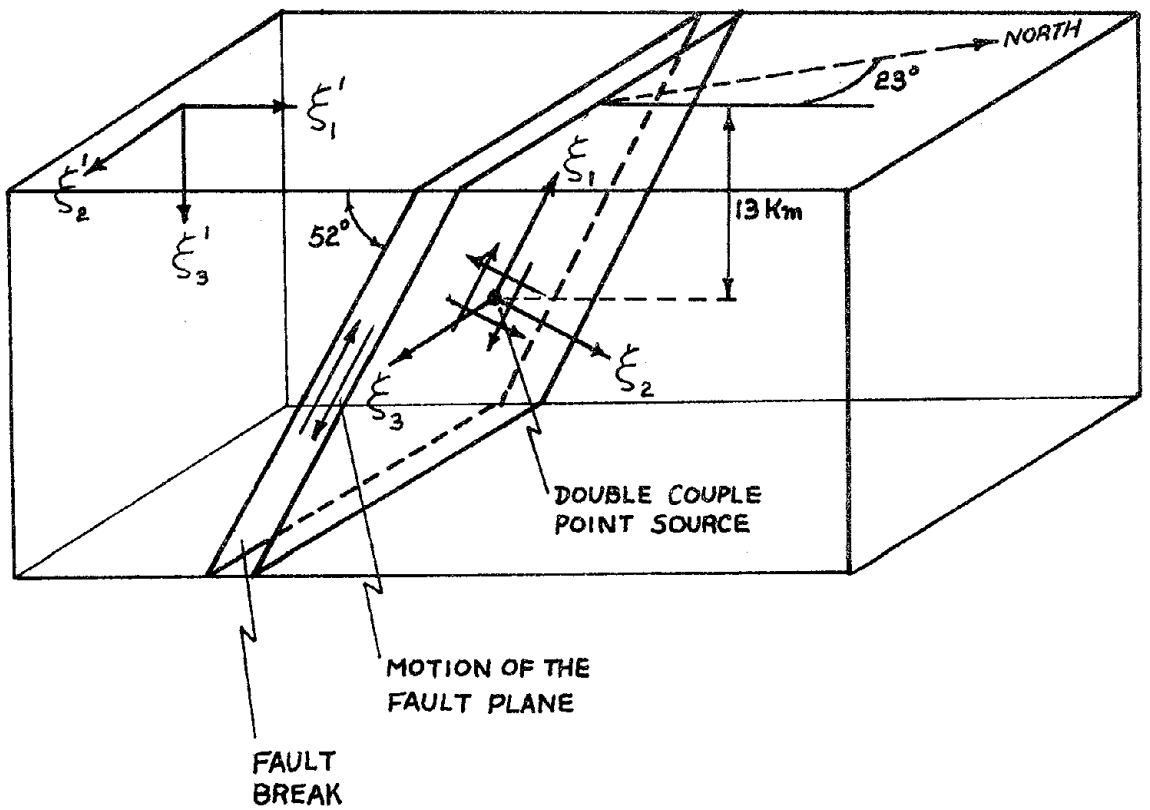

FOCAL DEPTH = 13 KM

DIP ANGLE = 52° (HANKS 1975)

Fig. 3.2 Double Couple Source Model for the San Fernando Mainshock

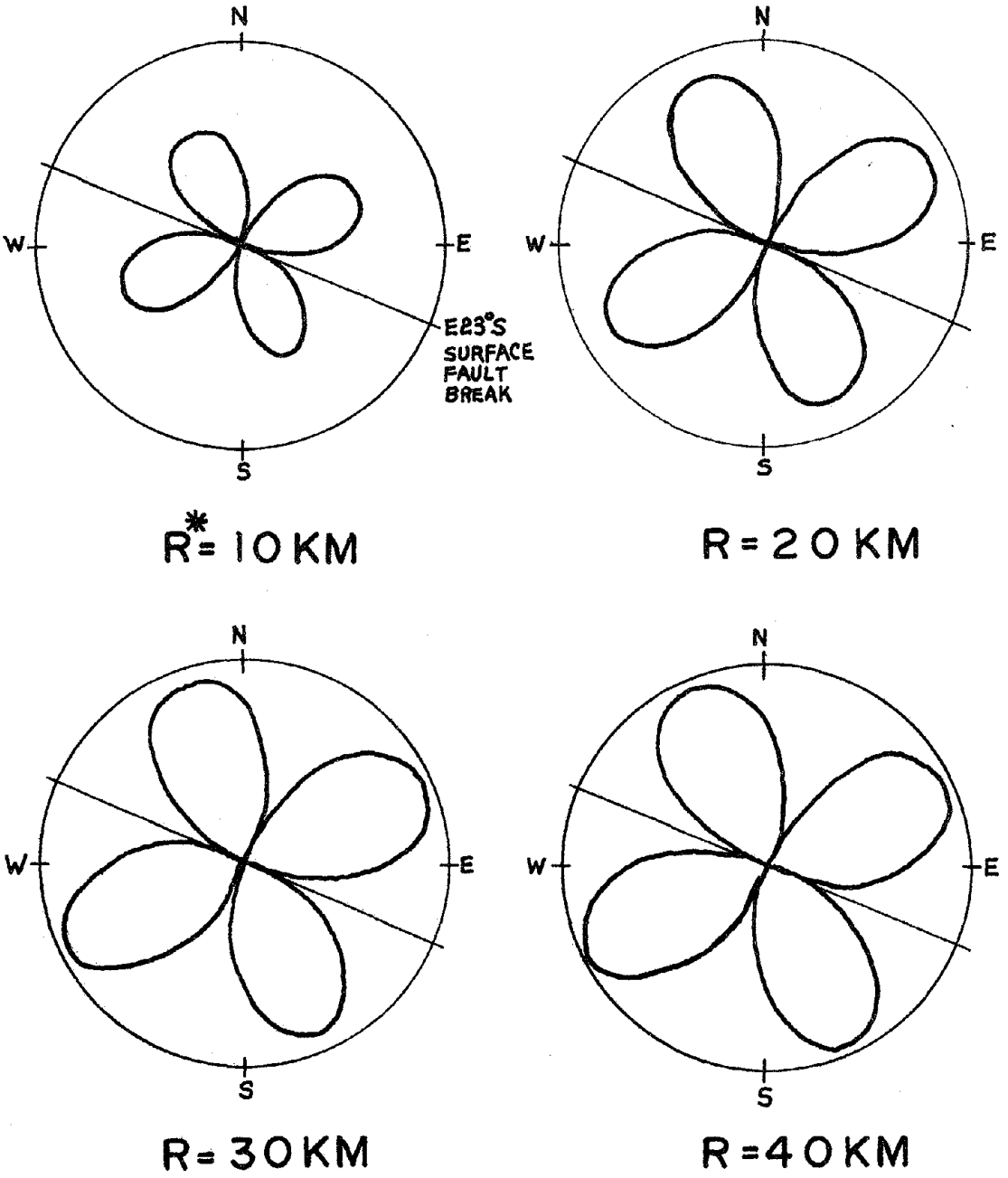

* R ≡ EPICENTRAL DISTANCE

Fig. 3.3 Radiation Patterns for the San Fernando Mainshock for a Double Couple Point Source

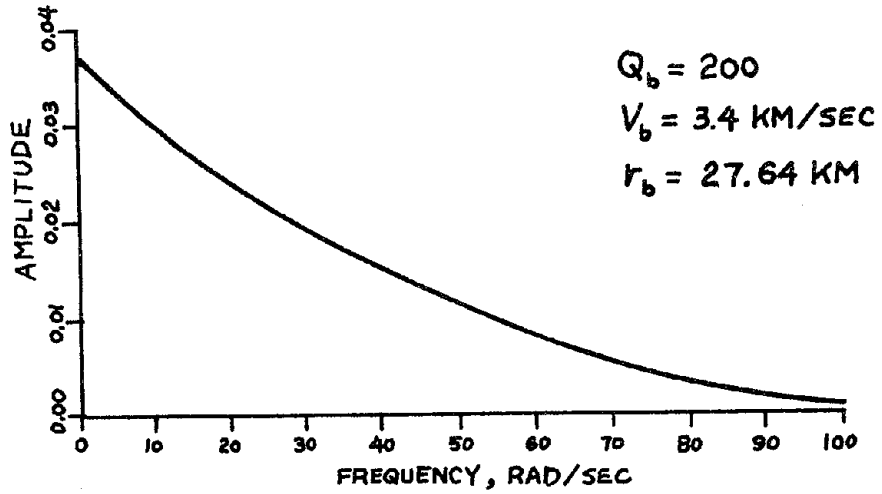

Fig. 3.4a Typical Body Wave Path Transfer Function

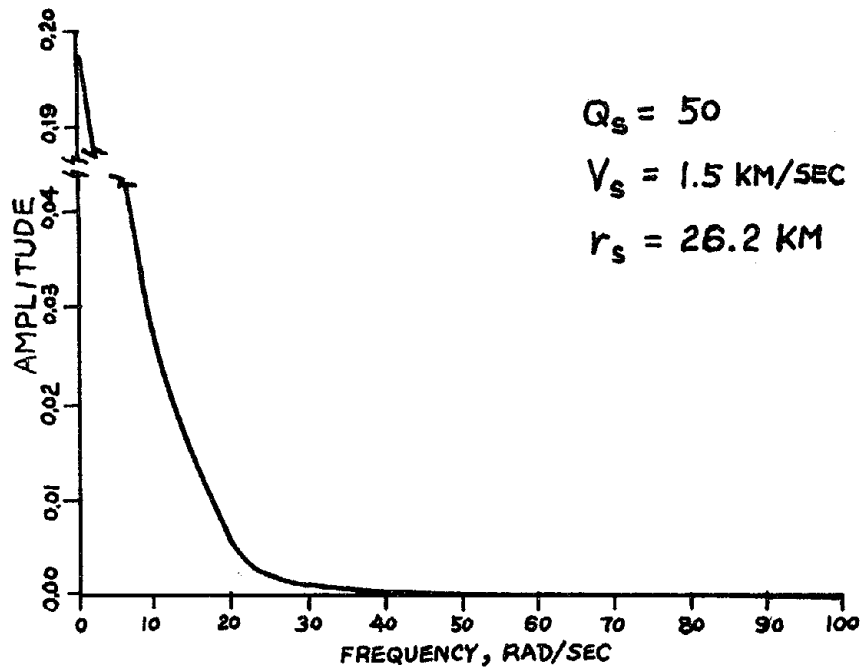

Fig. 3.4b Typical Surface Wave Path Transfer Function

velocity in the crystalline rock. A typical shape of W_b is illustrated in Fig. 3.4a.

SITE AMPLIFICATION EFFECTS FOR BODY WAVES The function X_b for the stations used in this analysis have been calculated by Johnsen (1972) and Engman (1973). The results termed in their reports as "X_{ALL}" are selected as the most appropriate ones to be used here. These incorporate a site model extending to the original ground surface. Fig. 3.5 illustrates these functions.

SURFACE WAVE EFFECTS Due to the nonavailibility of a convenient algorithm for surface wave site effects, the function X_s will be taken as unity in this analysis. The path functions W_s are calculated according to Eq. 1.13b. A value of 50 is selected for Q_s reflecting the average amount of damping in the top 0.6 km of geology in the San Fernando Valley (Duke et al. 1971). A value of 1.5 km/sec is set for V_s. This value is an average of shear wave velocity in the upper 0.6 km of geology in the San Fernando Valley. And it is assumed to be roughly the average velocity for the surface waves traveling in the wave guide of this depth. A typical shape of W_s is illustrated in Fig. 3.4b.

CONSIDERATION OF TIME DELAYS Based on the Fourier transform pair given in Eq. 1.2, the effect of time shift can be calculated from the following equation.

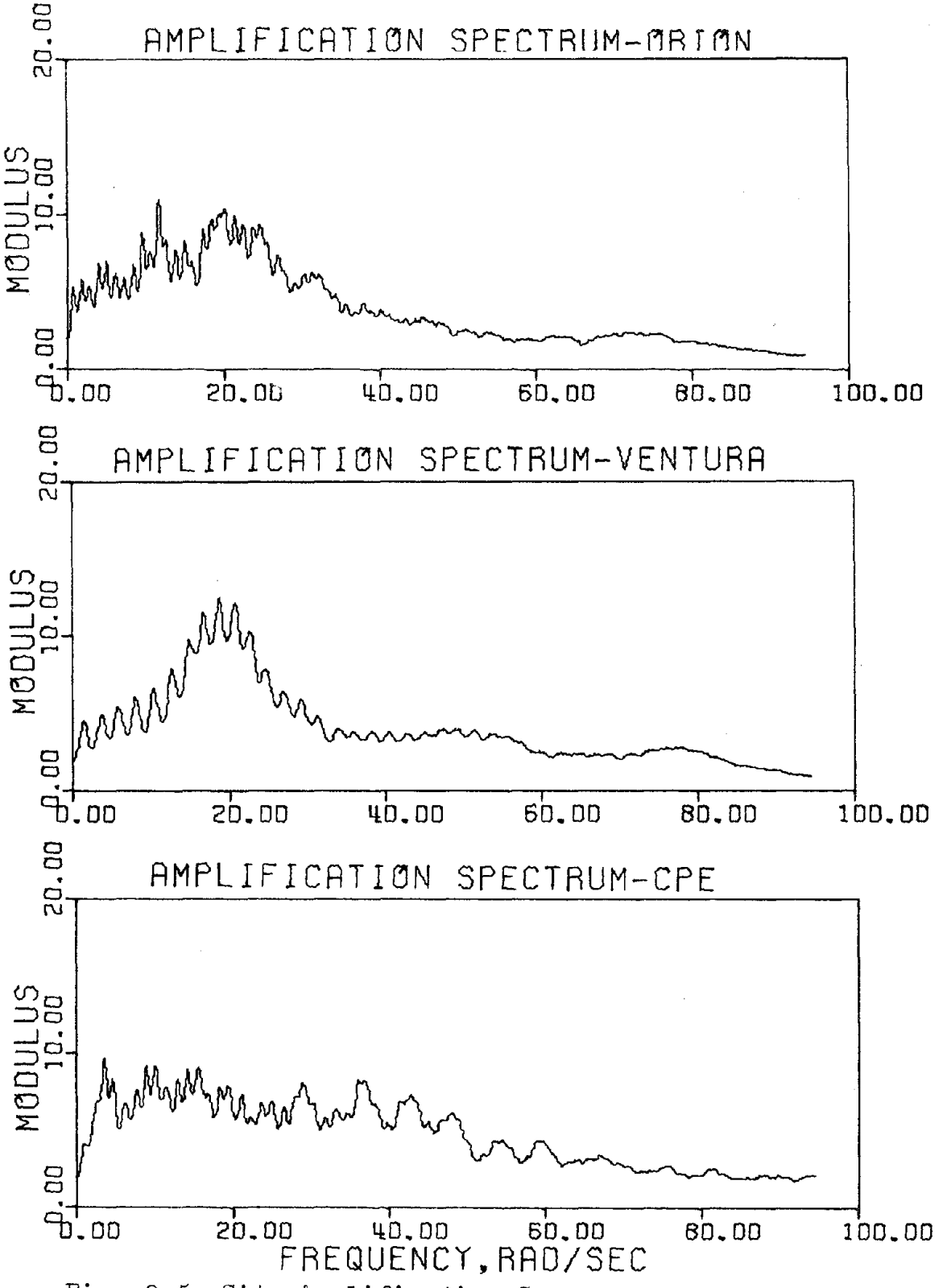

Fig. 3.5 Site Amplification Spectra For Vertically Traveling S-Waves

$$F(\omega)_{shifted} = F(\omega)_{original} \cdot e^{-i\omega t} \qquad \text{(Eq. 3.1)}$$

where t>0 gives positive time shift (delay), and t<0 gives negative time shift (advance). In this analysis, the arrival time difference for both the body waves and the surface waves between the two stations are considered. For the body waves, the estimation of the difference in arrival time is calculated by the following equation.

$$t_{delay} = \left[\frac{r_{w2}}{c_{rock}} + \frac{r_{x2}}{c_{x2}}\right] - \left[\frac{r_{w1}}{c_{rock}} + \frac{r_{x1}}{c_{x1}}\right] \qquad \text{(Eq. 3.2a)}$$

where the letter r denotes distance and c denotes velocity. For the surface waves, it is calculated by the following equation

$$t_{delay} = \frac{d_2 - d_1}{c_{surf}} \qquad \text{(Eq. 3.2b)}$$

where the letter d denotes epicentral distance and c_{surf} denotes the average surface wave velocity, which was used in the function W_s. Fig. 3.6 defines all the symbols used in Eq. 3.2a and 3.2b.

The errors resulting from the uncertainties in the distances and velocities, the delay time for the arrival of waves between stations, and the effect of surface wave dispersion have been ignored because of the exploratory nature of this research.

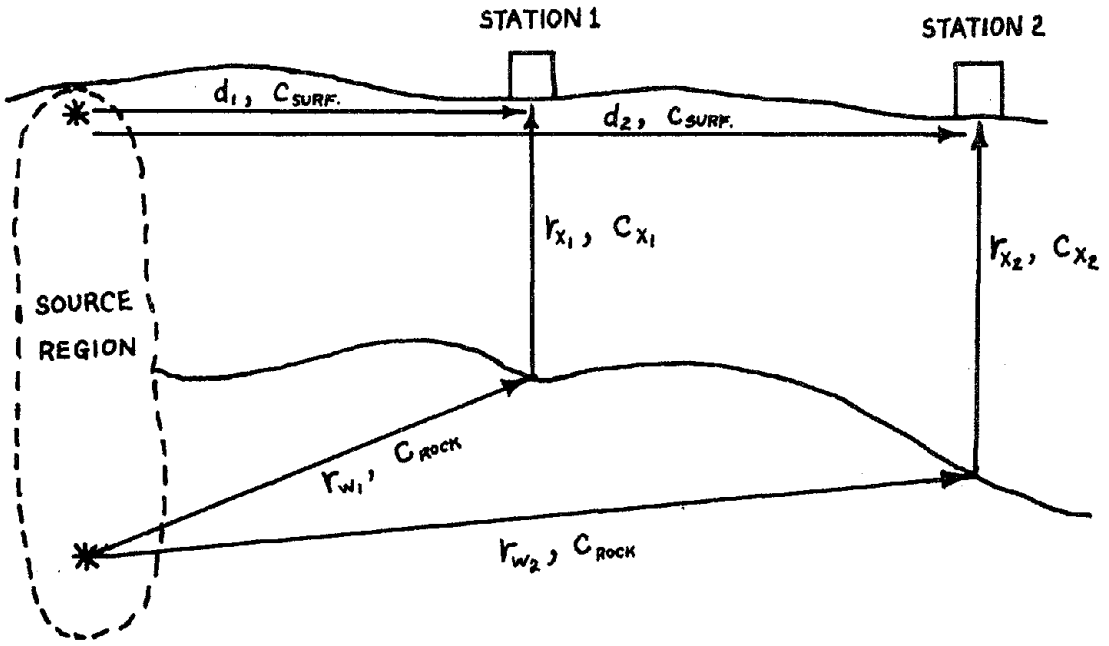

Fig. 3.6 Travel Paths used to Calculate the Differences in Arrival Times

3.2 THE PROBLEM IN COMPUTING SEPARATED WAVES

Based on the preliminary model provided in the above Section, the separated body and surface waves should show the following characteristics:

(1) Due to the relatively higher rate of damping specified in the transfer function W_s over W_b, one should expect the higher frequency contents in the surface waves to decay faster than those in the body waves as the distance increases. (2) One should expect the general amplitude for body waves to decay faster than surface waves as the distance increases. This is because the surface waves decay with a factor of $1/\sqrt{r}$ while the body waves decay with a factor of $1/r$. (3) The general shapes of the pair of separated body and surface wave spectra should not differ from each other too much. The reason being that the various characteristics of the surface waves, such as the dispersion phenomenon and the amplification due to the effects of wave guides have not been modeled. Therefore, the surface wave and the body wave characteristics are governed primarily by the W_s and W_b transfer functions, respectively, which are similar in shape.

Using Eq. 2.5 and the transfer functions discussed in the last section, a set of separated surface and body waves for the pair of stations, Holiday Inn and Century City, and the pair, Holiday Inn and Bank of California were obtained. The numerators, the denominators, the original ground motions, the separated body and surface waves and the inverse transforms of the body and surface waves are presented in Fig. 3.7 and Fig. 3.8 for the above two station pairs in that order. Fig. 3.7 presents the calculations for the pair of stations, Holiday Inn and Century City; Fig. 3.8 presents the calculations for the pair of stations, Holiday Inn and Bank of California.

After examining the results, it was found that some of the computed results exhibited large unrealistic peaks. This is especially evident in the calculations shown in Fig. 3.8b. The periodic appearance of these large peaks and the fact that they exist at the same sets of frequencies reinforce the doubt of their validity.

In the previous work done with Linear System Theory, similar spurious peaks have appeared on numerous occasions. In the work by Johnson (1975), the occurrance of a large number of spurious peaks had hampered his analysis of the testing of the procedure

known as "Method II". In his inverse Fourier transforms, the spurious peaks in the spectra caused the time history to continue without decay. The reason for this is that the large peaks are like impulse functions in the frequency domain. And their inverse transforms are continuous sine waves. So, when a few of these large peaks exist in the Fourier spectrum, its inverse transform will be dominated by a superposition of a set of sine waves corresponding to the frequencies of these spurious peaks. A typical pair of his results is illustrated in Fig. 3.9. The same problem with spurious peaks had appeared earlier in the work by Johnson and Yee (1972), Johnsen (1972), and Engman (1973).

From a step by step examination of the processes of the separation calculation, it was found that these large peaks seem to correlate well with the dips in the amplitude of the denominators, N-M. Note in Fig. 3.7 and 3.8 that the spurious peaks occur wherever the denominator approaches zero. This phenomenon also existed in the works referenced in the above paragraph. In the next chapter, this observation will be demonstrated with the various testings performed. Chapter 5 will then present some possible methods for eliminating the spurious peaks and their effects.

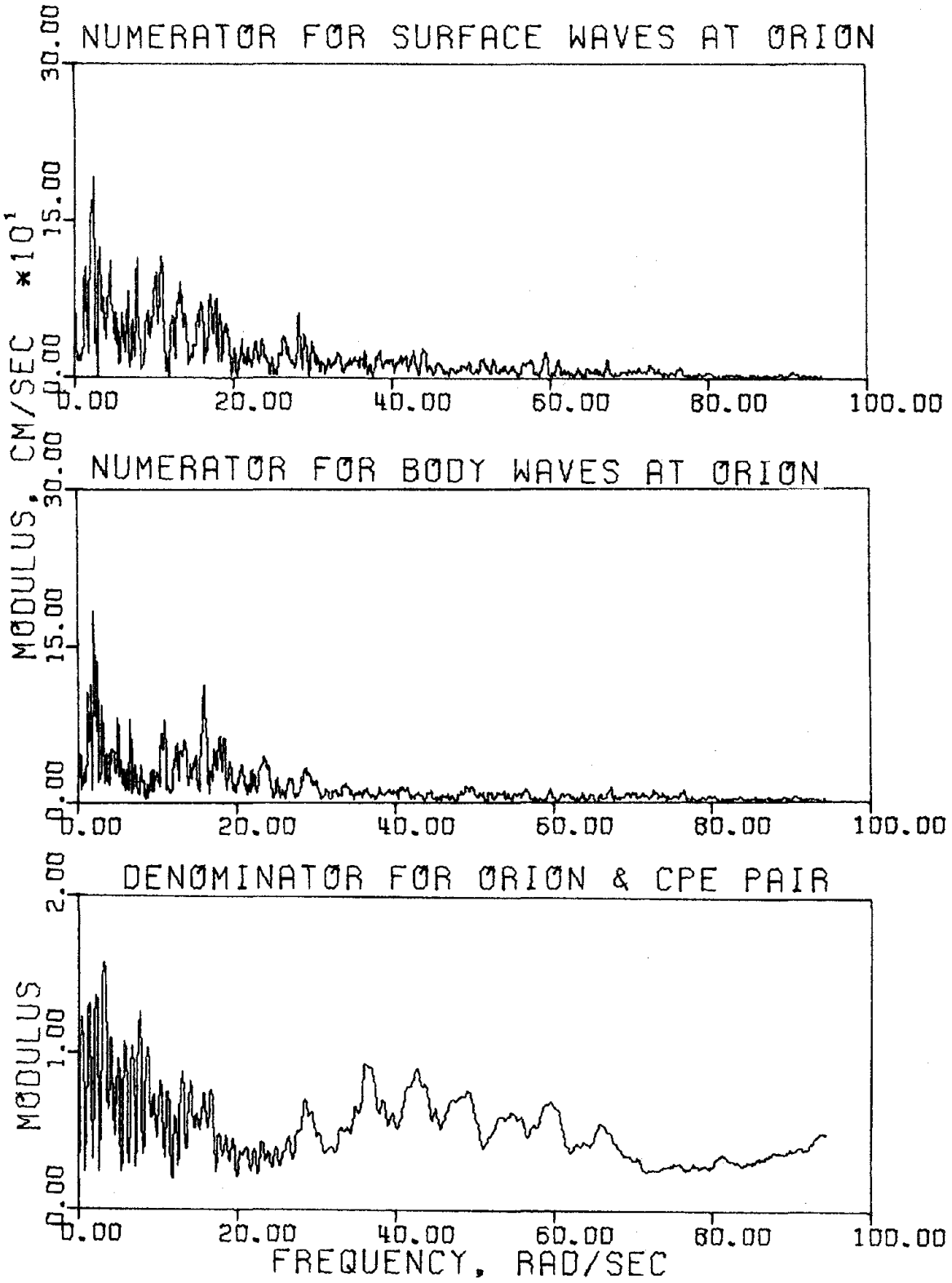

Fig. 3.7a Numerators and Denominator for Orion, Orion and CPE Pair

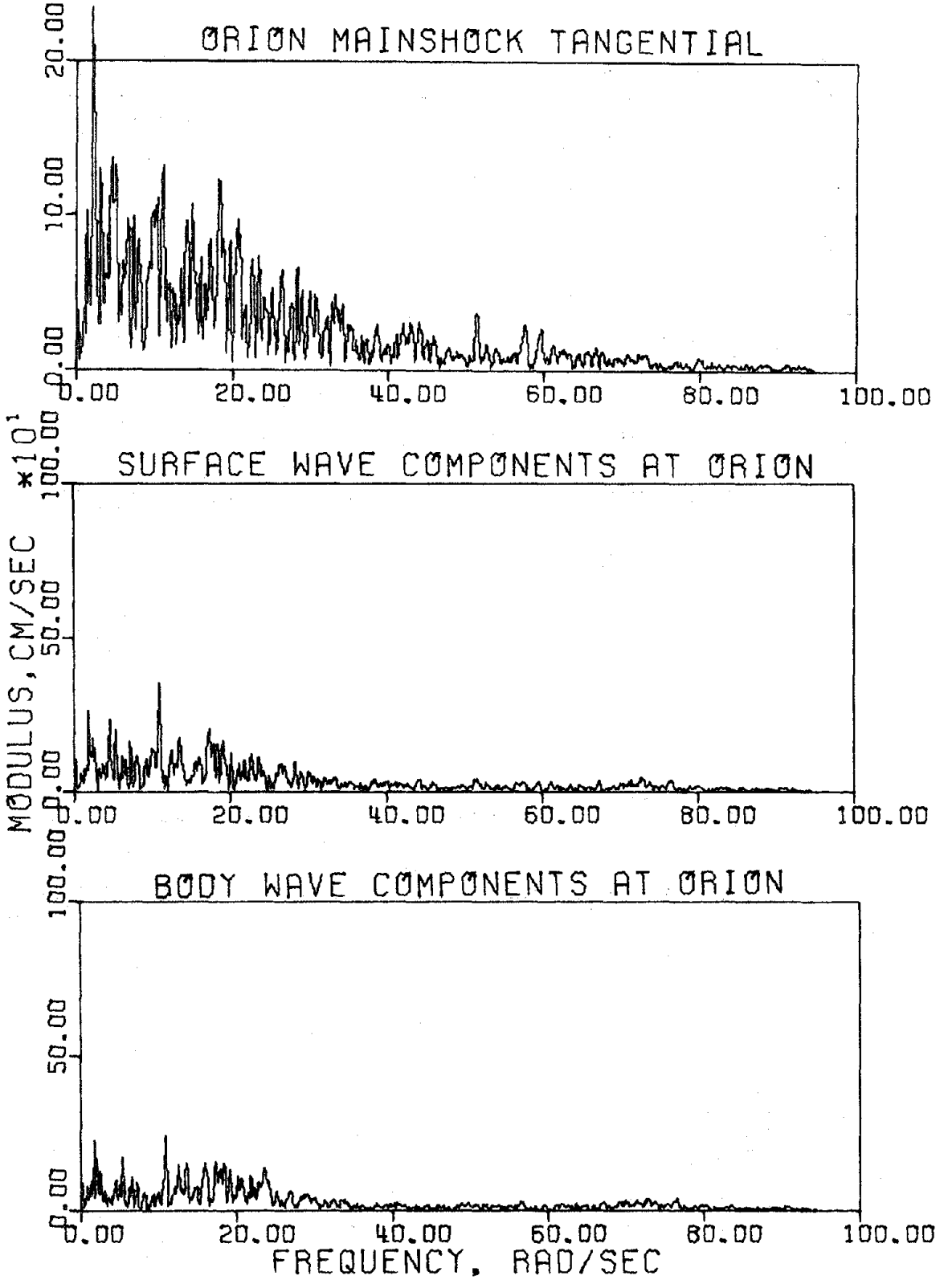

Fig. 3.7b Original Ground Motion and The Separated Spectra for Orion, Orion and CPE Pair

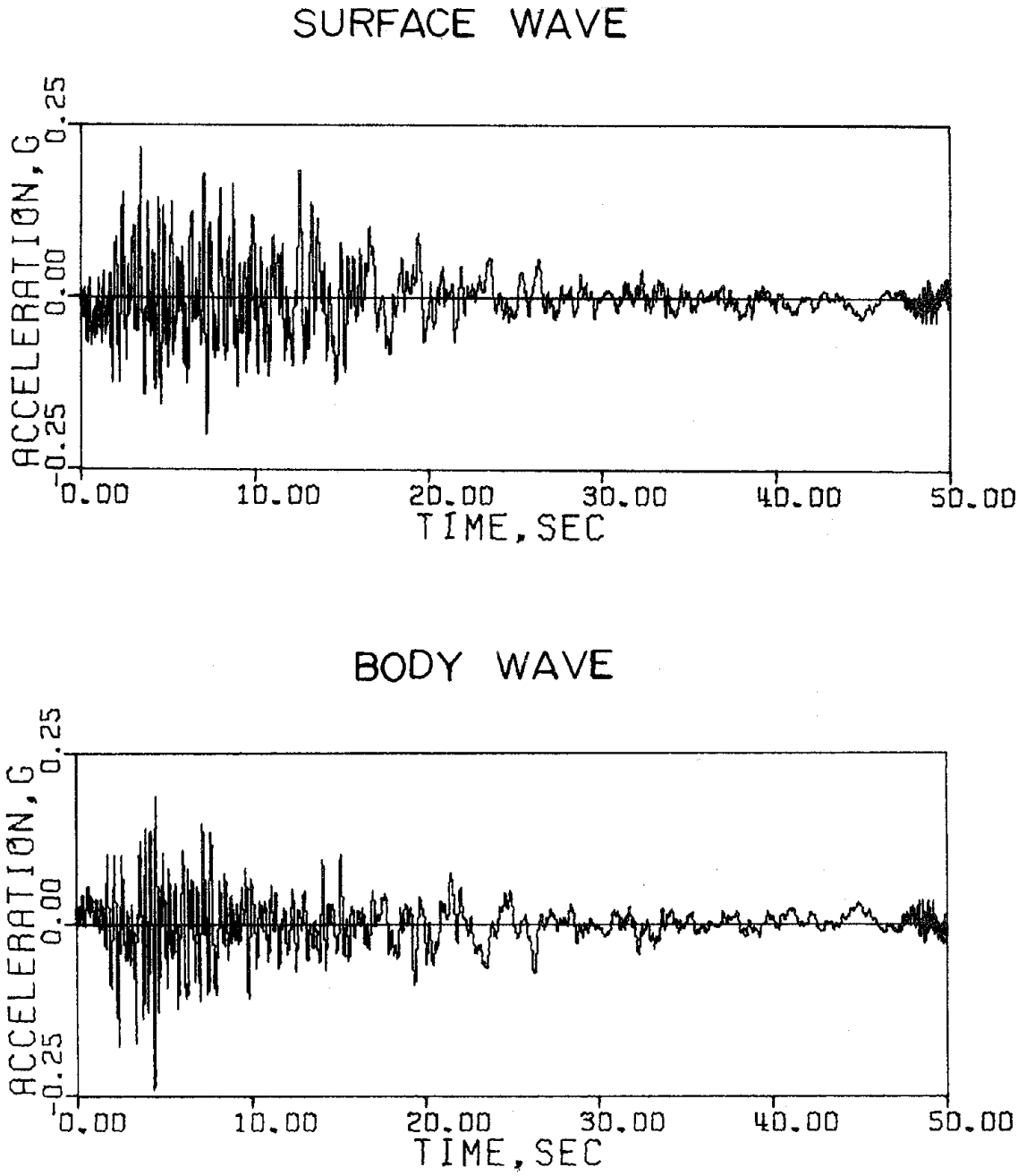

Fig. 3.7c Inverse Transforms of the Separated Surface Wave (top) and Body Wave (bottom) Spectra for Orion, Orion and CPE Pair

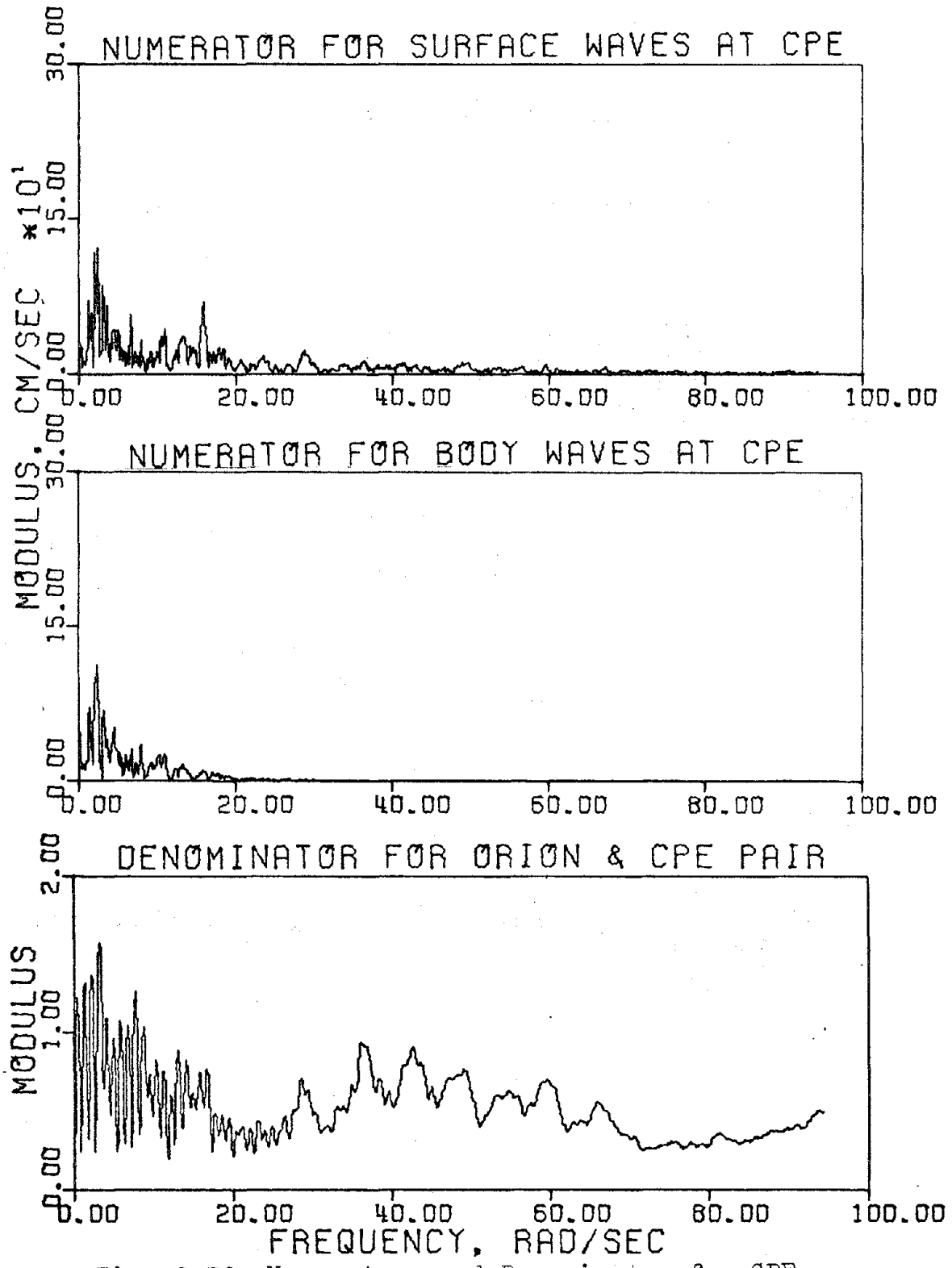

Fig. 3.7d Numerators and Denominator for CPE, Orion and CPE Pair

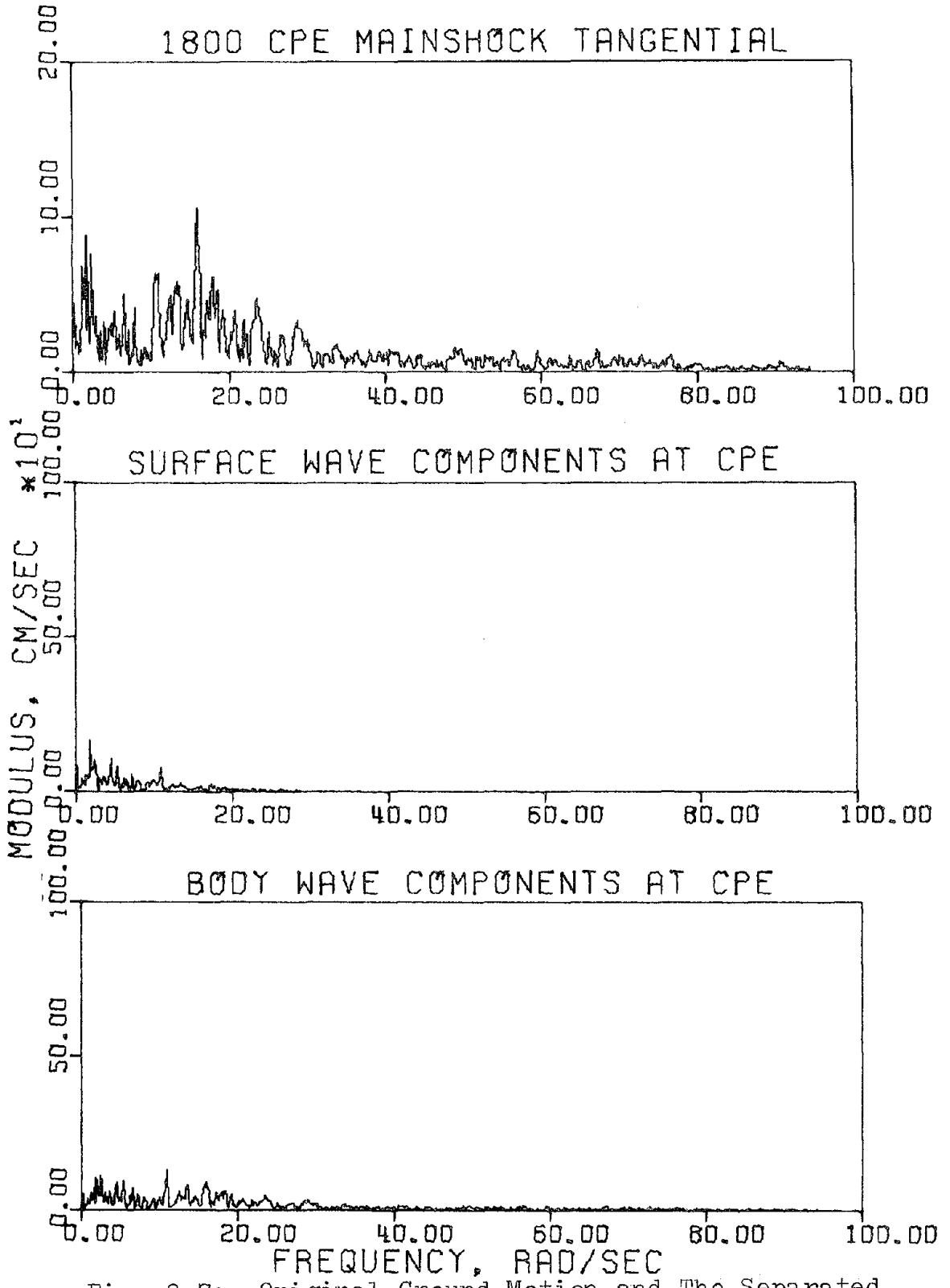

Fig. 3.7e Original Ground Motion and The Separated Spectra for CPE, Orion and CPE Pair

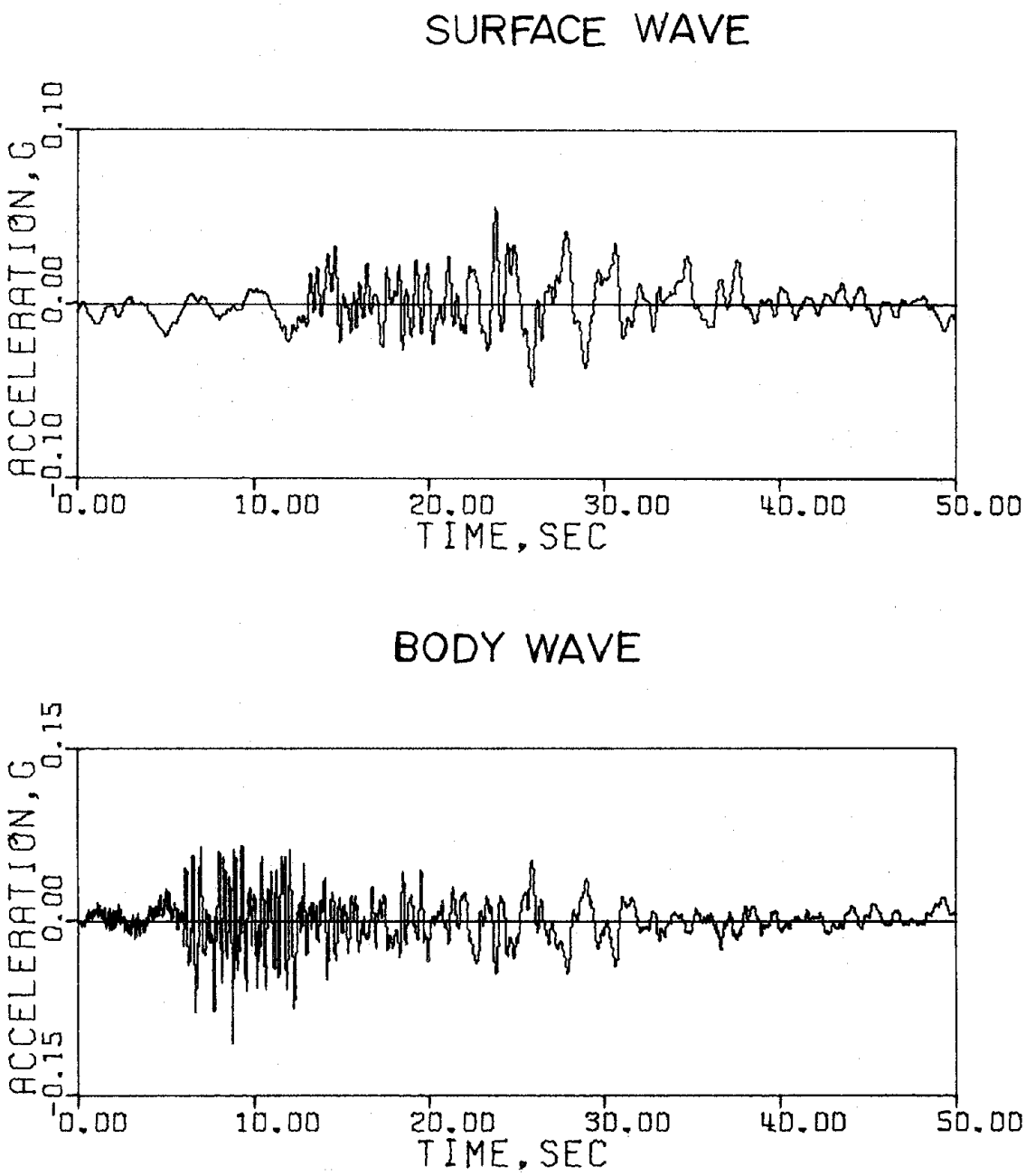

Fig. 3.7f Inverse Transforms of the Separated Surface Wave (top) and Body Wave (bottom) Spectra for CPE, Orion and CPE Pair

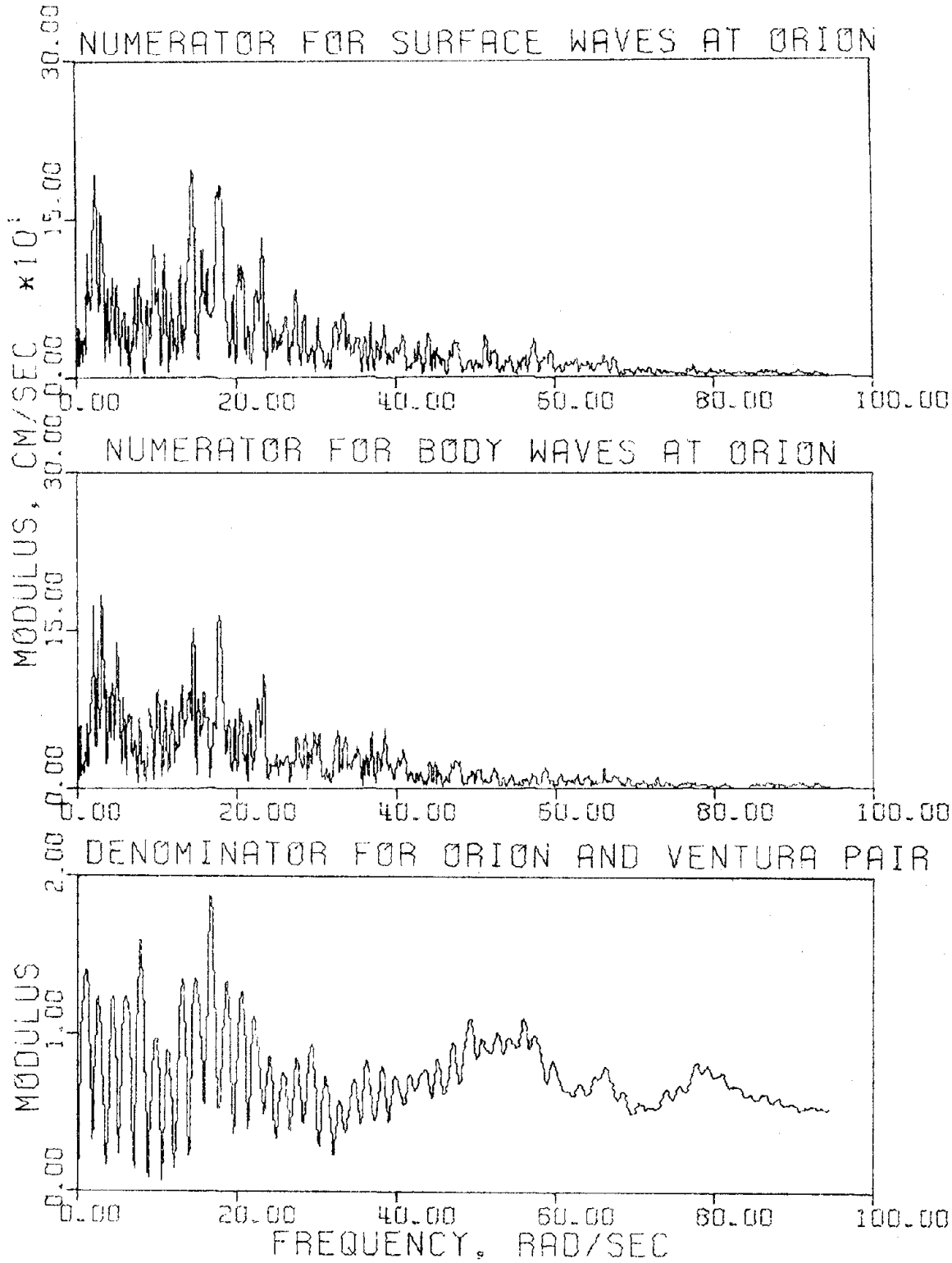

Fig. 3.8a Numerators and Denominator for Orion, Orion and Ventura Pair

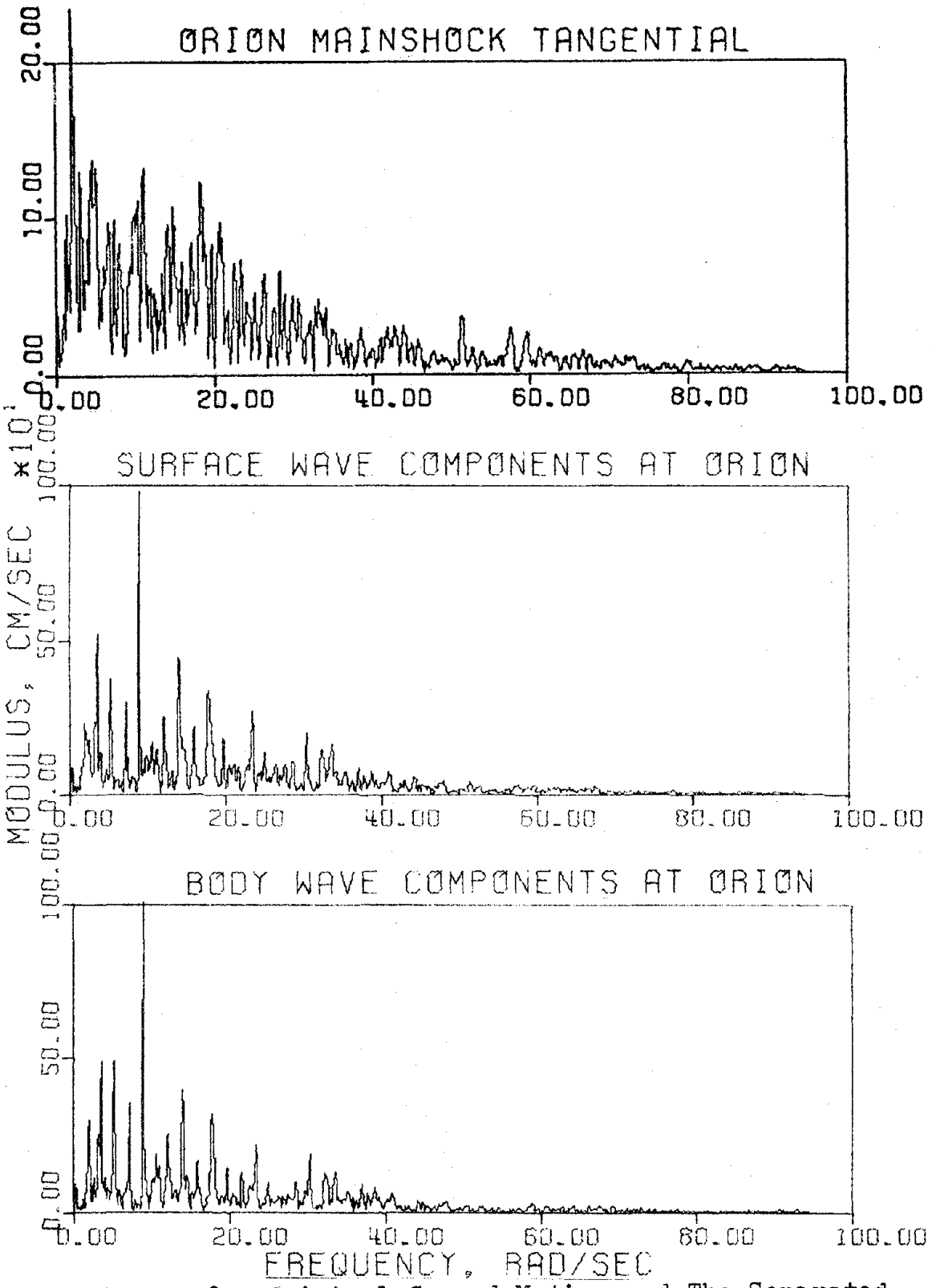

Fig. 3.8b Original Ground Motion and The Separated Spectra For Orion, Orion and Ventura Pair

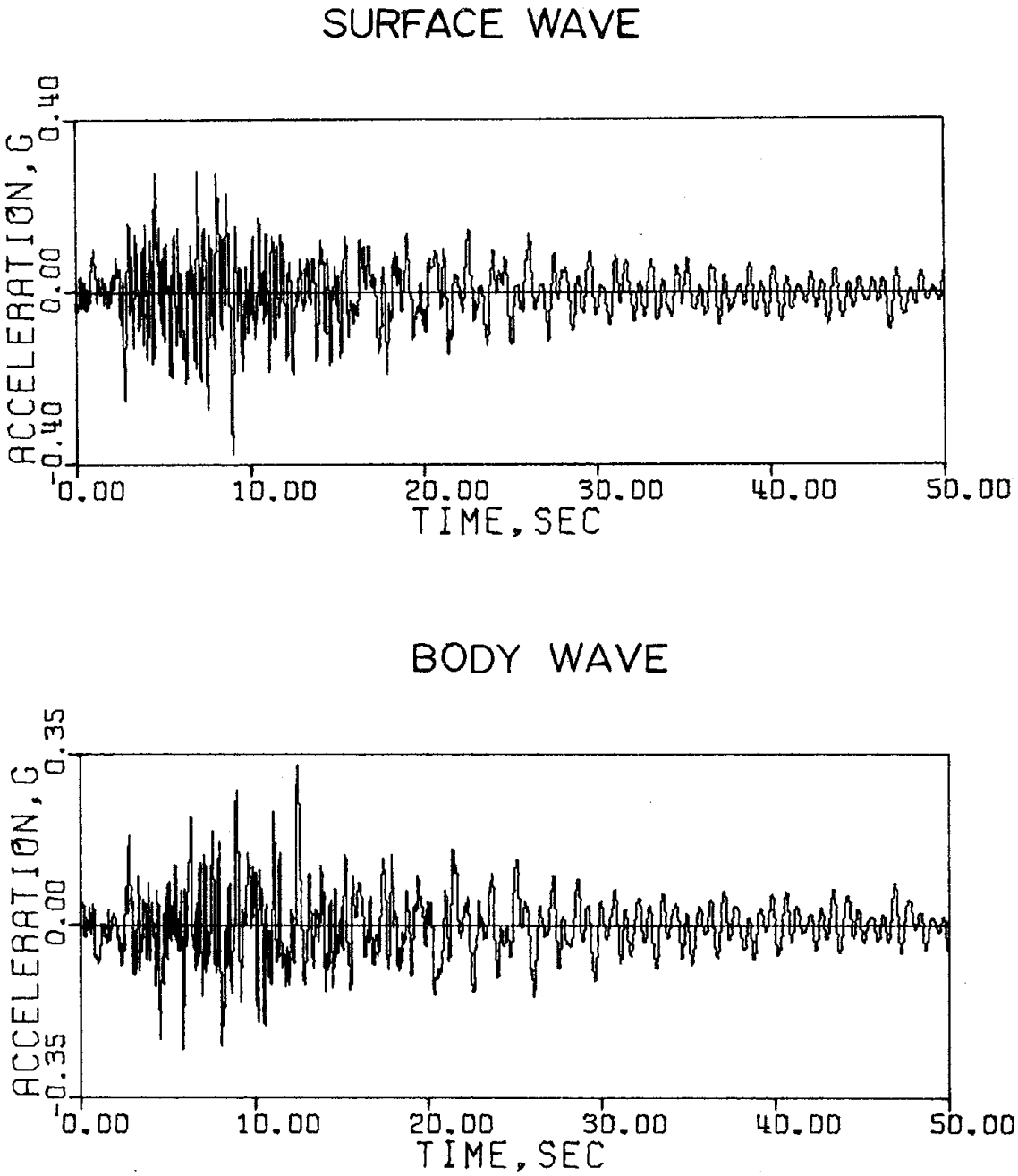

Fig. 3.8c Inverse Transforms of the Separated Surface Wave (top) and Body Wave (bottom) Spectra for Orion, Orion and Ventura Pair

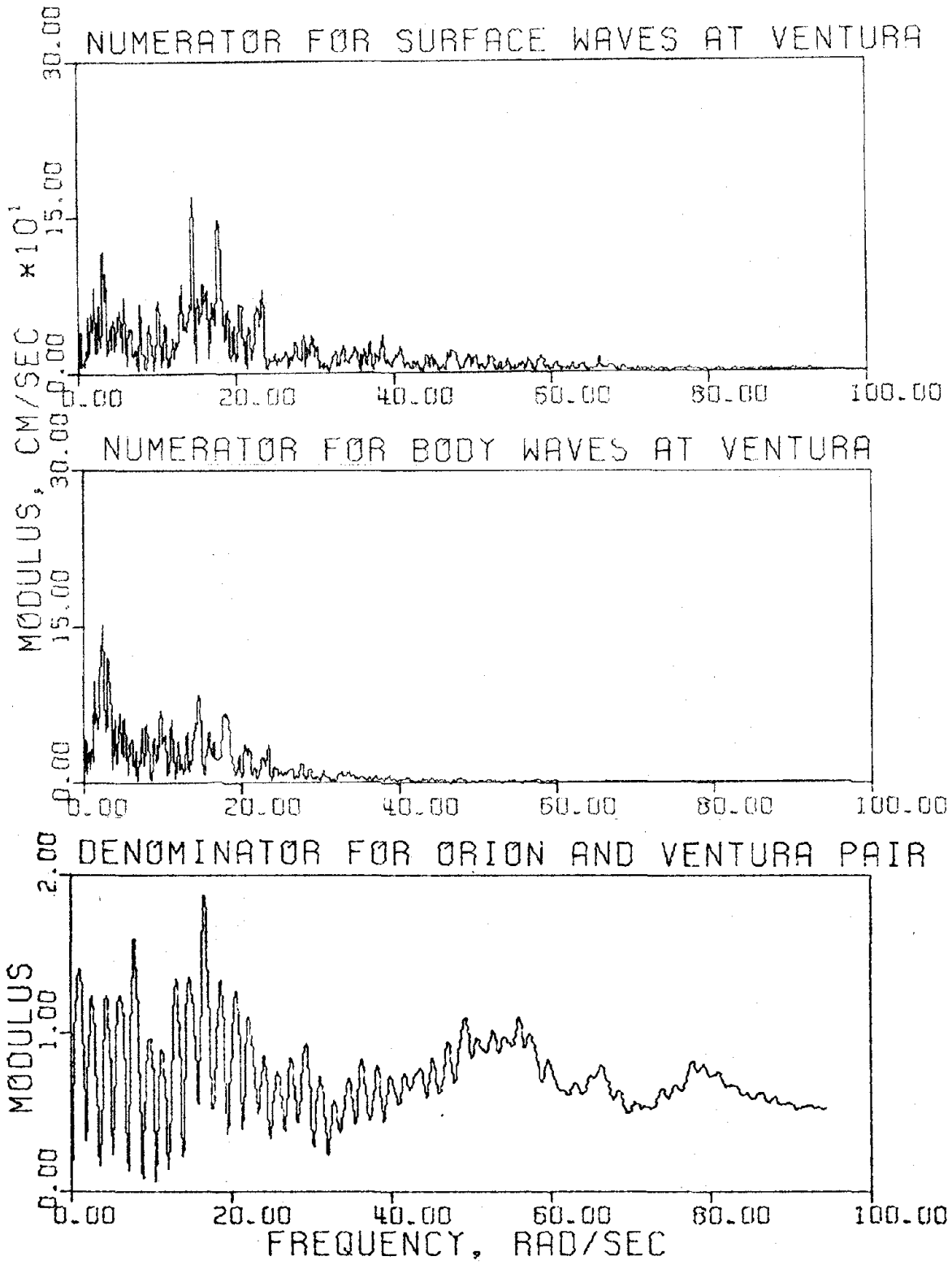

Fig. 3.8d Numerators and Denominator for Ventura, Orion and Ventura Pair

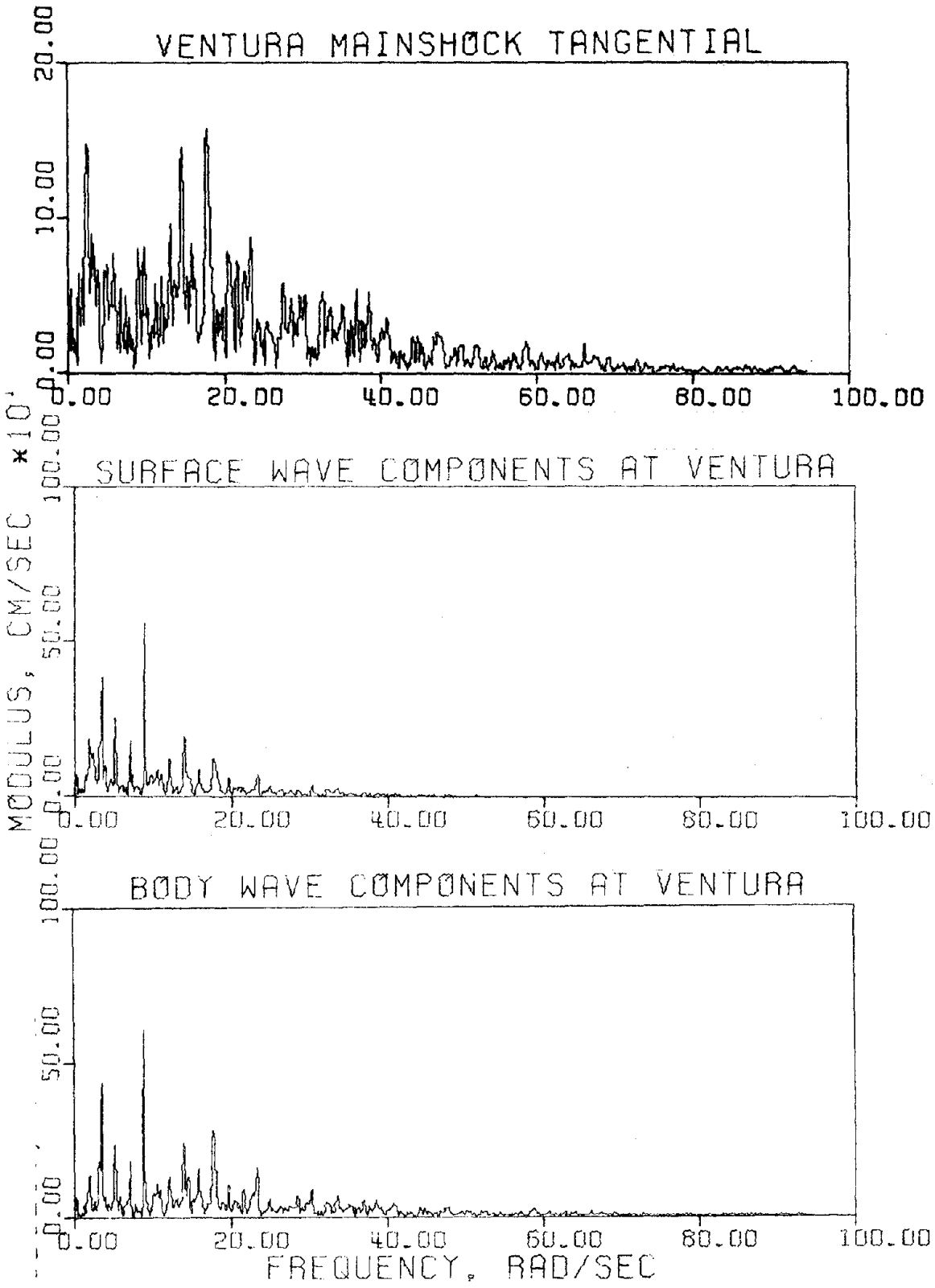

Fig. 3.8e Original Ground Motion and The Separated Spectra for Ventura, Orion and Ventura Pair

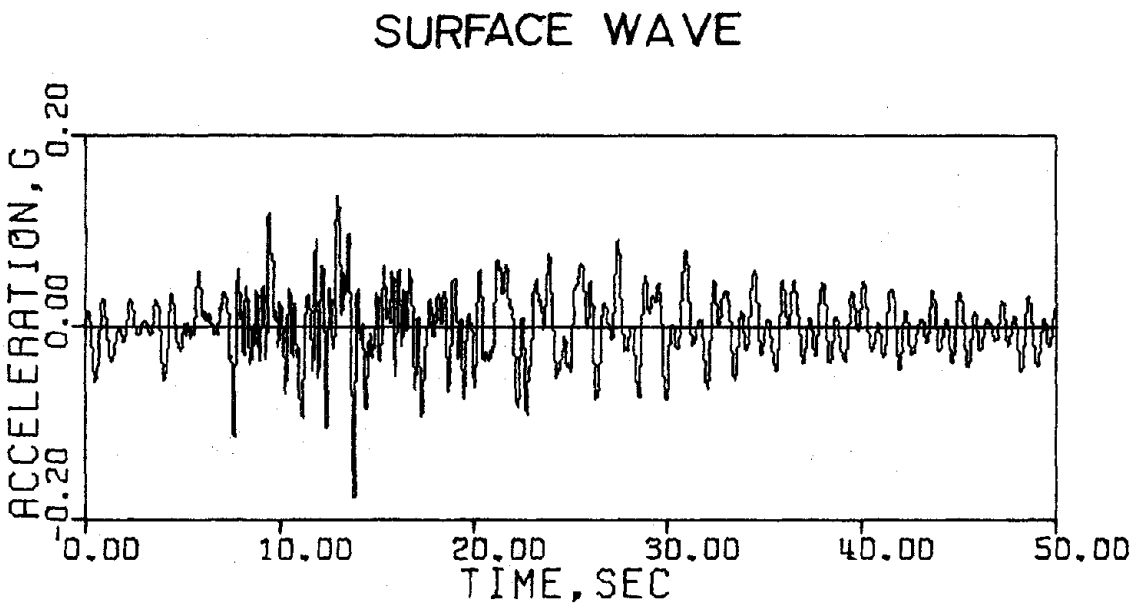

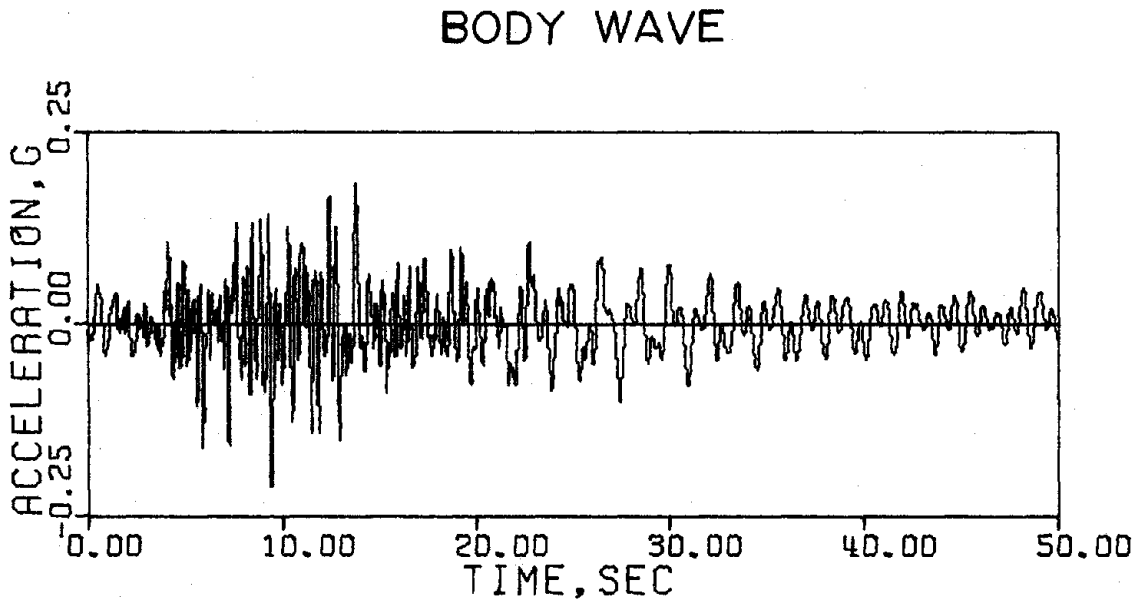

Fig. 3.8f Inverse Transforms of the Separated Surface Wave (top) and Body Wave (bottom) Spectra for Ventura, Orion and Ventura Pair

Reproduced from best available copy.

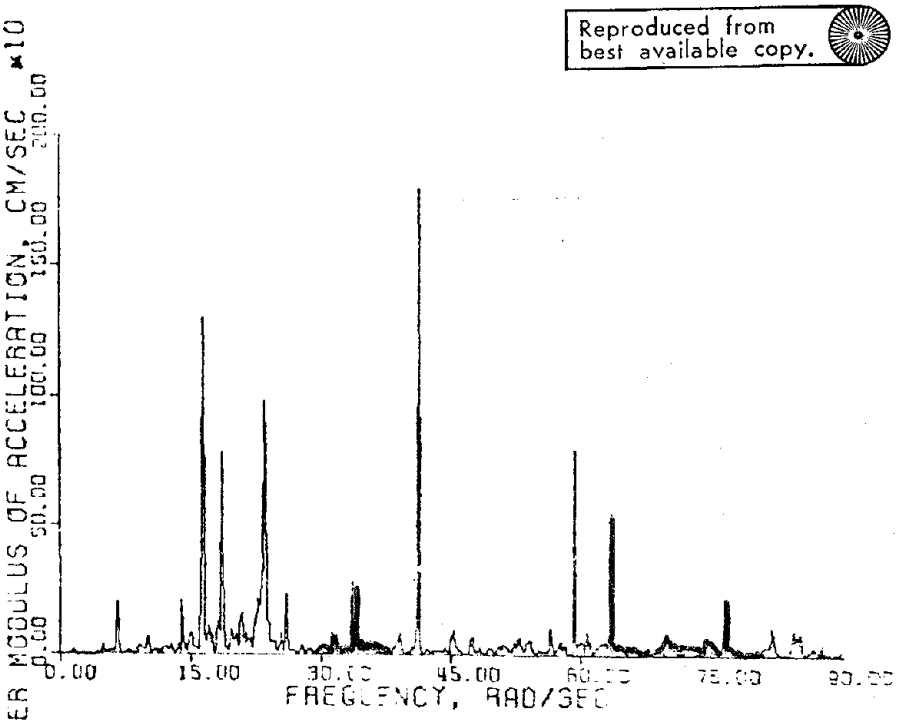

Figure 4.12. Calculated Fourier Modulus, Method II, BANC Events 1/2/72M and 1/2/72 IAS East.

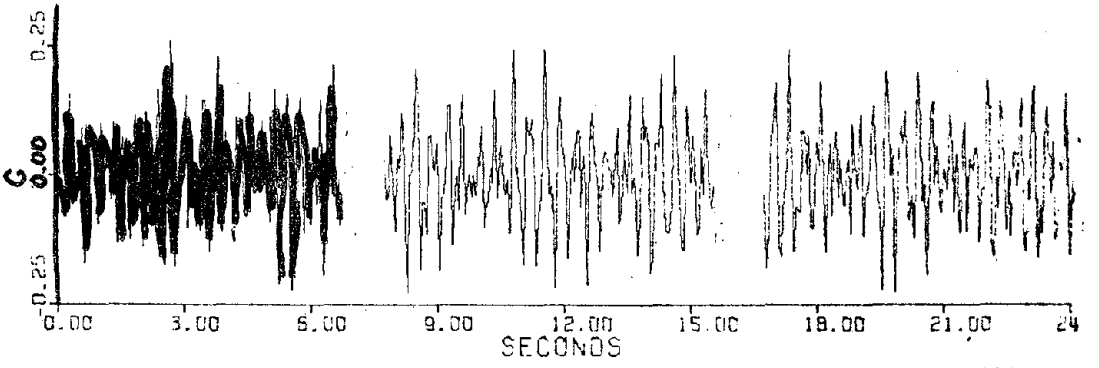

Figure 4.14. Calculated Time History, Method II, BANC Events 1/2/72 and 1/2/72 IAS East.

Fig. 3.9 Effect of Large Peaks in the Fourier Spectrum on the Inverse Transformed Time History (Johnson 1975)

CHAPTER 4

A DEMONSTRATION OF THE CAUSE OF THE SPURIOUS PEAKS PROBLEM

Before any attempt is made in eliminating the spurious peaks from the results of the separated waves, a brief examination of the causes of the spurious peaks is done in this chapter. Two arbitrary stations will be used for this purpose. This chapter will serve as a demonstration for confirming the spuriousness of these large peaks, and also verify their correspondence with the dips in the denominator, N-M. No rigorous parametric study will be attempted.

In order to properly perform the study on the causes of the spurious peaks, a controlled condition on the system is established. A set of exact solutions to the body wave and surface wave contents must be known. All transfer functions must also be exact. If these conditions exist one will be able to observe the possible errors that each parameter contributes by comparing basic theory with computed results. However, since this is only a test case, it is not necessary to base the test system on any real physical event. In addition, no actual physical units will be attached to any of the parameters. These simplifications can help ease the analyses performed in this chapter.

4.1 PREPARATION OF TEST DATA

The simplest way to create a controlled set of data is to design a source function and a set of transfer function, and then to generate the body and surface wave contents and the total ground motions at two arbitrary stations based on the method described in Eq. 2.1.

For the source, time function with exponential decay of the form shown below was arbitrarily chosen.

$$e(t) = (220/\pi)^{\frac{1}{2}} e^{-220t^2} \qquad \text{(Eq. 4.1)}$$

Knowing that the Fourier transform of $h(t)=(\alpha/\pi)^{\frac{1}{2}}\exp(-\alpha t^2)$ is $H(\omega)=\exp(-\omega/4\alpha)$*, the Fourier transform of Eq. 4.1 with an arbitrary time delay of 1.0 unit gives a source function of the following form.

$$E(\omega) = e^{\frac{-\omega^2}{880} - i(1.0)\omega} \qquad \text{(Eq. 4.2)}$$

For simplicity, this function will be used to represent both E_b and E_s.

The path transfer function W_b and W_s are those described in Eq. 1.13. The parametric values are listed in Table 4.1.

For the X_b's one layer site amplification models based on the site conditions at Holiday Inn and Bank of

---

*See Brigham (1974), page 27 for the description of this function.

STATIONS	1	2
r_b	23.4	39.5
r_s	6.0	24.0
Q_b	100	100
Q_s	100	100
V_b	3.4	3.4
V_s	3.2	3.2

Table 4.1 Values of the Parameters Used in Designing W_b and W_s

California are used for station #1 and Station #2, respectively. The two models are illustrated in Fig. 4.1.

The transfer functions R_b, R_s and X_s are set at unity in the analysis.

Using the above functions, the separate spectra of body and surface waves and their combined spectra of total ground motion are calculated. These results are shown in Fig. 4.2.

These spectra provide the bases for the testing pursued in this chapter. The subsequent analyses will test the separation equations based on the test data provided above.

4.2 TESTING THE SEPARATION EQUATIONS

Before performing any parametric studies, the separation equations are tested to check for their validity. Using the unaltered transfer functions created above, the two ground motions were separated to obtain their body and surface wave parts. The results obtained are exact. These results are not presented here since they resemble the original spectra shown in Fig. 4.2 exactly. This test indicates that the separation equation proposed in Sec. 2.2 is valid.

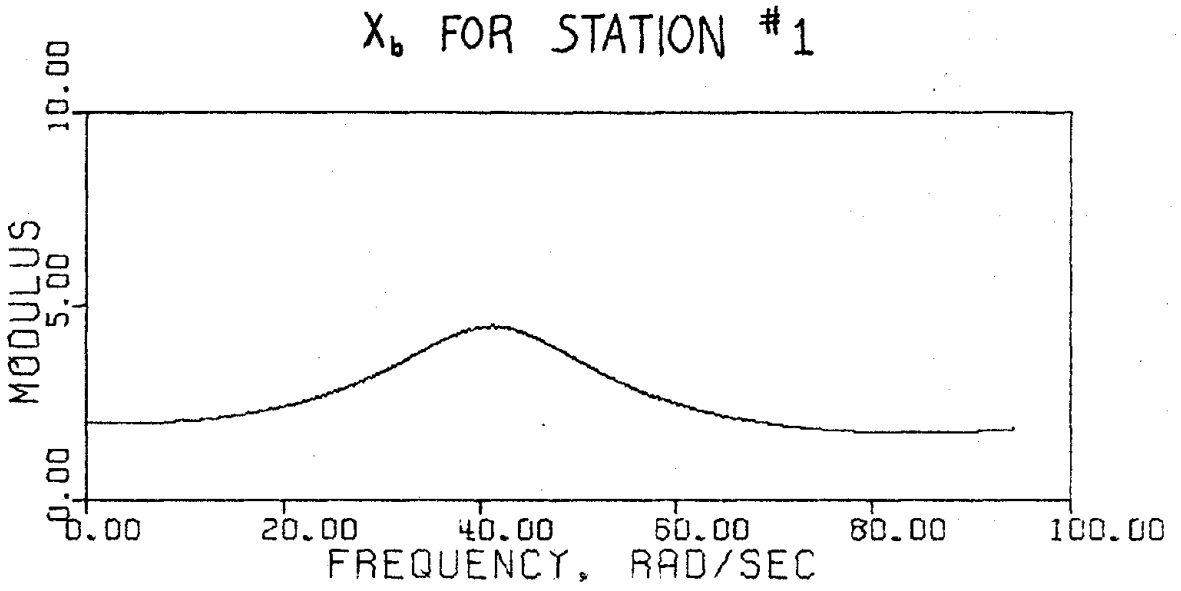

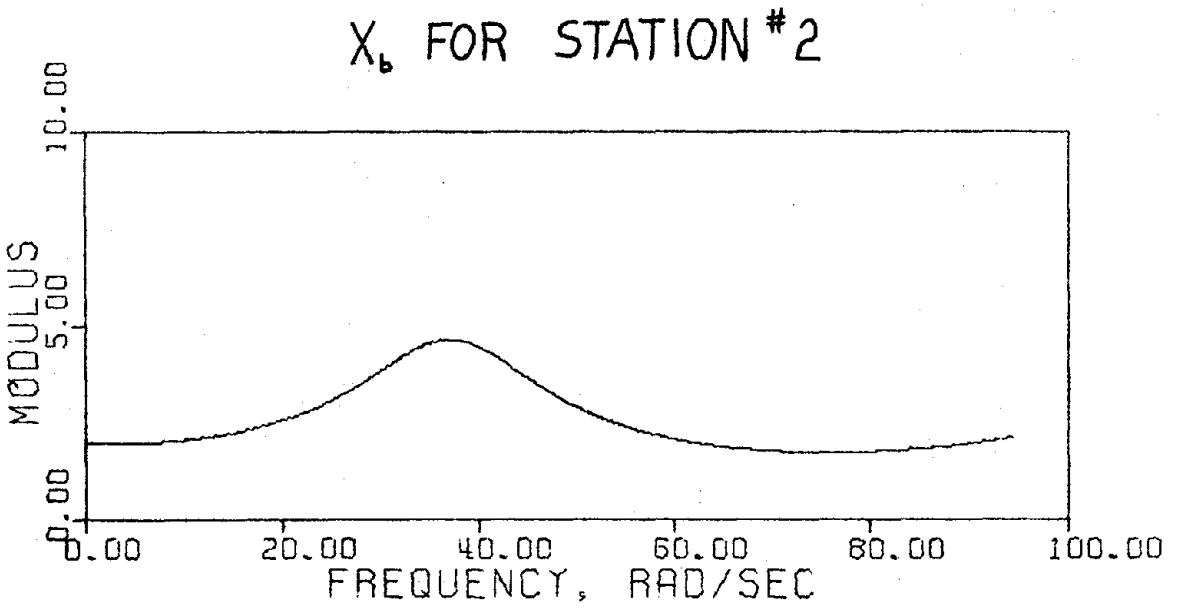

Fig. 4.1 One Layer Site Amplification Model

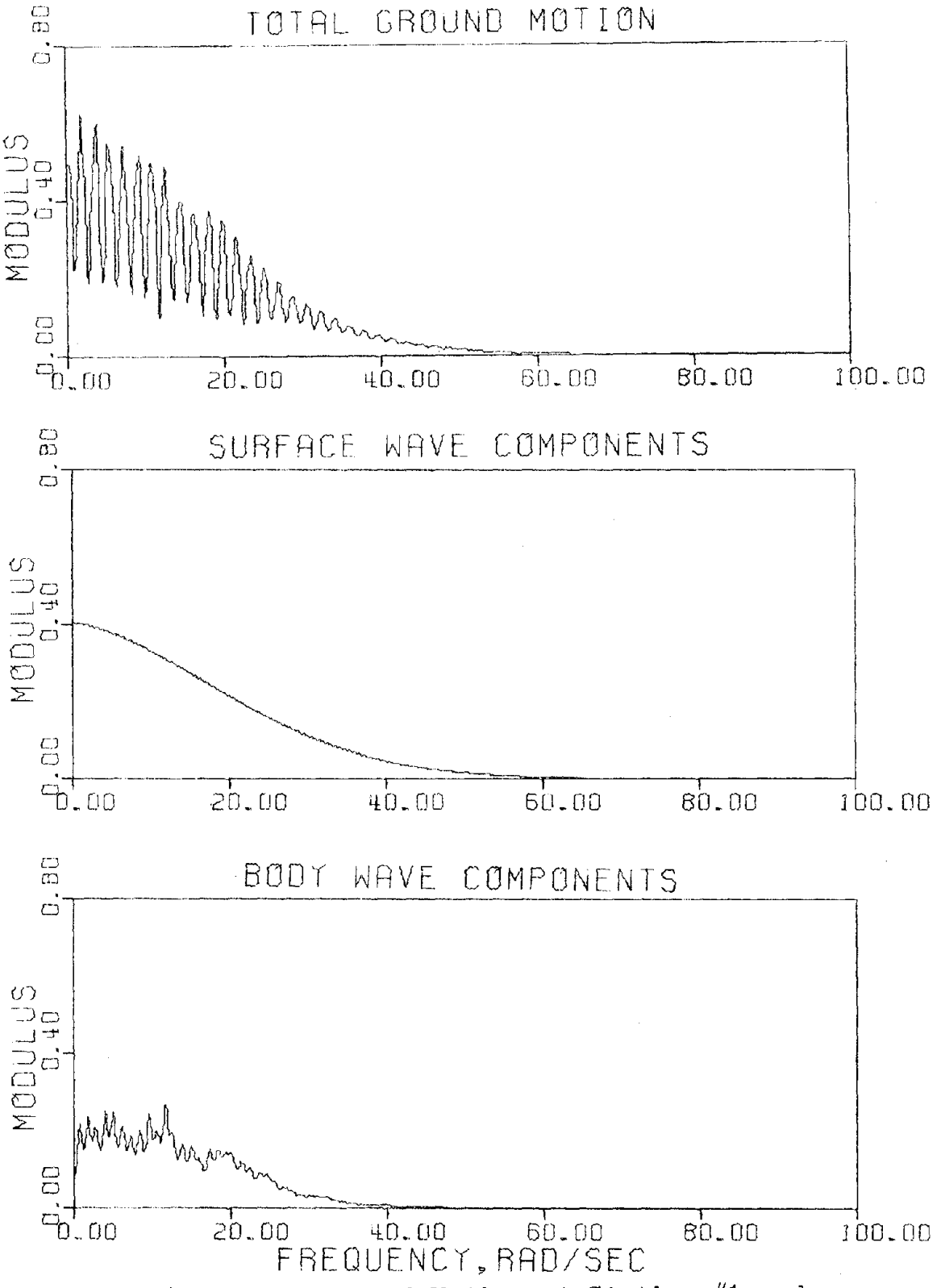

Fig. 4.2a The Ground Motion at Station #1 and Its Exact Surface and Body Wave Contents

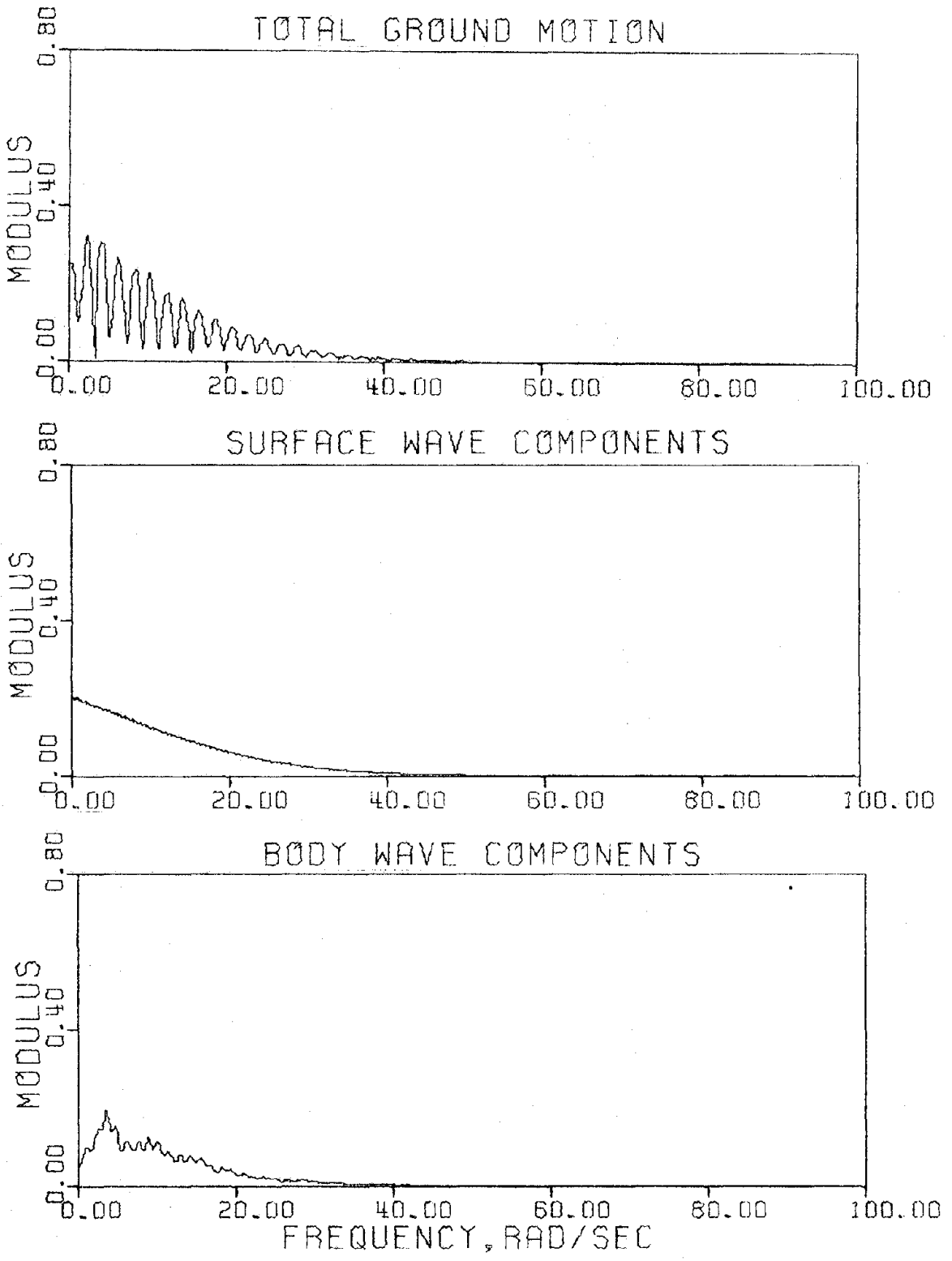

Fig. 4.2b The Ground Motion at Station #2 and Its Exact Surface and Body Wave Contents

4.3 PARAMETRIC STUDIES

Using the artificial model established in Sec. 4.1, three types of parametric studies are performed to test for the problem of spurious peaks.

The first study examines the effects on the separated body and surface waves due to variations on the epicentral distances. For this study, the epicentral distance of station #2 is altered both +2 units and also -2 units. Fig. 4.3 and 4.4 presents the resulting separated body and surface wave components along with the denominators N-M.

The second study examines the effects on the separated body and surface waves due to variations on the differences of arrival times for the two types of waves between the two stations. Fig. 4.5, 4.6 and 4.7 presents the resulting separated body and surface wave components along with their denominators, N-M, for the cases with the time delays for both waves increased 0.001, 0.01, and 0.1 units.

The third and the last study compares the significantness of the spurious peak problem for systems with different amounts of high frequency contents. To do this, three differnet source functions of the form shown in Eq. 4.3 below and in Fig. 4.8 are used to create the test data.

$$E_1 = e^{\frac{-\omega^2}{150} - i\omega}$$

$$E_2 = e^{\frac{-\omega^2}{880} - i\omega} \qquad \text{(Eq. 4.3)}$$

$$E_3 = e^{\frac{-\omega^2}{4400} - i\omega}$$

The procedure is same as those described in Sec. 4.1. Besides the source function, the system model remains the same. Note that the second source function, E_2, is the one used in the first two studies.

The two types of parametric studies used earlier are performed again with these three systems. The first study involves an increase of the epicentral distance of station #2 by 5 units. The second study has the station to station time lags for both the body waves and the surface waves increased by 0.01 units. The exact results and the results with the two testings are presented in Fig. 4.9 for the first source function, in Fig. 4.10 for the second source function, and in Fig. 4.11 for the third source function. And the denominators for all cases are presented along with the test results.

From the above three studies, a definite correspondence can be observed between the dips of the denominators, N-M, and the large peaks. Comparing the resulting

separated body and surface wave spectra from the parametric studies with the exact spectra, it becomes clear that these large peaks are definitely spurious. And for this reason, these peaks ought to be somehow avoided in order to improve the results obtained from the inaccurate models used in this analysis. In the next chapter, precedures will be presented to eliminate the spurious peaks.

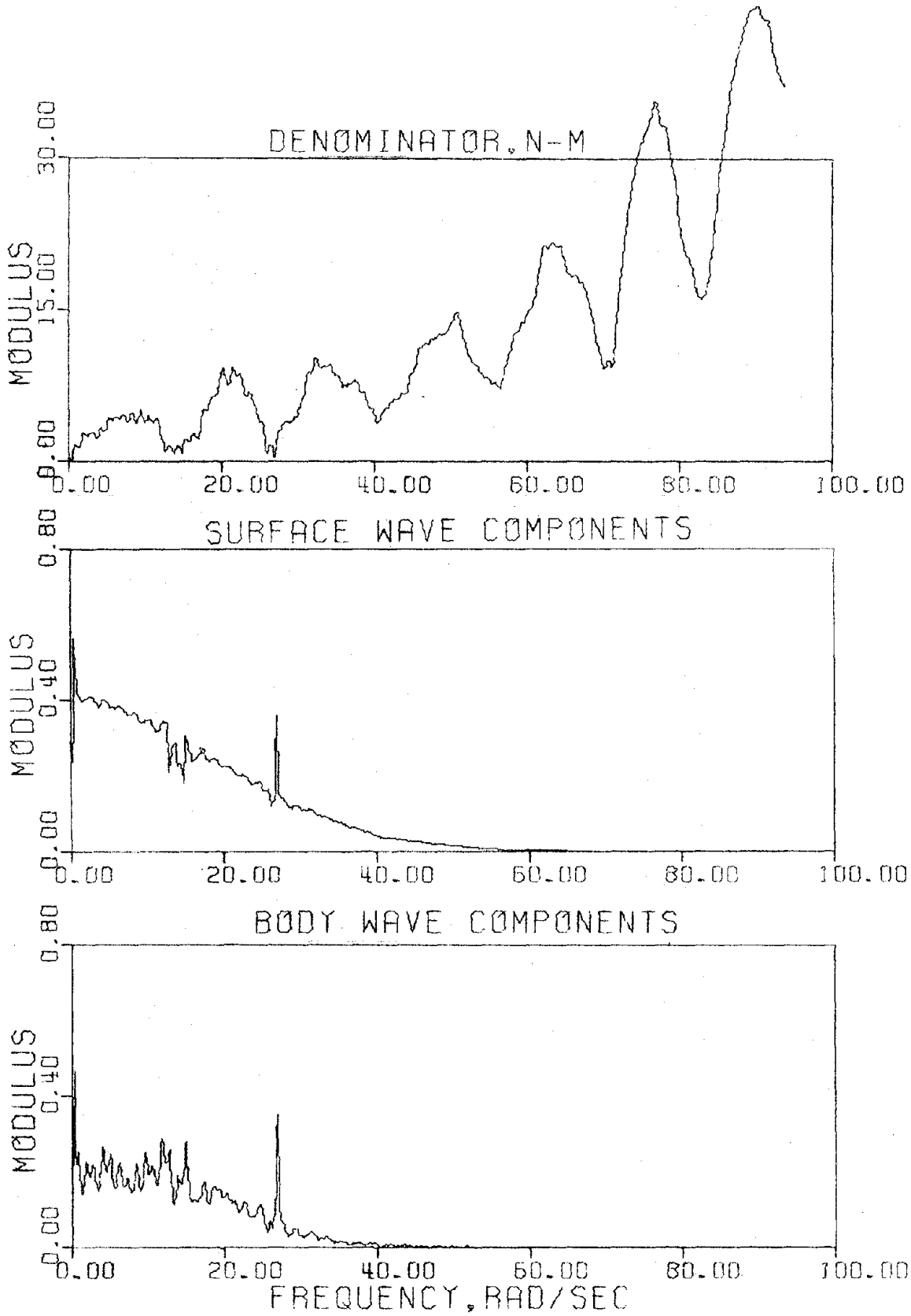

Fig. 4.3a The Denominator and The Resulting Surface and Body Waves at Station #1 With The Epicentral Distance of Station #2 Increased by 2 Units

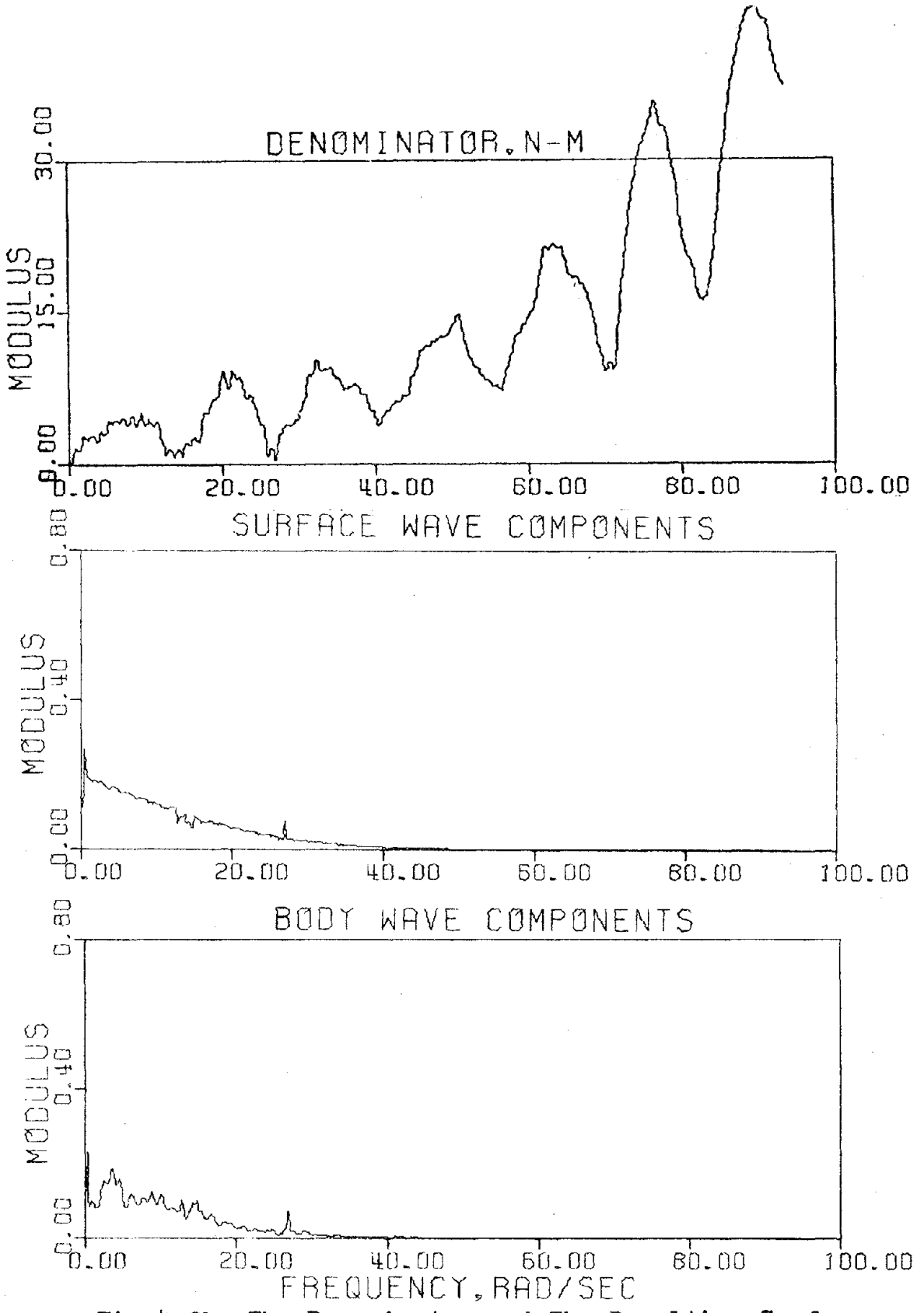

Fig 4.3b The Denominator and The Resulting Surface and Body Waves at Station #2 With The Epicentral Distance of Station #2 Increased by 2 Units

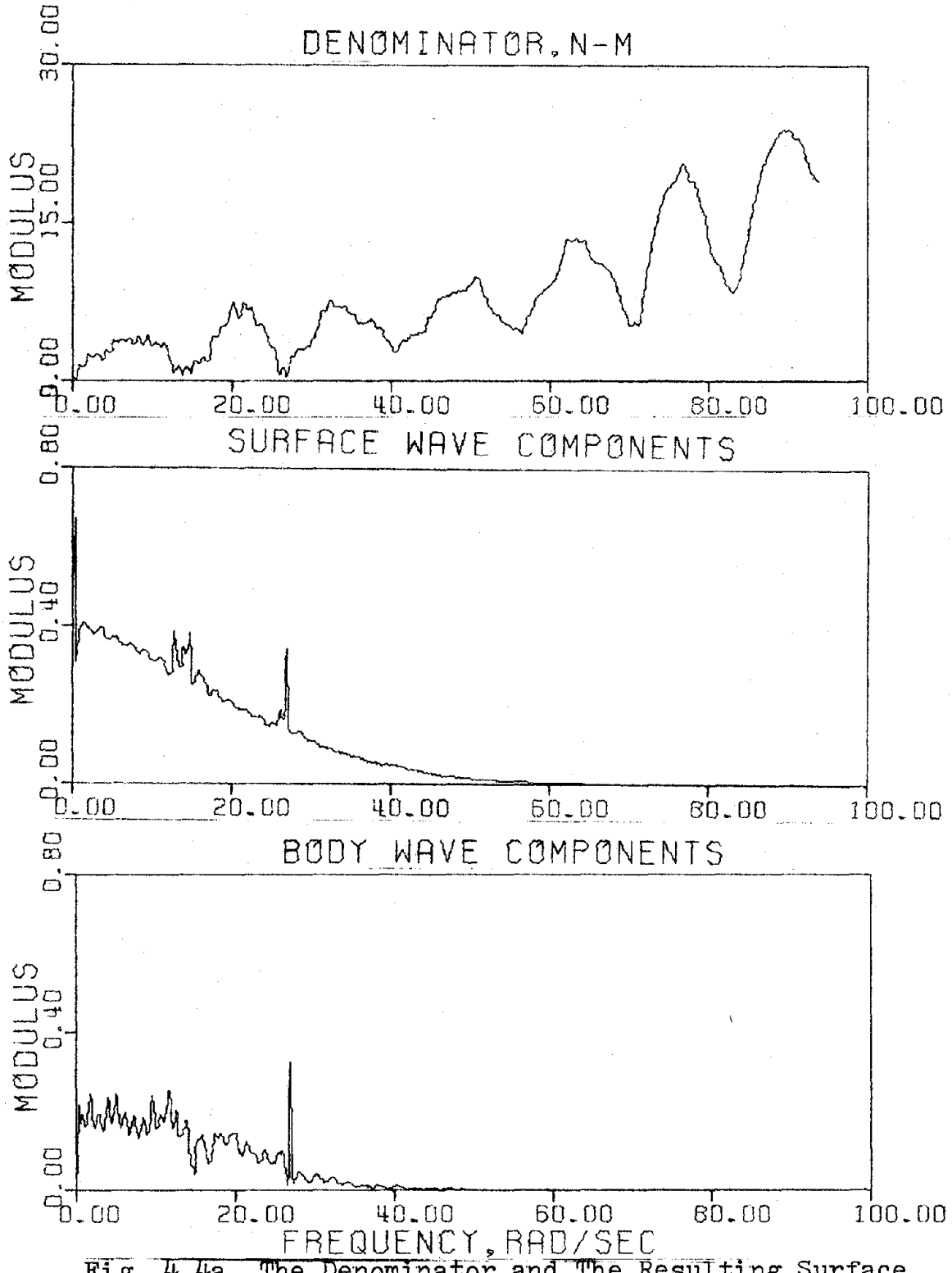

Fig. 4.4a The Denominator and The Resulting Surface and Body Waves at Station #1 With The Epicentral Distance of Station #2 Decreased by 2 Units

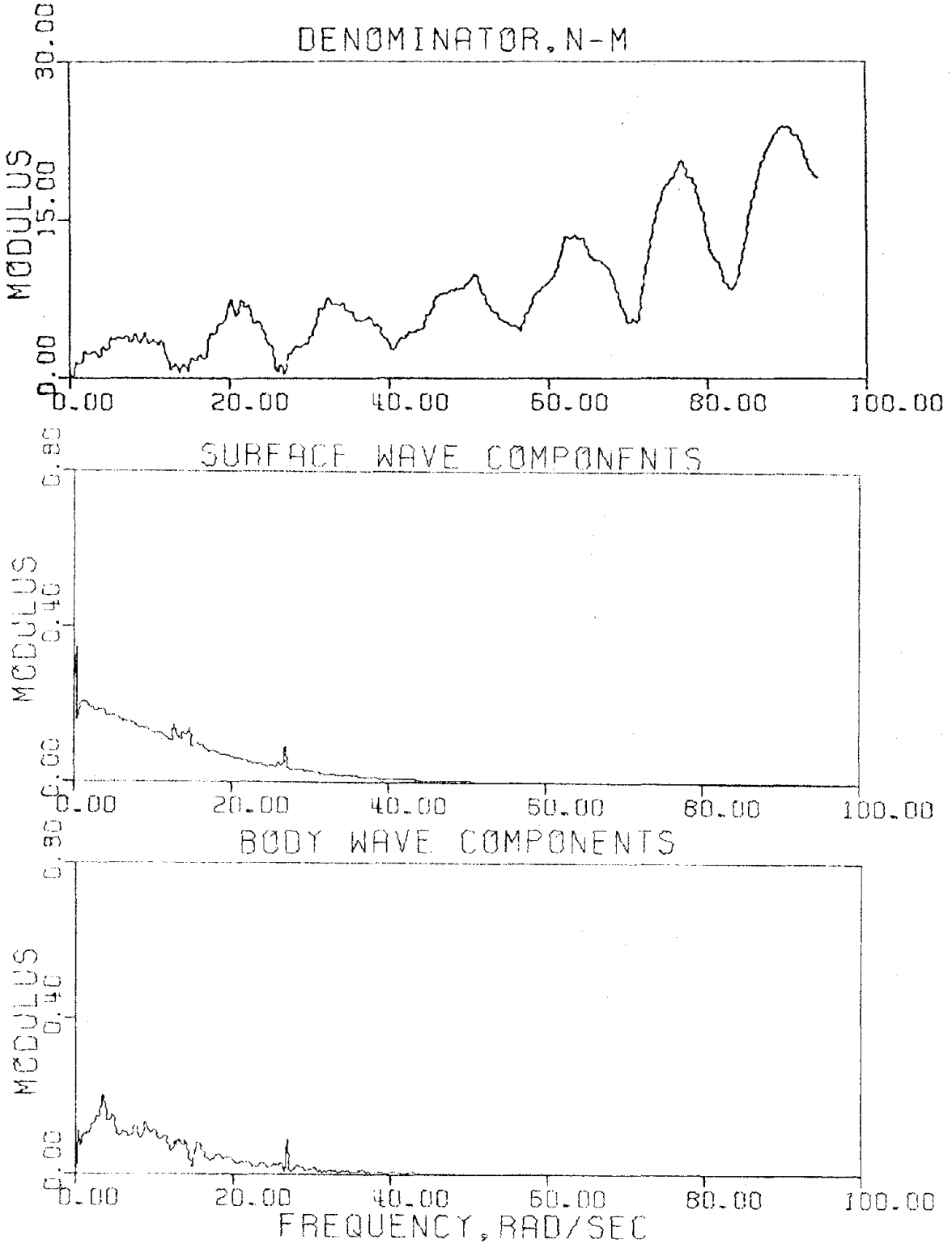

Fig. 4.4b The Denominator and The Resulting Surface and Body Waves at Station #2 With The Epicentral Distance of Station #2 Decreased by 2 Units

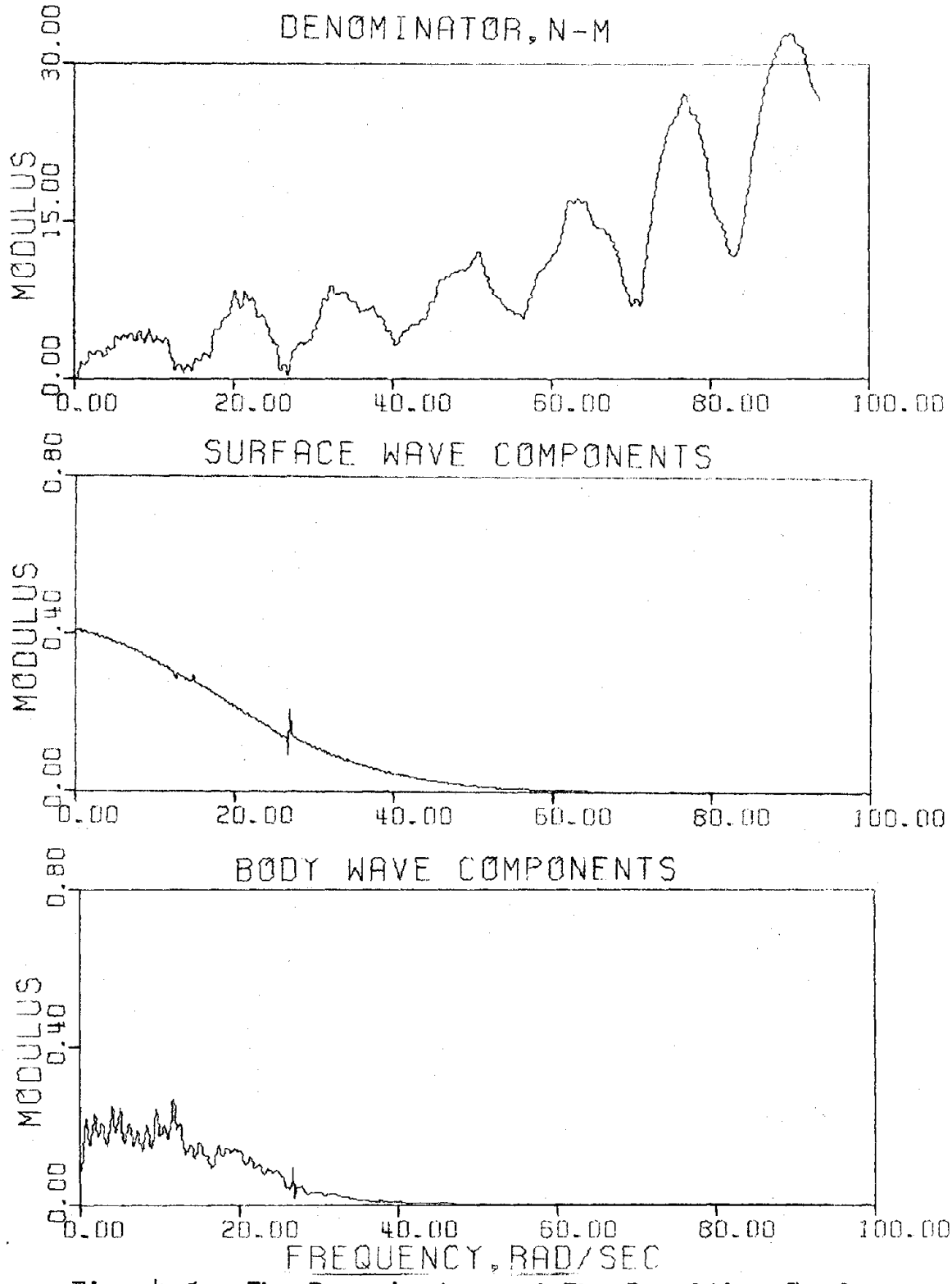

Fig. 4.5a The Denominator and The Resulting Surface and Body Waves for Station #1 With The Arrival Time Differences for Both Types of Waves Increased by 0.001 Unit

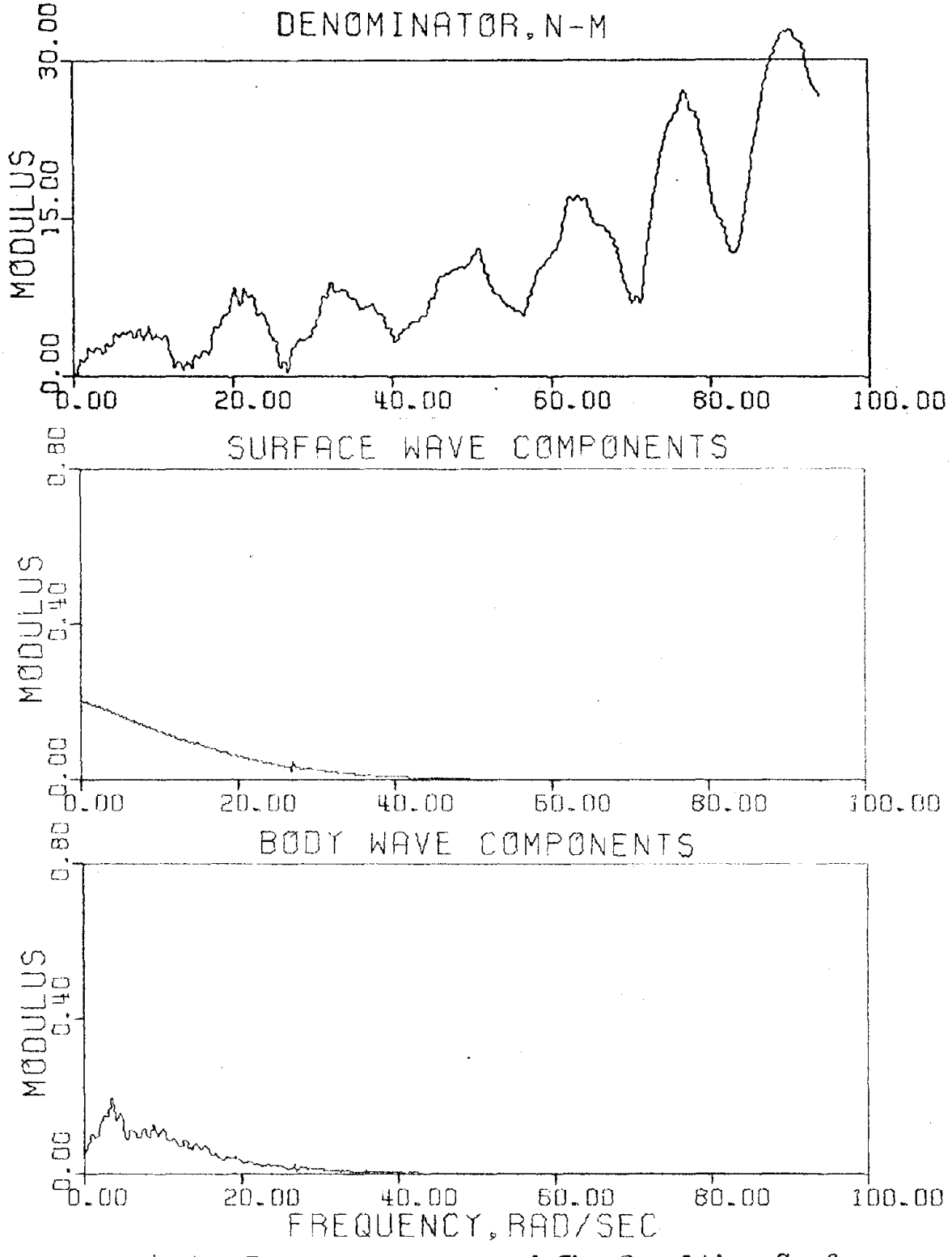

Fig. 4.5b The Denominator and The Resulting Surface and Body Waves for Station #2 With The Arrival Time Differences for Both Types of Waves Increased by 0.001 Unit

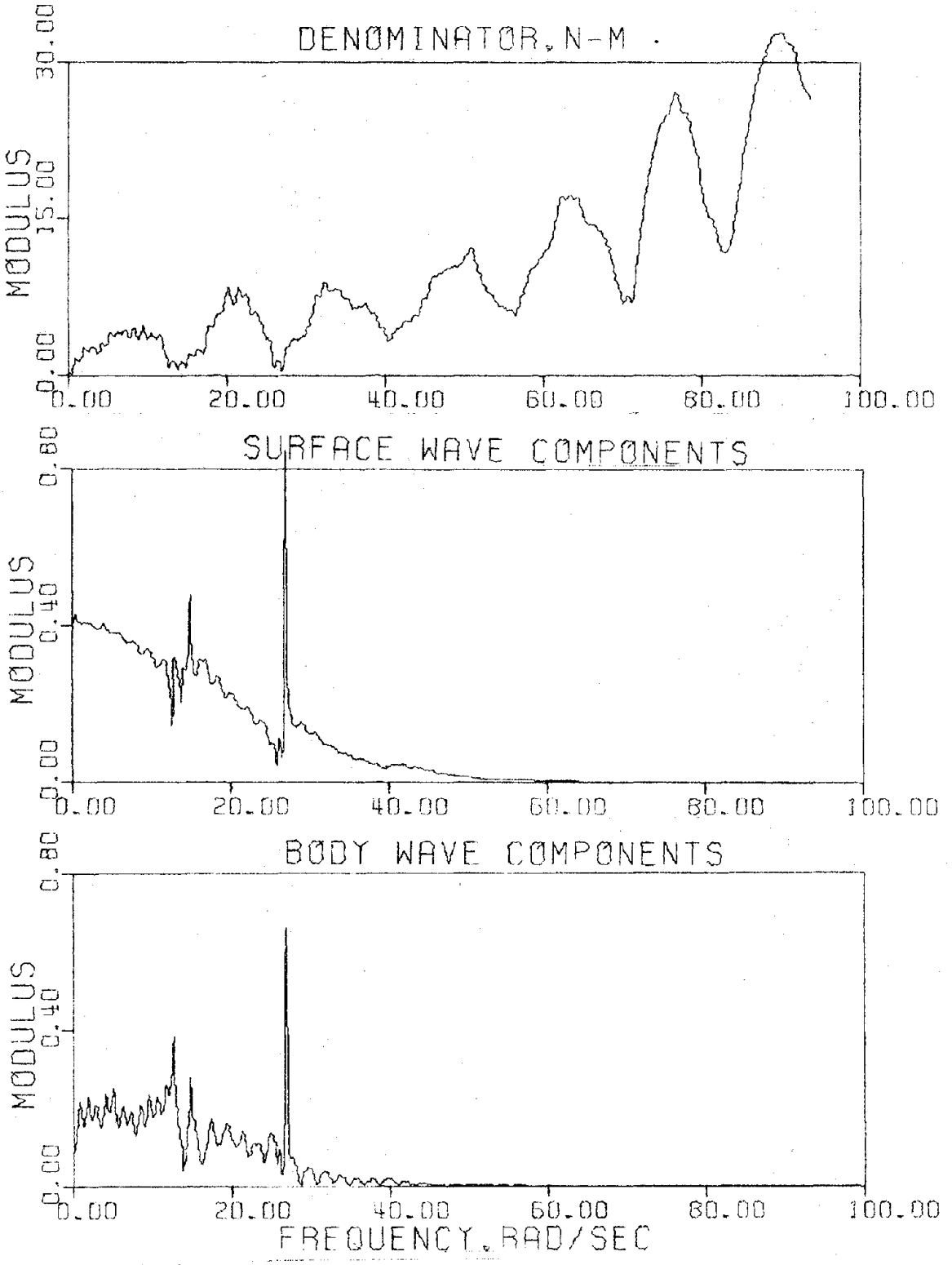

Fig. 4.6a The Denominator and The Resulting Surface and Body Waves for Station #1 With The Arrival Time Differences for Both Types of Waves Increased by 0.01 Unit

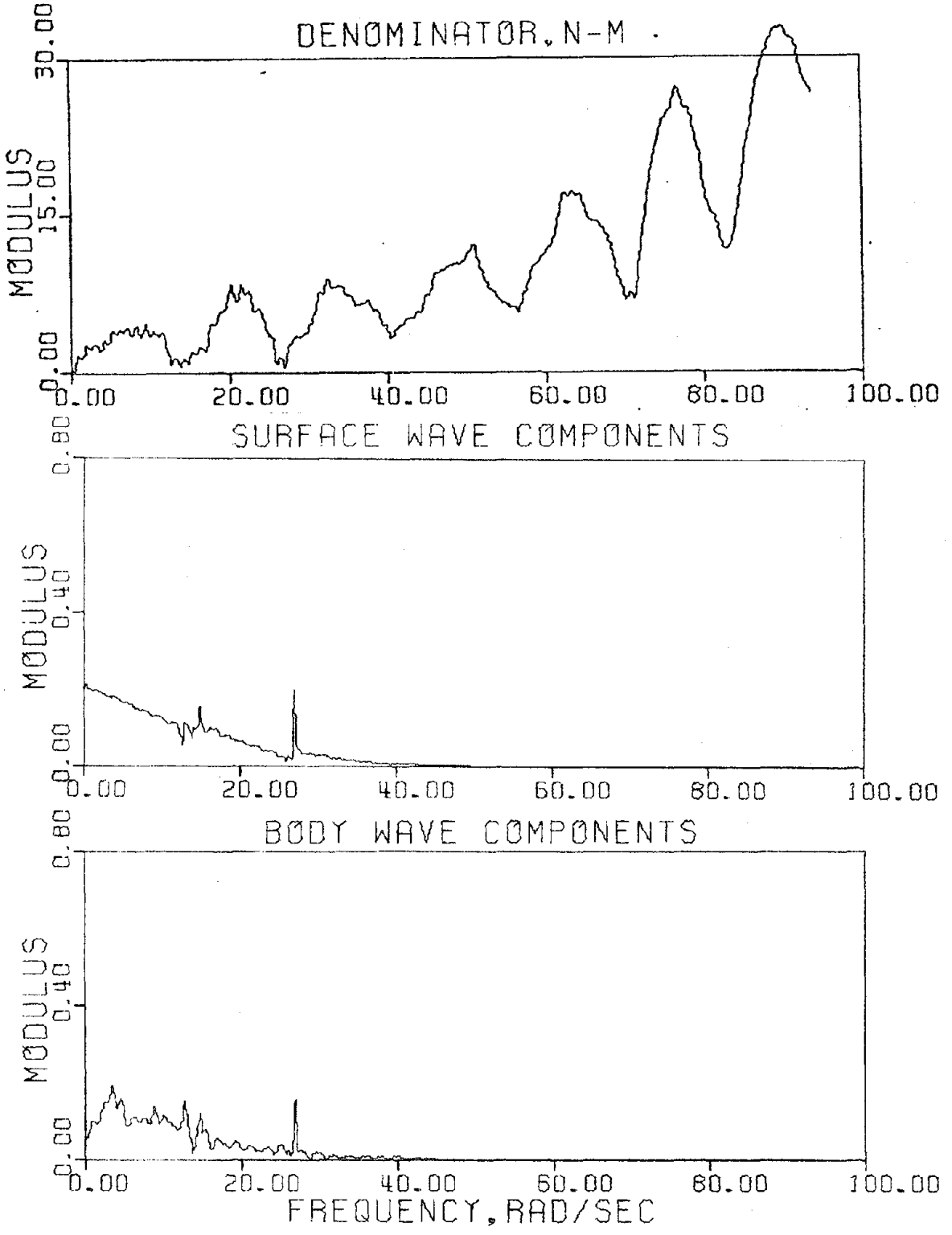

Fig. 4.6b The Denominator and The Resulting Surface and Body Waves for Station #2 With The Arrival Time Differences for Both Types of Waves Increased by 0.01 Unit

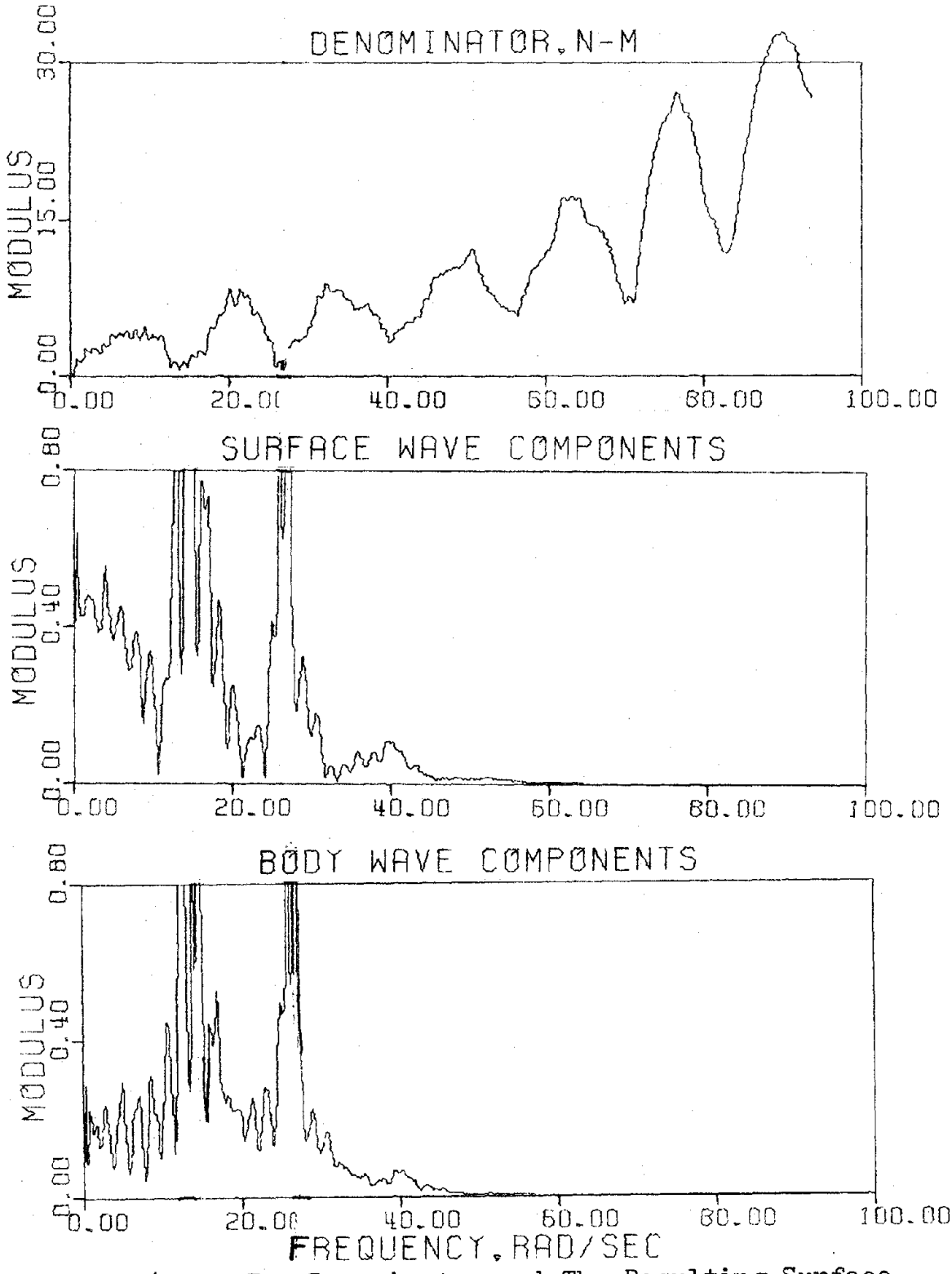

Fig. 4.7a The Denominator and The Resulting Surface and Body Waves for Station #1 With The Arrival Time Differences for Both Types of Waves Increased by 0.1 Unit

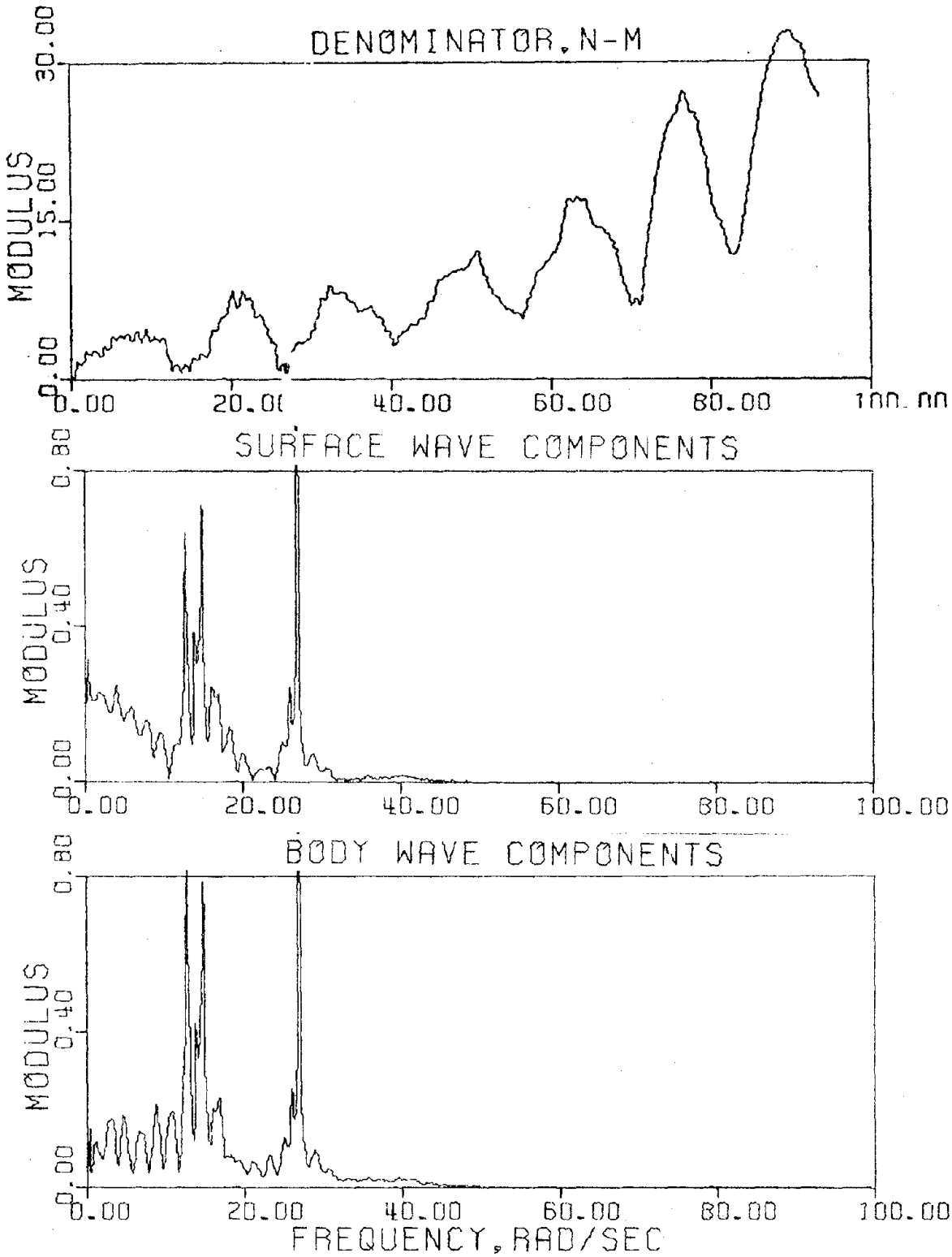

Fig. 4.7b The Denominator and The Resulting Surface and Body Waves for Station #2 With The Arrival Time Differences for Both Types of Waves Increased by 0.1 Unit

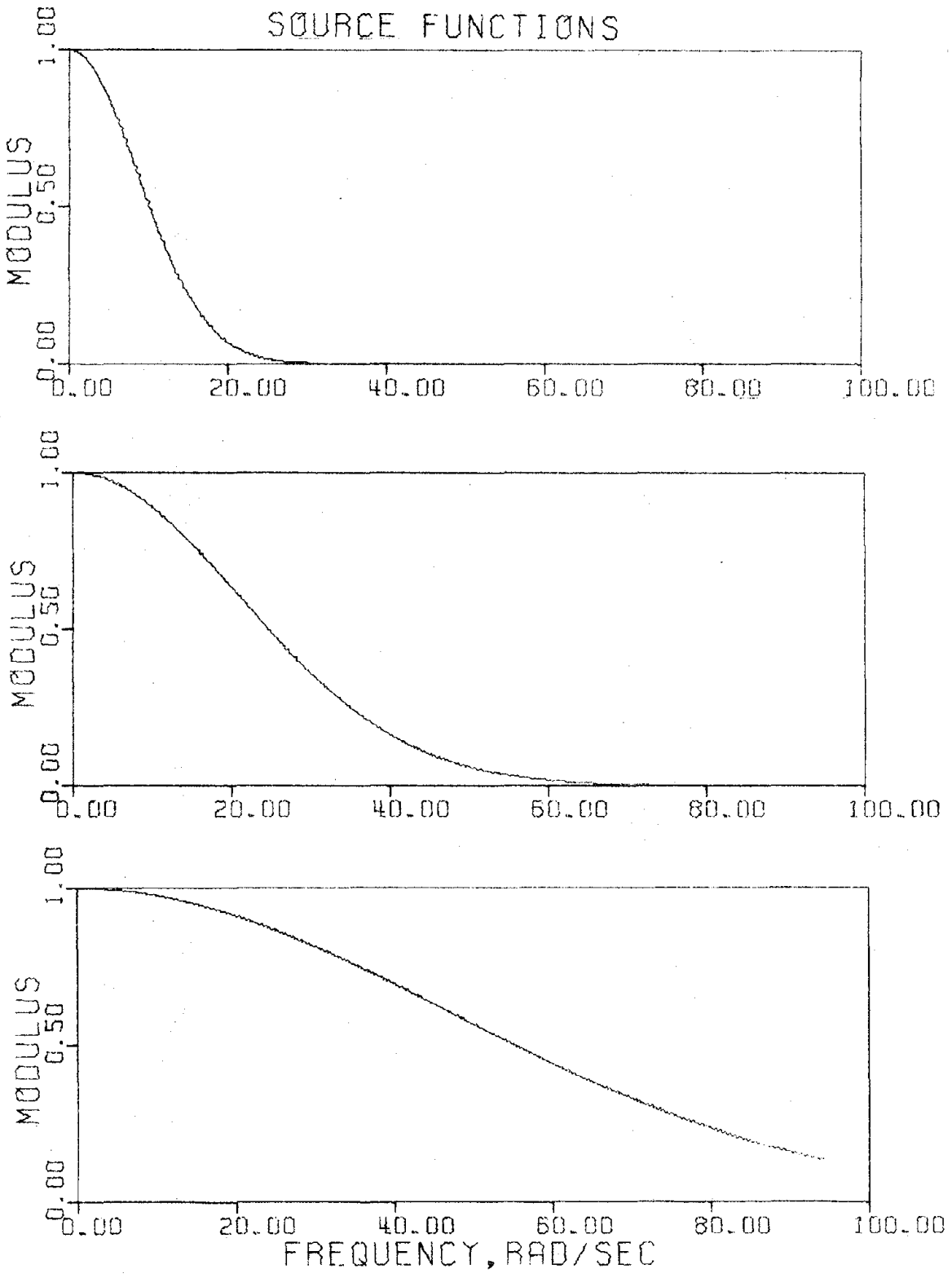

Fig. 4.8 Artificial Source Functions Used for the Third Study

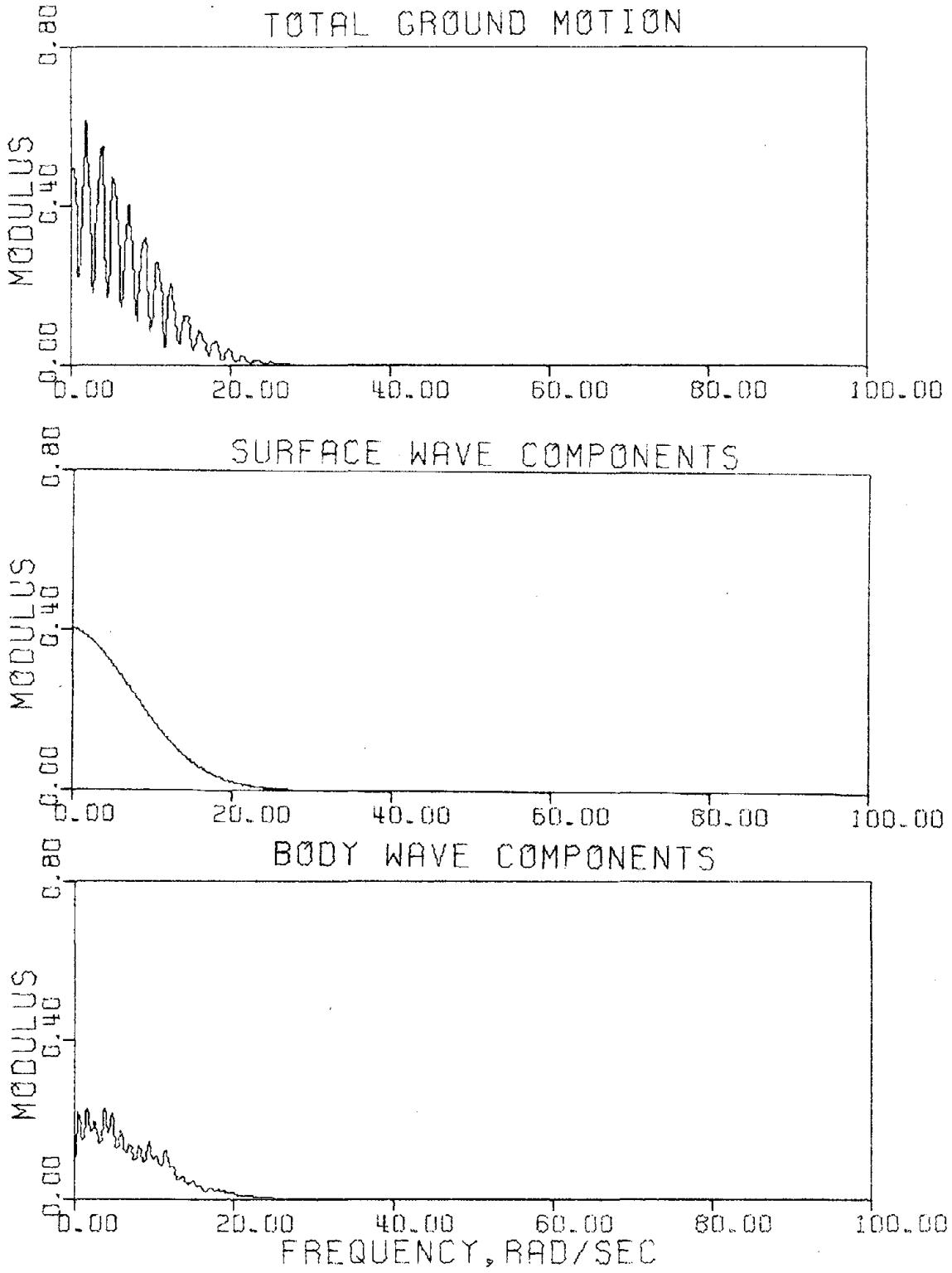

Fig. 4.9a The Ground Motion at Station #1 and Its Exact Surface and Body Wave Contents With Source Function E_1

Reproduced from best available copy.

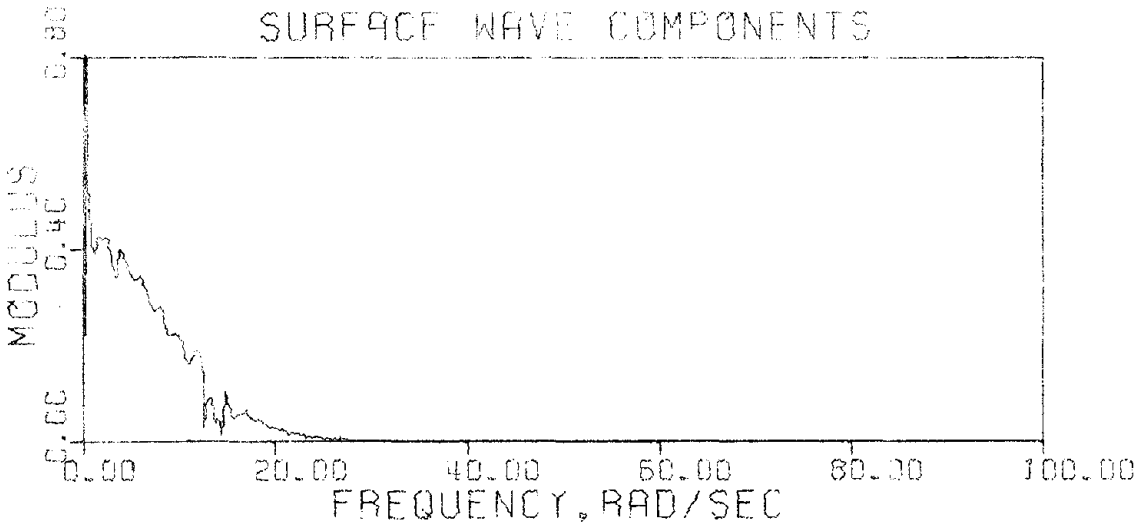

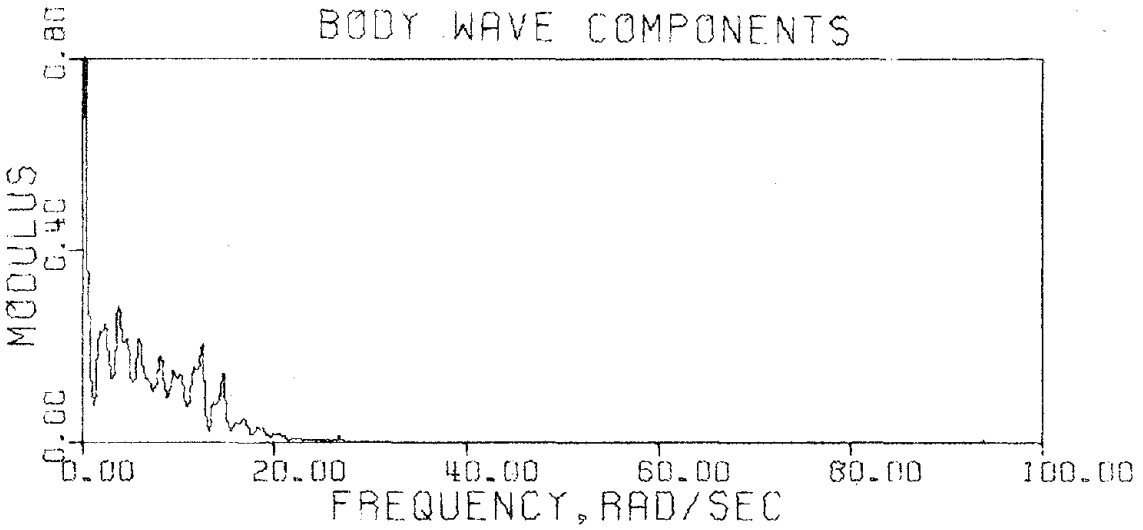

Fig. 4.9b Resulting Surface and Body Waves at Station #1 With Source Function E_1, And the Epicentral Distance of Station #2 Increased by 5 Units

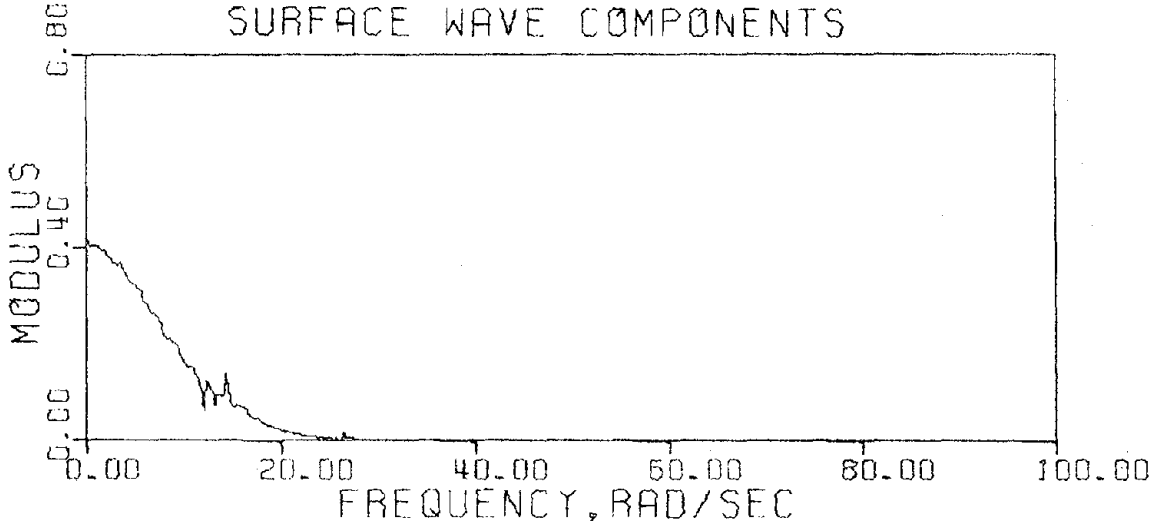

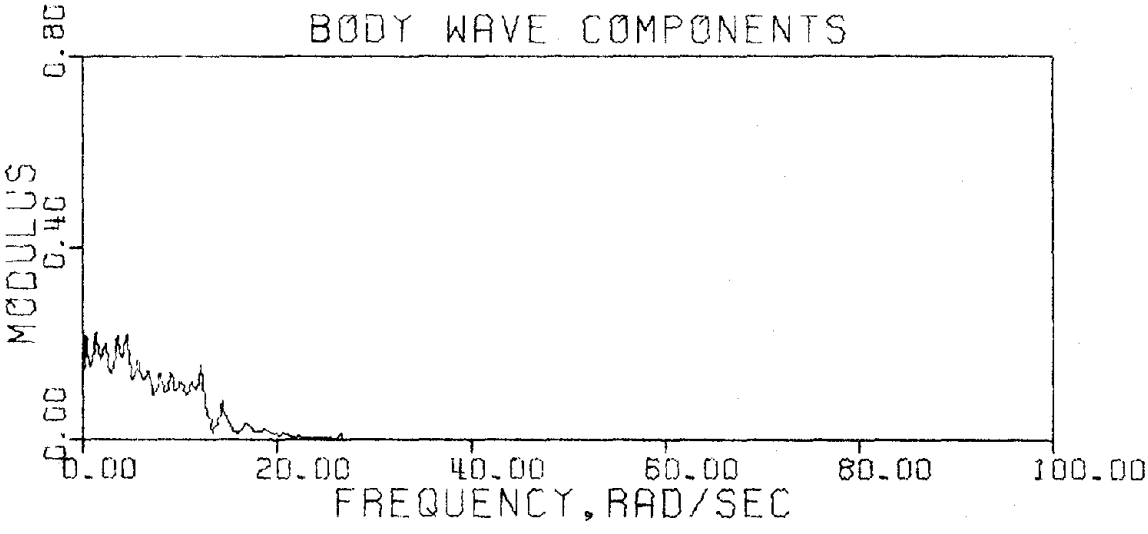

Fig. 4.9c Resulting Surface and Body Waves at Station #1 with Source Function E_1, And the Arrival Time Differences for both Types of Waves Increased by 0.01 Unit

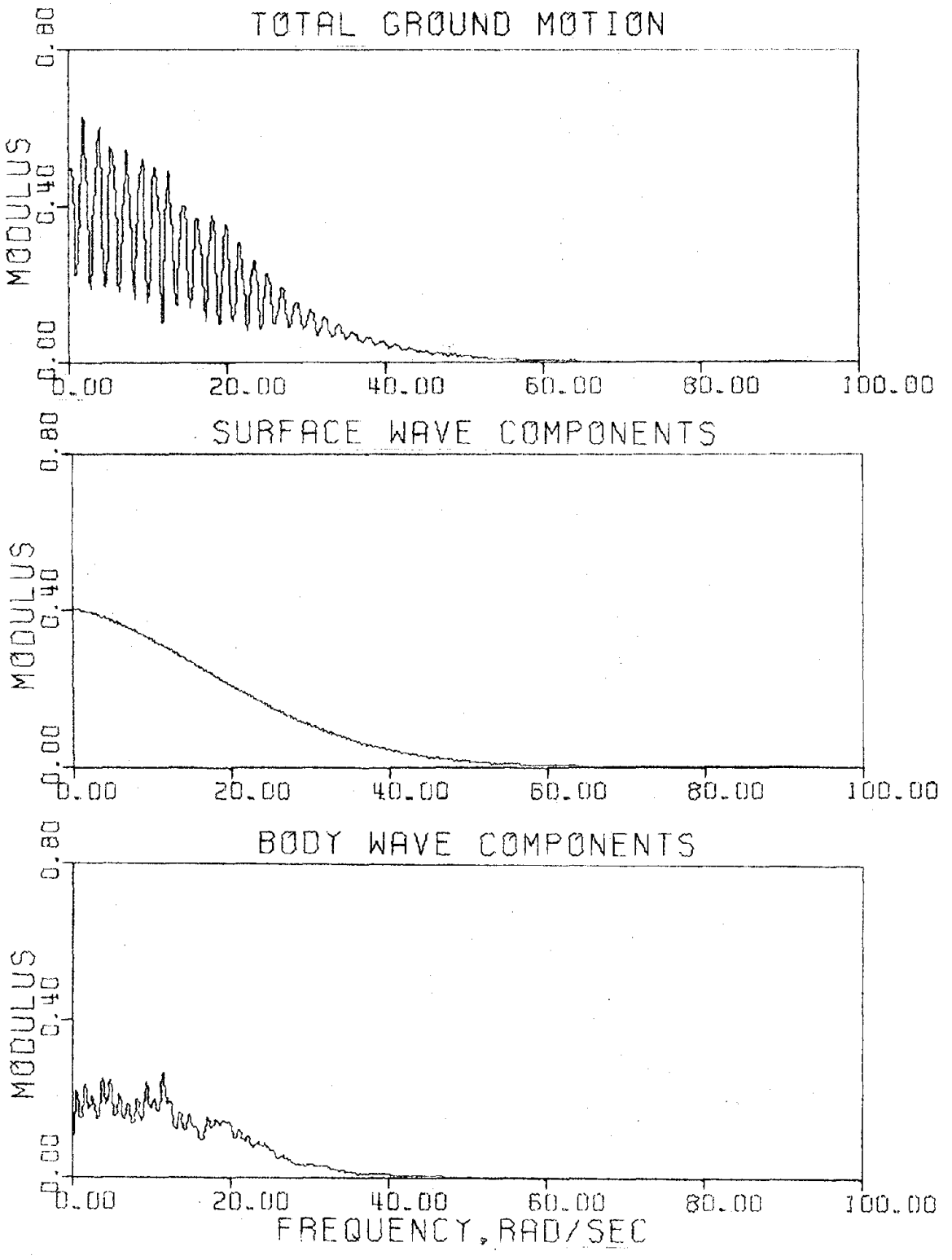

Fig. 4.10a The Ground Motion at Station #1 and Its Exact Surface and Body Wave Contents With Source Function E_2

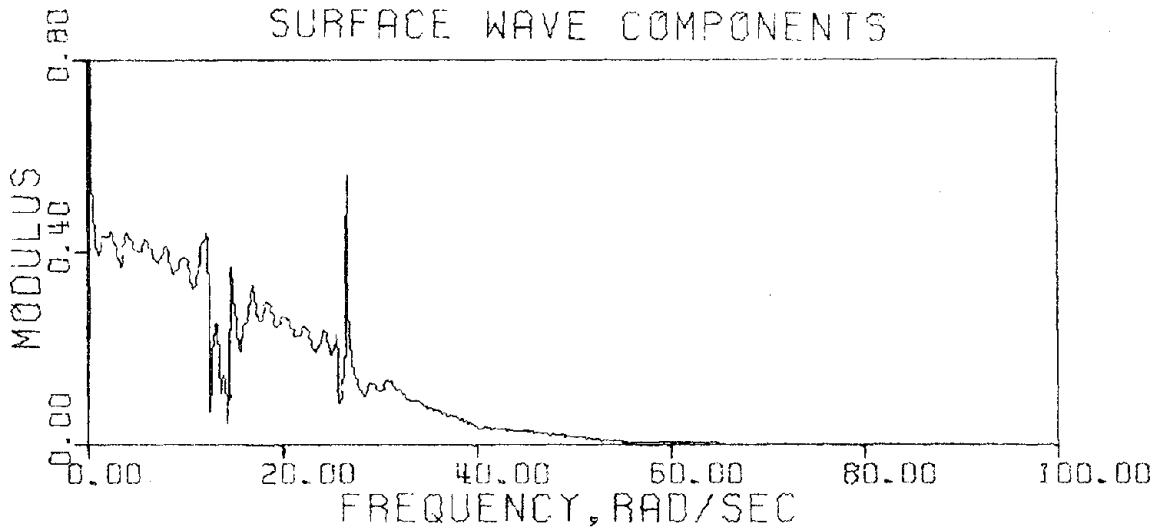

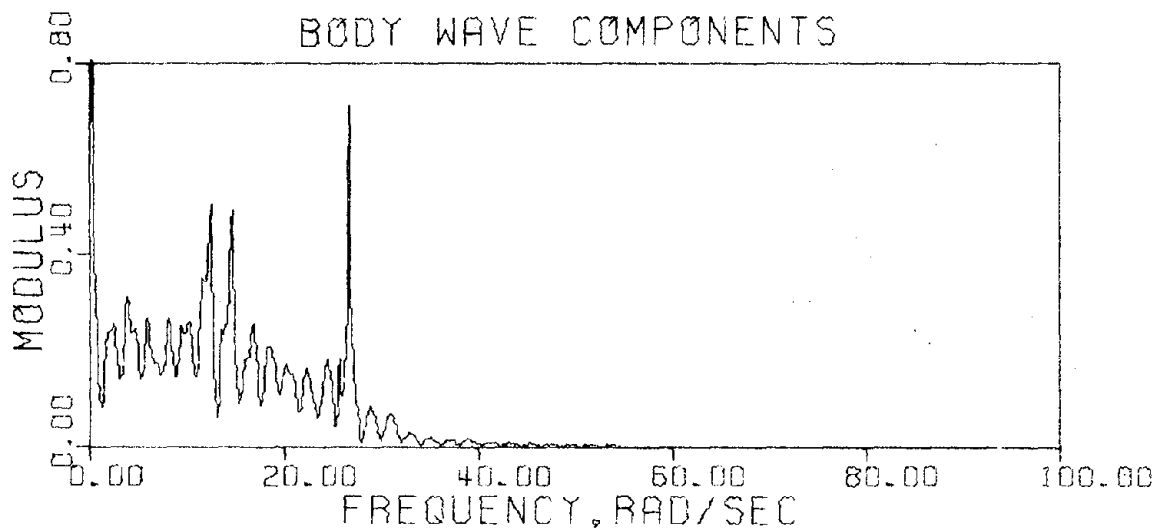

Fig. 4.10b Resulting Surface and Body Waves at Station #1 With Source Function E_2, And the Epicentral Distance of Station #2 Increased by 5 Units

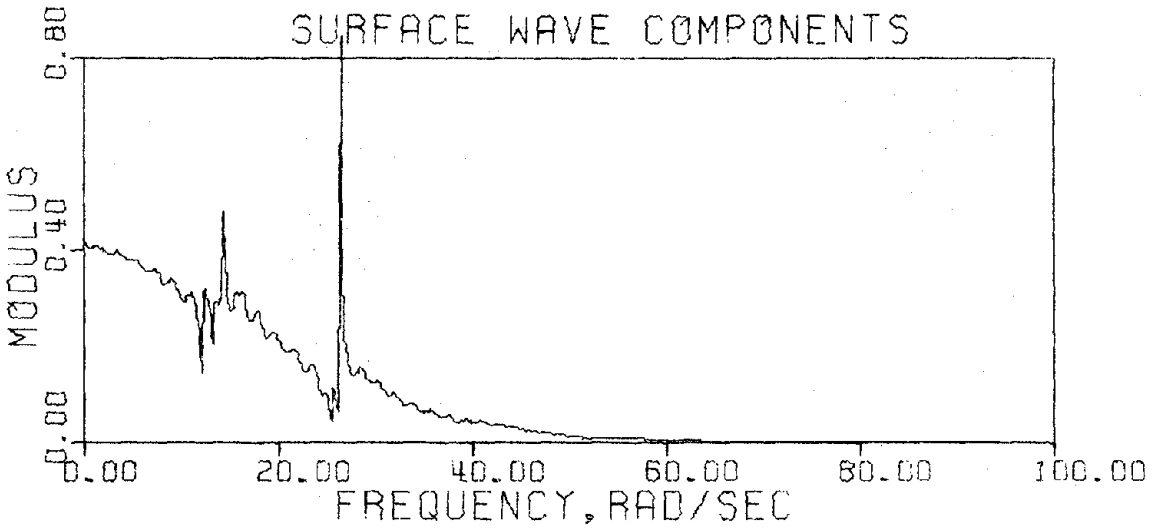

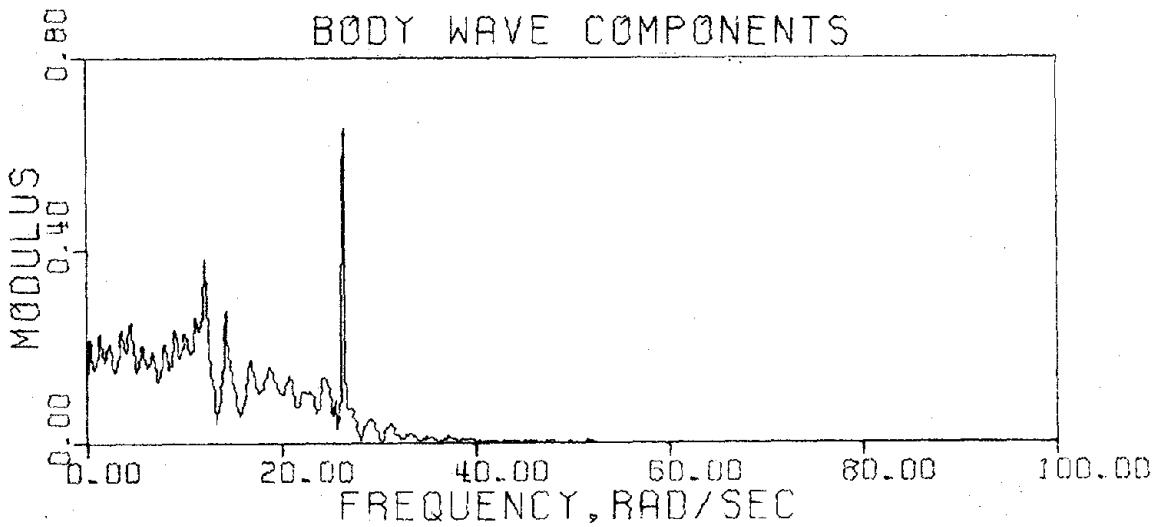

Fig. 4.10c Resulting Surface and Body Waves at Station #1 With Source Function E_2, And the Arrival Time Differences for both Types of Waves Increased by 0.01 Unit

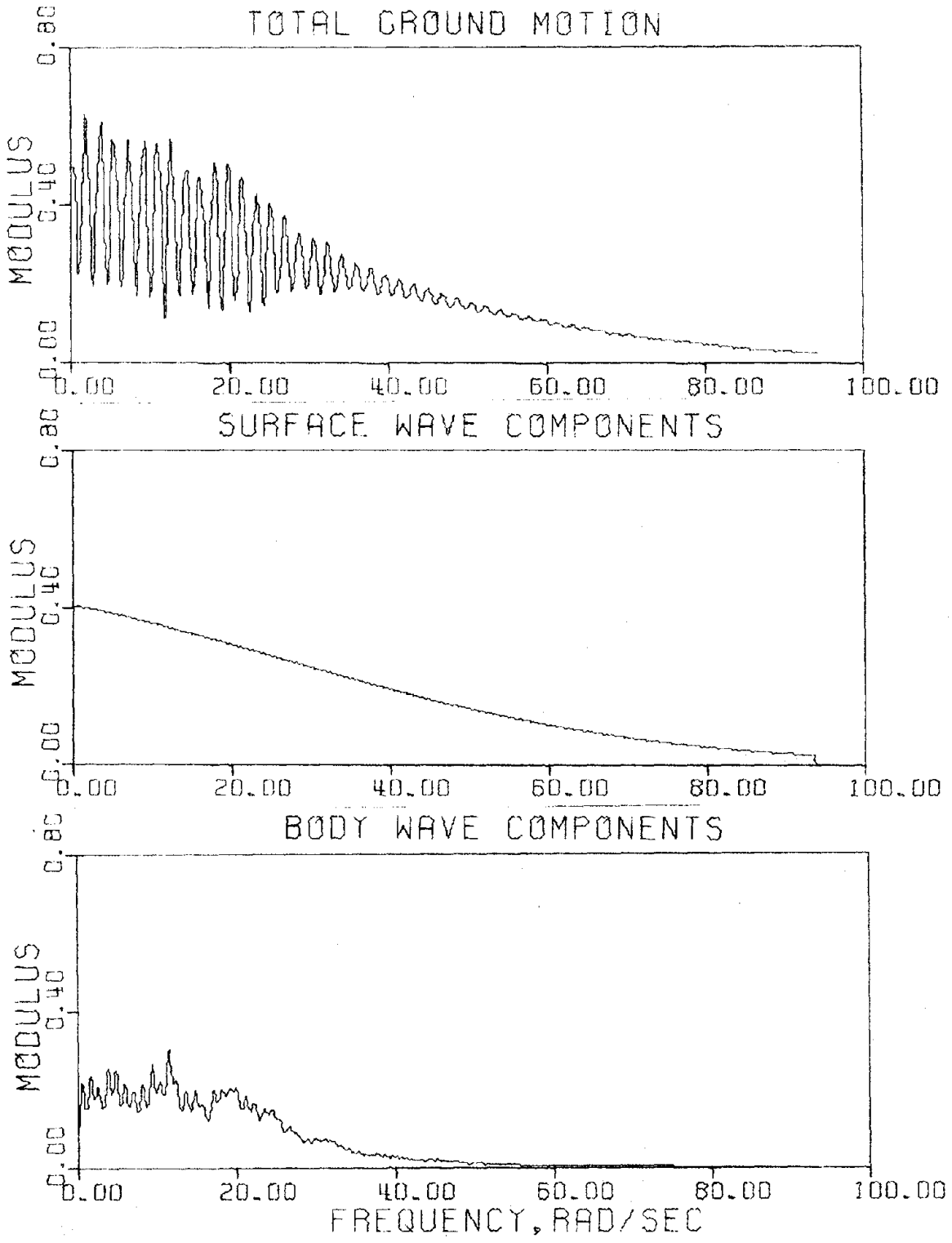

Fig. 4.11a The Ground Motion at Station #1 and Its Exact Surface and Body Wave Contents With Source Function E_3

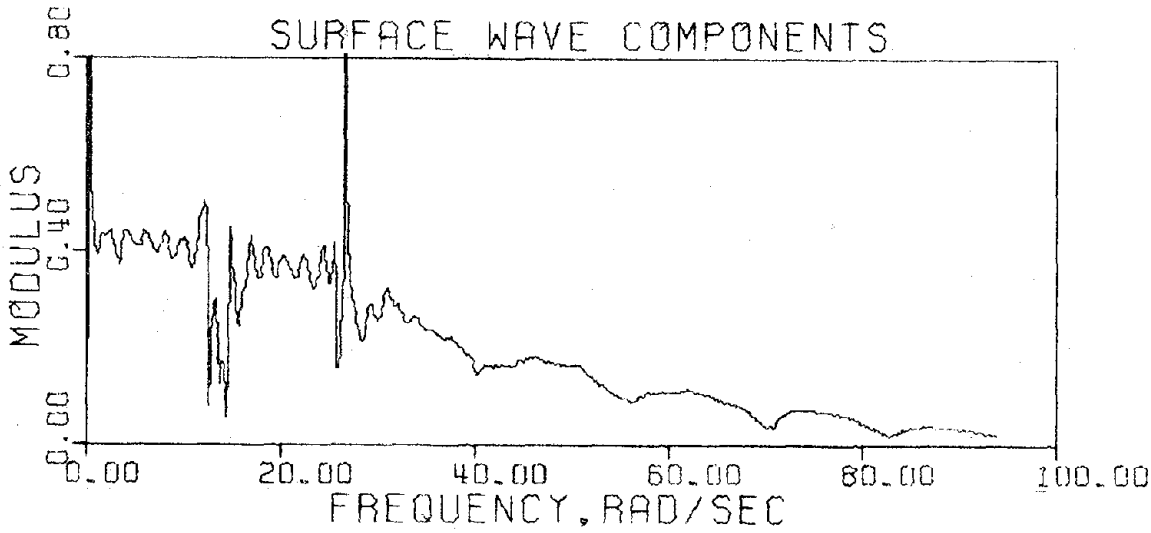

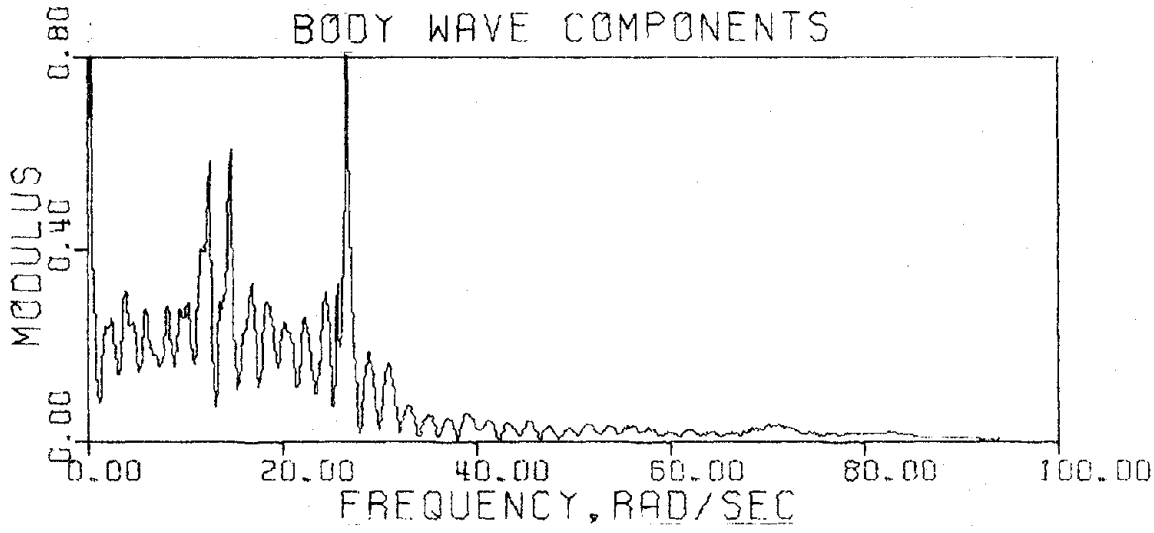

Fig. 4.11b Resulting Surface and Body Waves at Station #1 With Source Function E_3, And the Epicentral Distance of Station #2 Increased by 5 Units

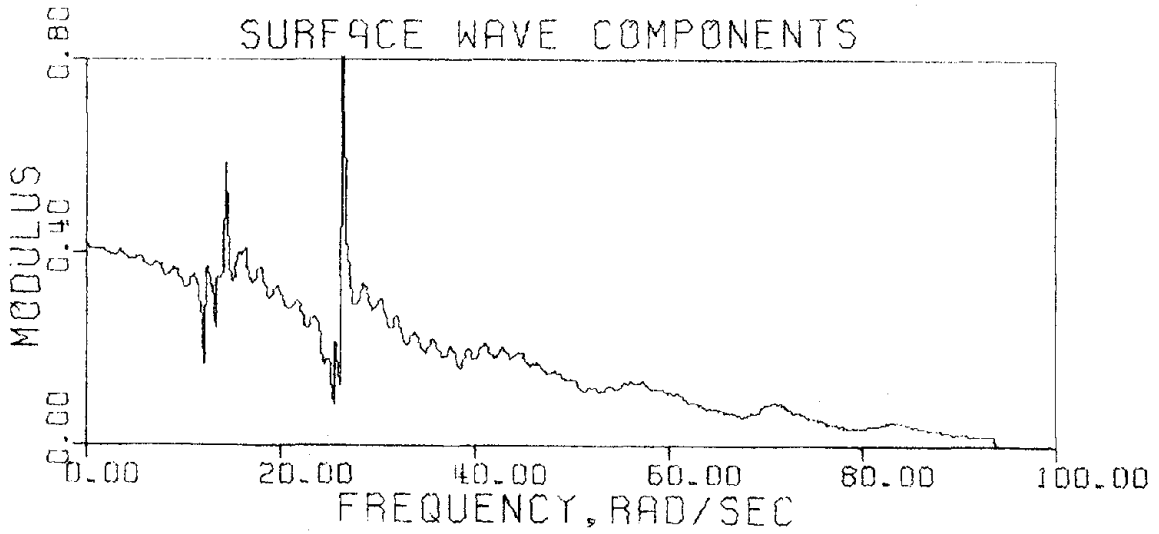

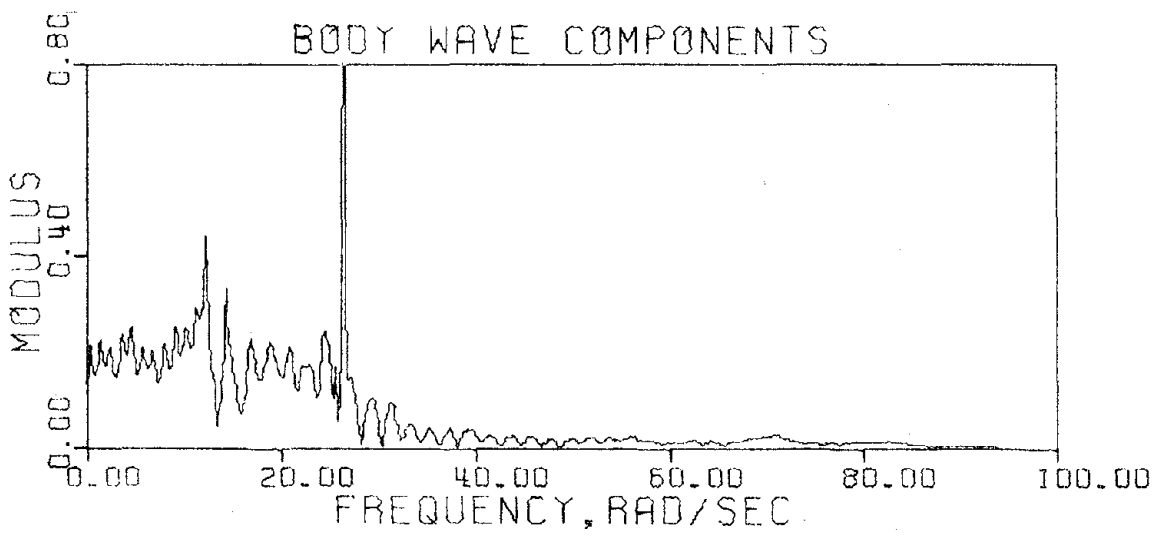

Fig. 4.11c Resulting Surface and Body Waves at Station #1 With Source Function E_3, And the Arrival Time Differences for both Types of Waves Increased by 0.01 Unit

CHAPTER 5

COMPUTATIONAL PROCEDURE

The preceeding chapter demonstrated that the spurious peaks are indeed false information. These peaks were due to errors introduced by the computational procedure. In this chapter, four methods are introduced for the purpose of eliminating the spurious peaks from the separated body and surface wave spectra. The station pair, Orion and Ventura are used for a majority of the studies presented in this chapter. The results obtained should be compared with Figs. 3.8b and 3.8e.

5.1 METHOD A: A ROUGH TREATMENT

One of the simplest ways to treat the spurious peaks is to cut them off from the spectrum at an arbitrary level. This method, although crude, does serve the purpose of producing "believable" inverse transform. However, the reliability of this procedure is quite poor, because there is no predetermined rule on the level of amplitude where the spurious peaks should be cut off. For this reason, no effort will be attempted in this thesis to treat any of the results using this method.

5.2 METHOD B: SMOOTHING

Spectra with large fluctuations of peaks and valleys have often been smoothed for various purposes. In the problem of avoiding spurious peaks from divisions of two spectra, both Båth (1974) and Dobry (1971) have recommended that the numerator and the denominator be pre-smoothed in an amount determined by trial and error.

In this section, the same procedure will be attempted on the separation equations given in Eq. 2.5, where the numerators (NG_2-G_1), $M(NG_2-G_1)$, (G_1-MG_2), and $N(G_1-MG_2)$, and the denominator, $(N-M)$, will all be smoothed before dividing. A smoothing algorithm which smoothes complex spectra with a triangular function was developed for this purpose*. By trial and error, it was found that the best scheme is to use 7 weights on the triangular function and to smooth both the numerator and denominator twice. The resulting surface wave and body wave contents for the Orion and Ventura pair are presented in Fig 5.1 through 5.4 along with their numerators, denominators and inverse transforms.

---

*See Appendix B, Program #3, Subroutine CMOOTH.

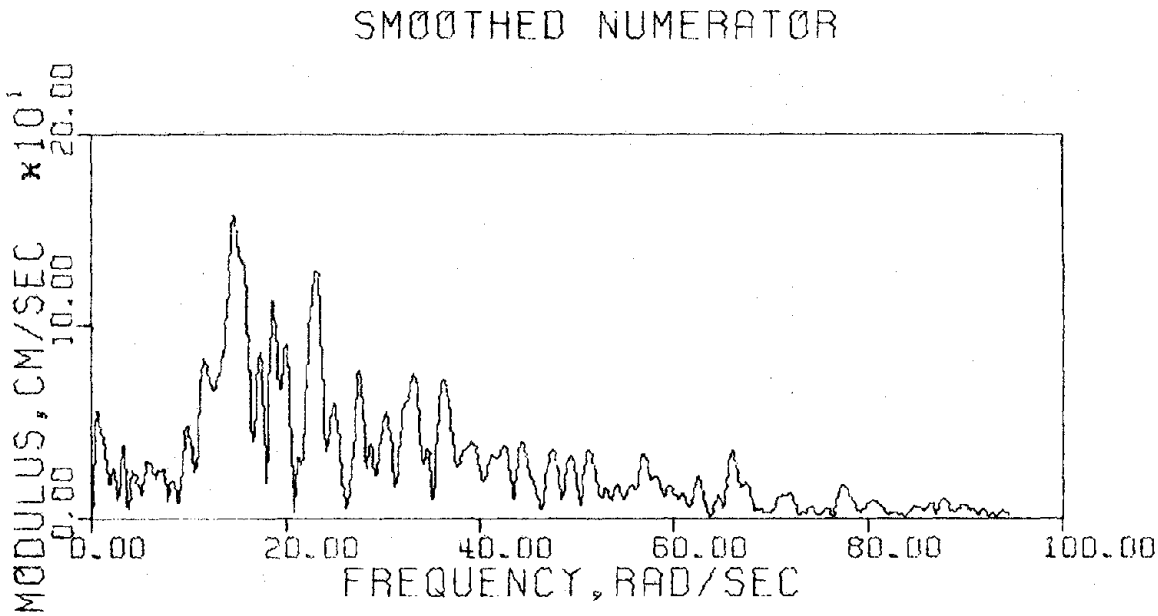

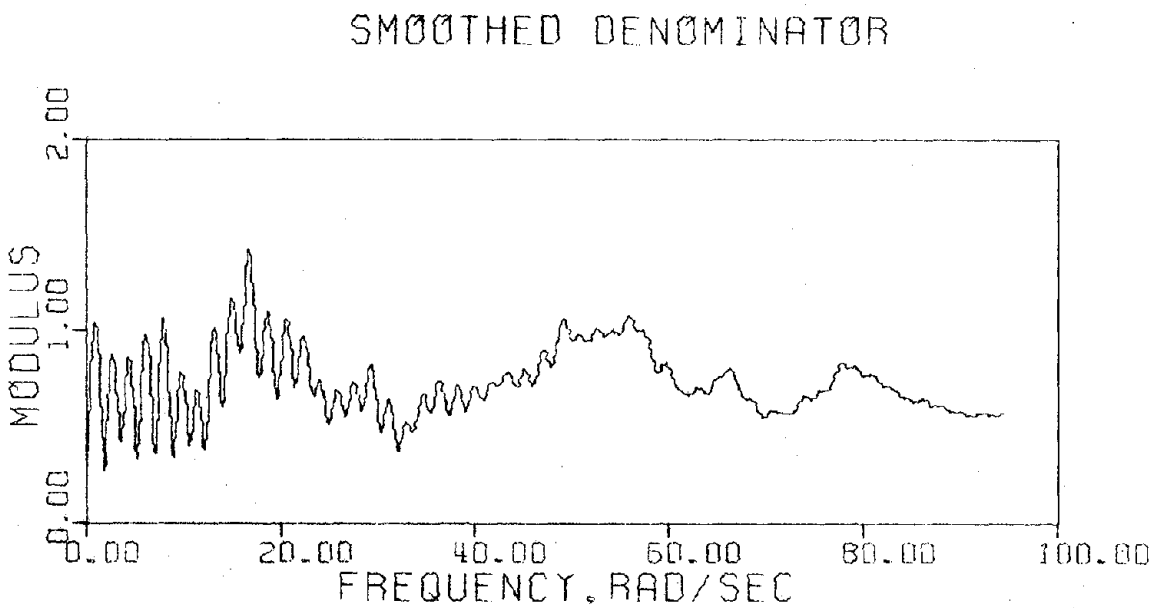

Fig. 5.1a Smoothed Numerator and Denominator for Surface Waves at Orion, Orion and Ventura Pair

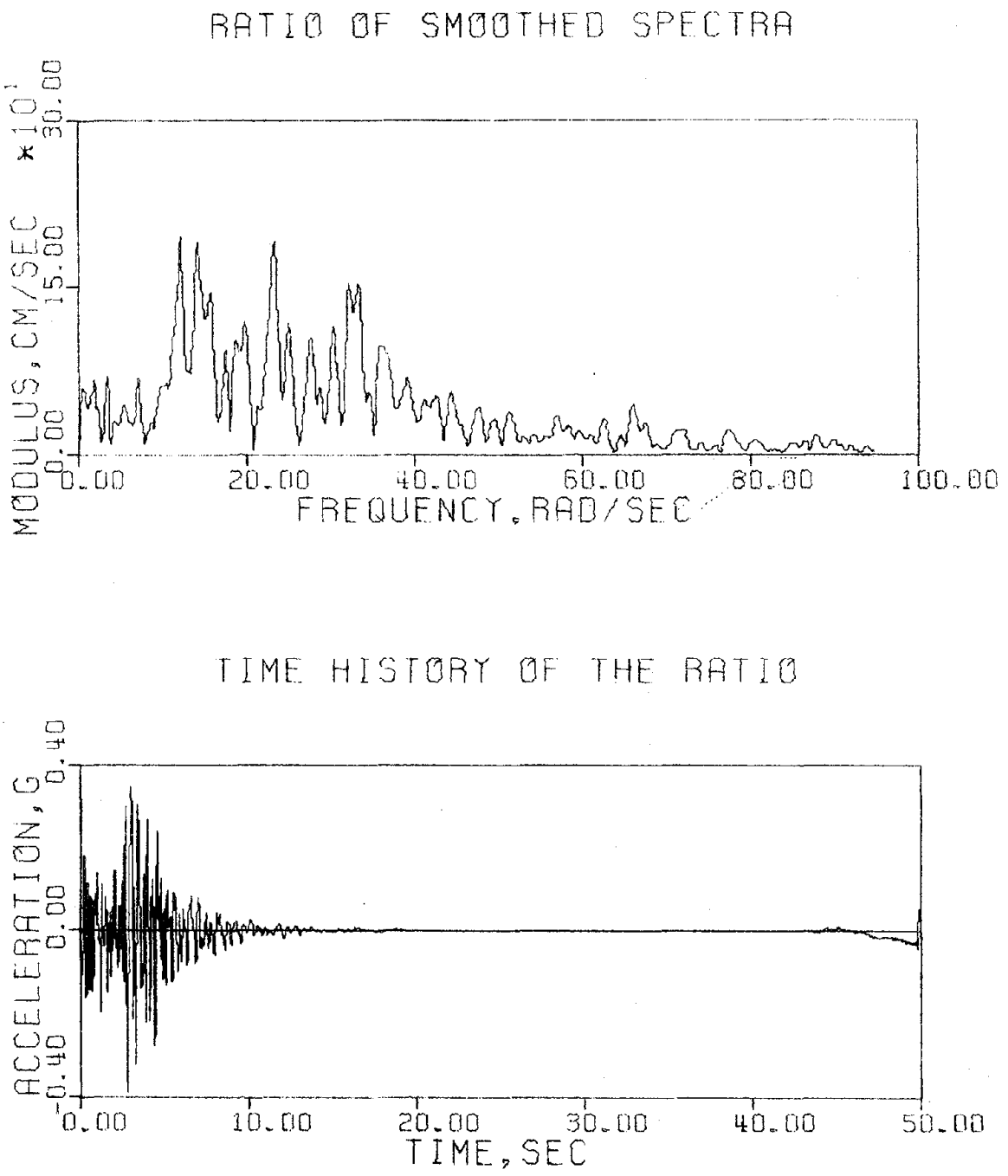

Fig. 5.1b Surface Wave Spectrum and Its Inverse Transform at Orion, Obtained from the Smoothed Numerator and Denominator

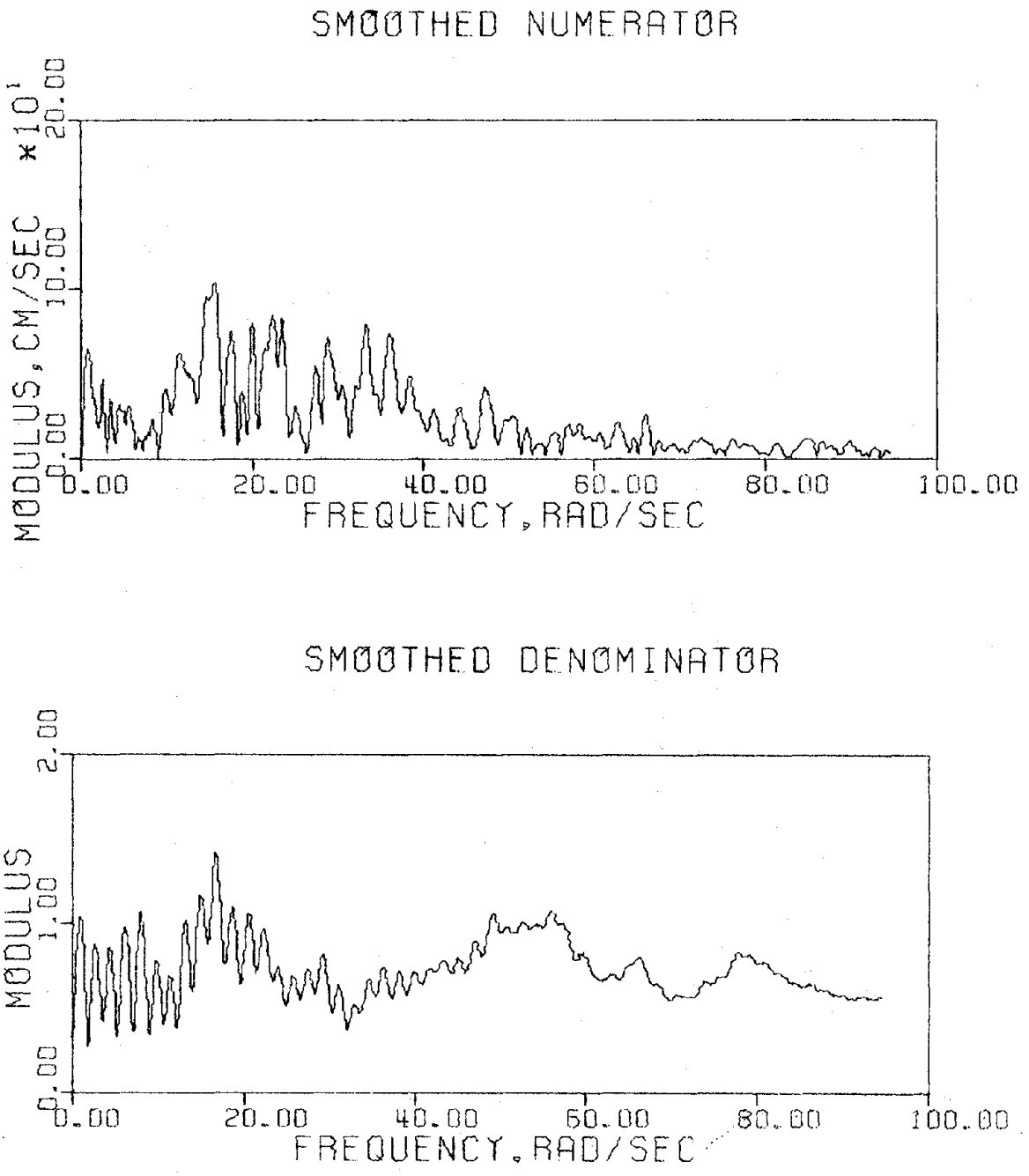

Fig. 5.2a Smoothed Numerator and Denominator for Body Waves at Orion, Orion and Ventura Pair

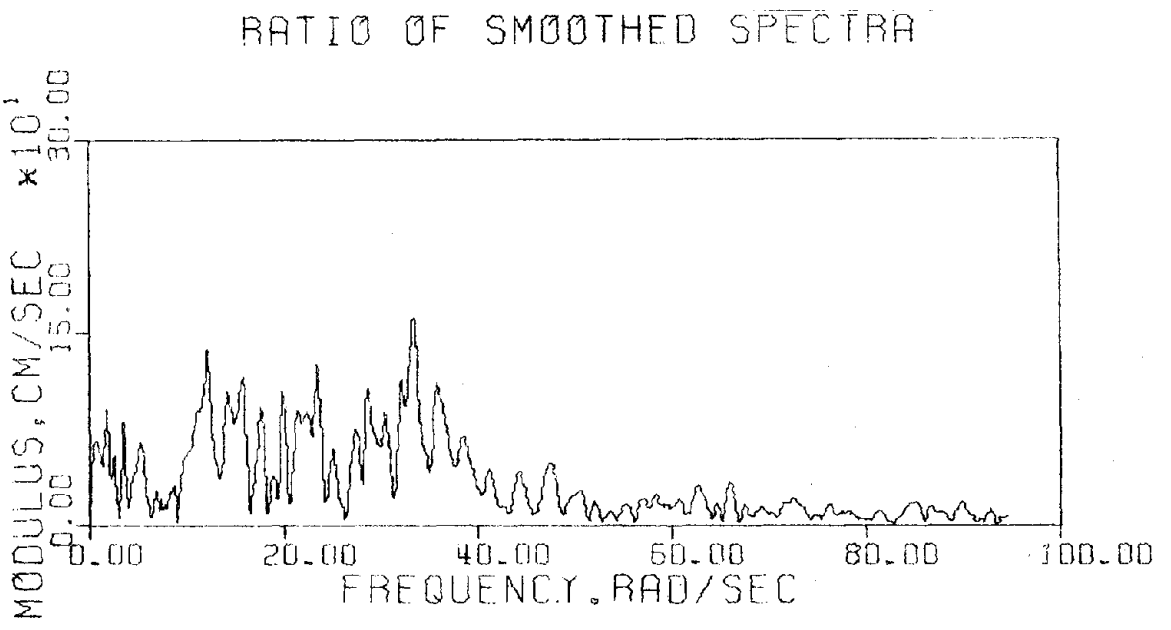

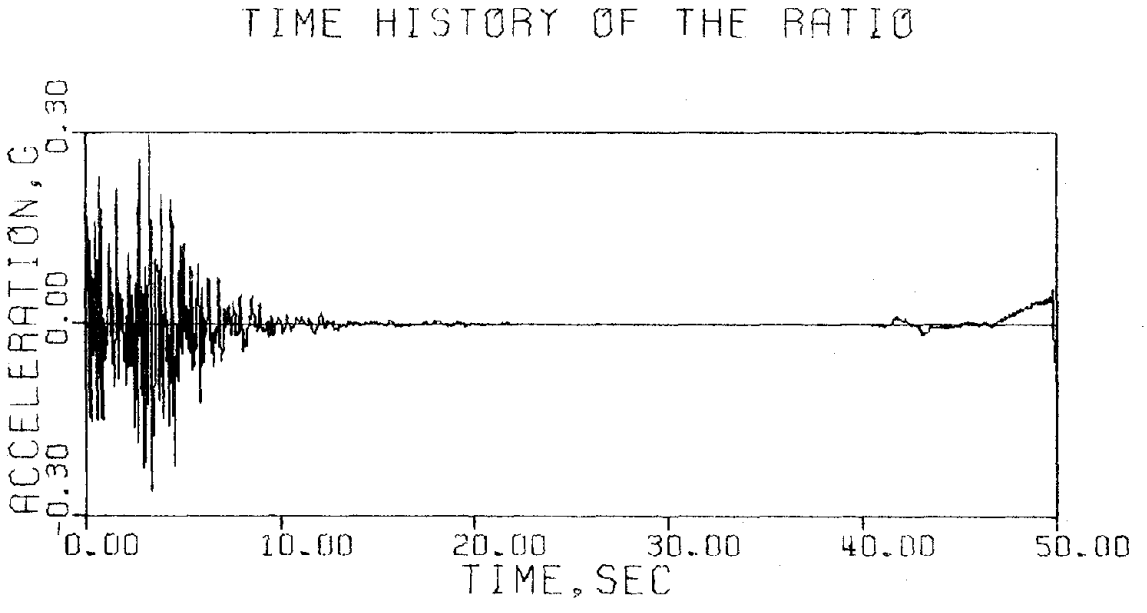

Fig. 5.2b Body Wave Spectrum and Its Inverse Transform at Orion, Obtained from the Smoothed Numerator and Denominator

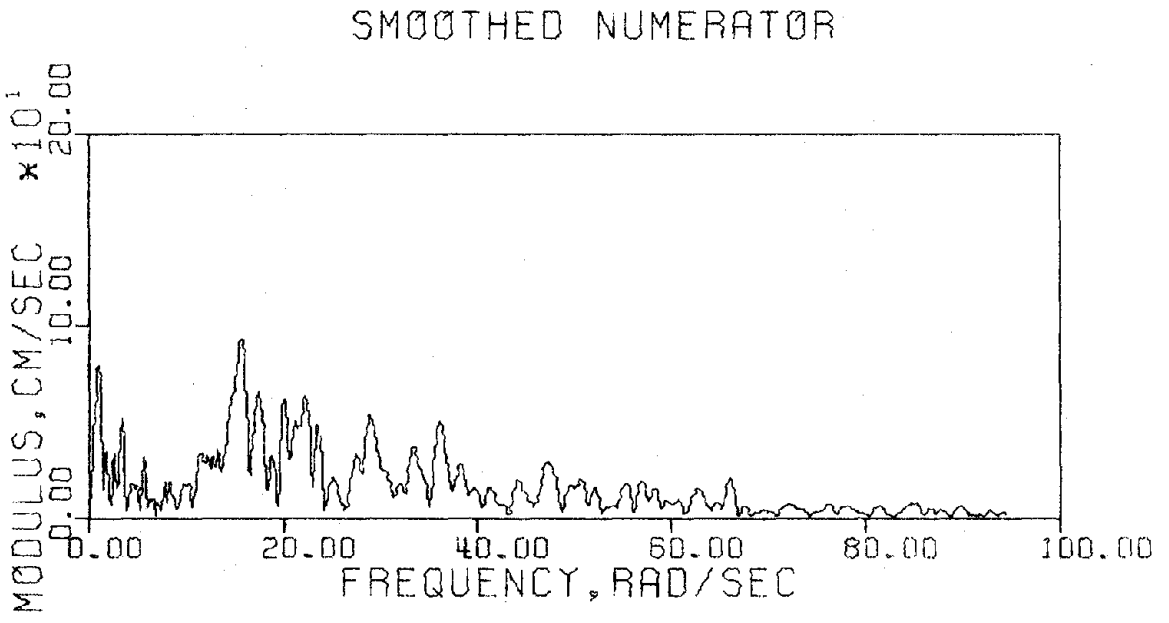

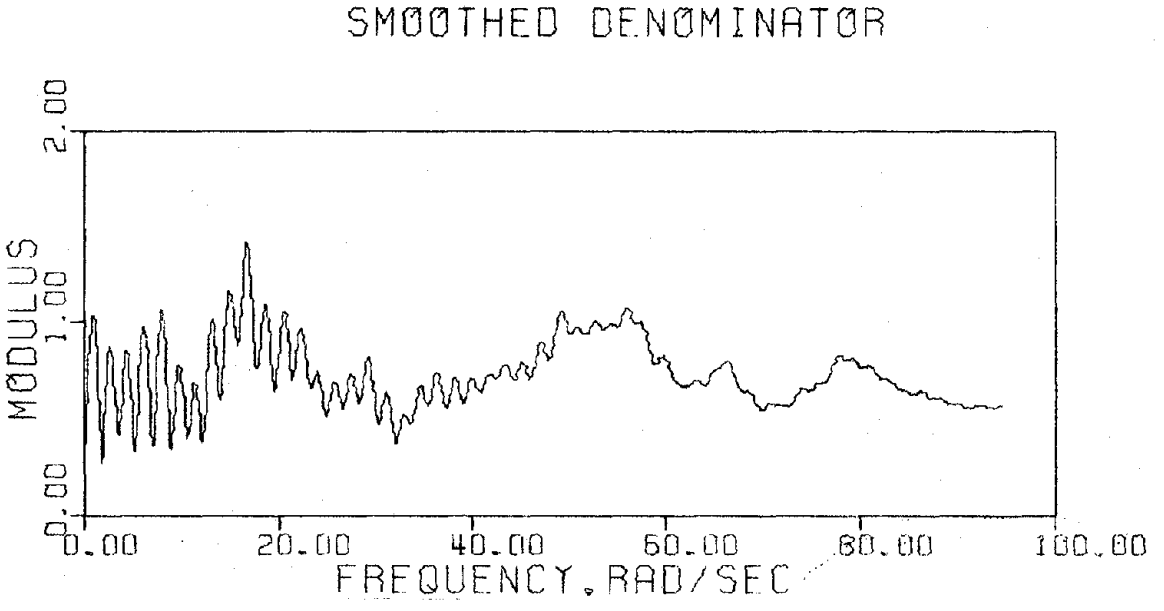

Fig. 5.3a Smoothed Numerator and Denominator for Surface Waves at Ventura, Orion and Ventura Pair

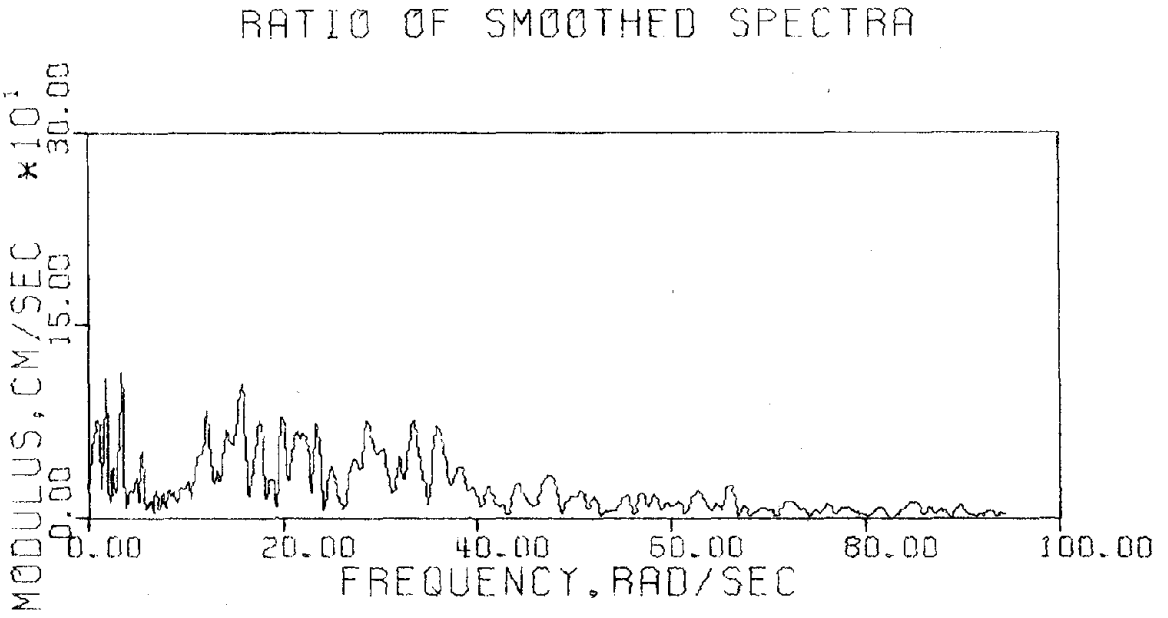

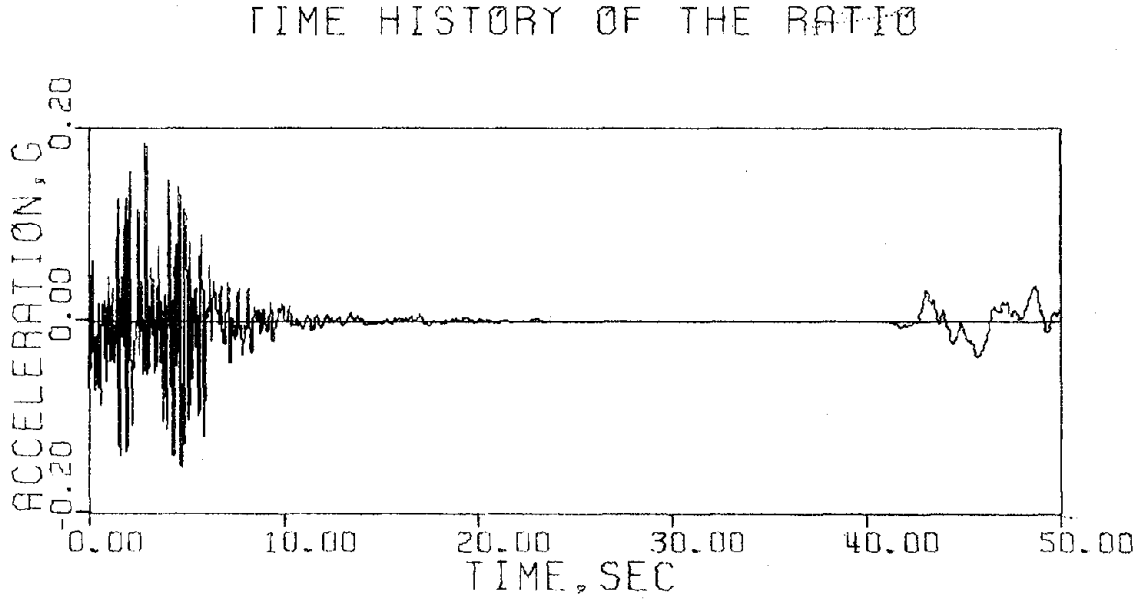

Fig. 5.3b Surface Wave Spectrum and Its Inverse Transform at Ventura, Obtained from the Smoothed Numerator and Denominator

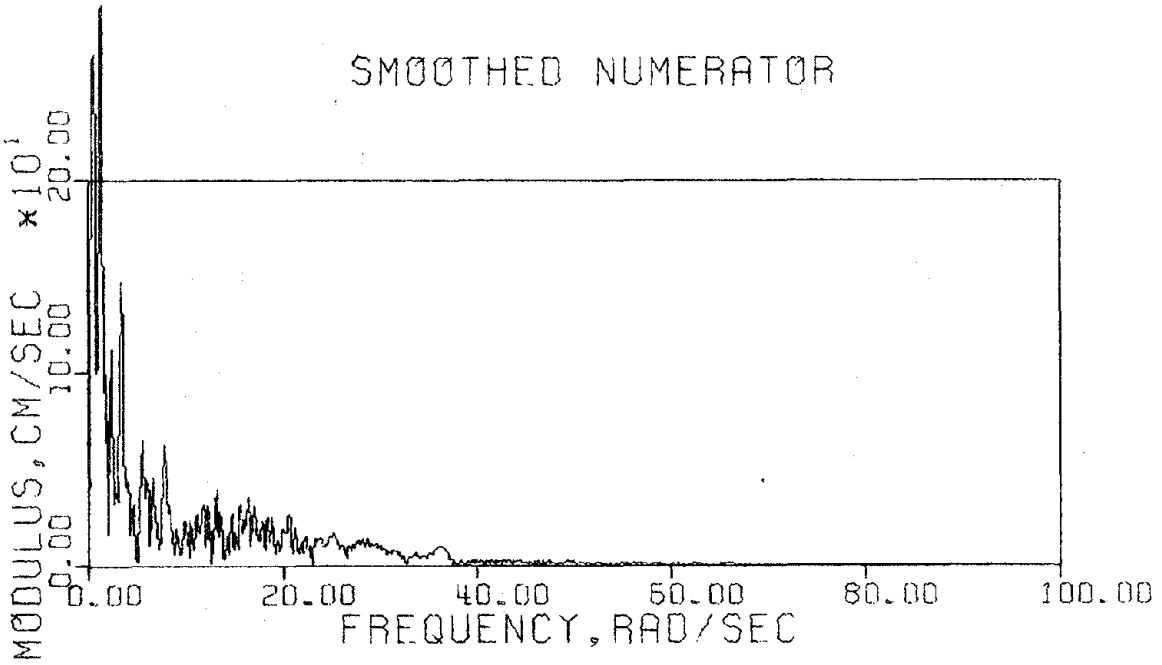

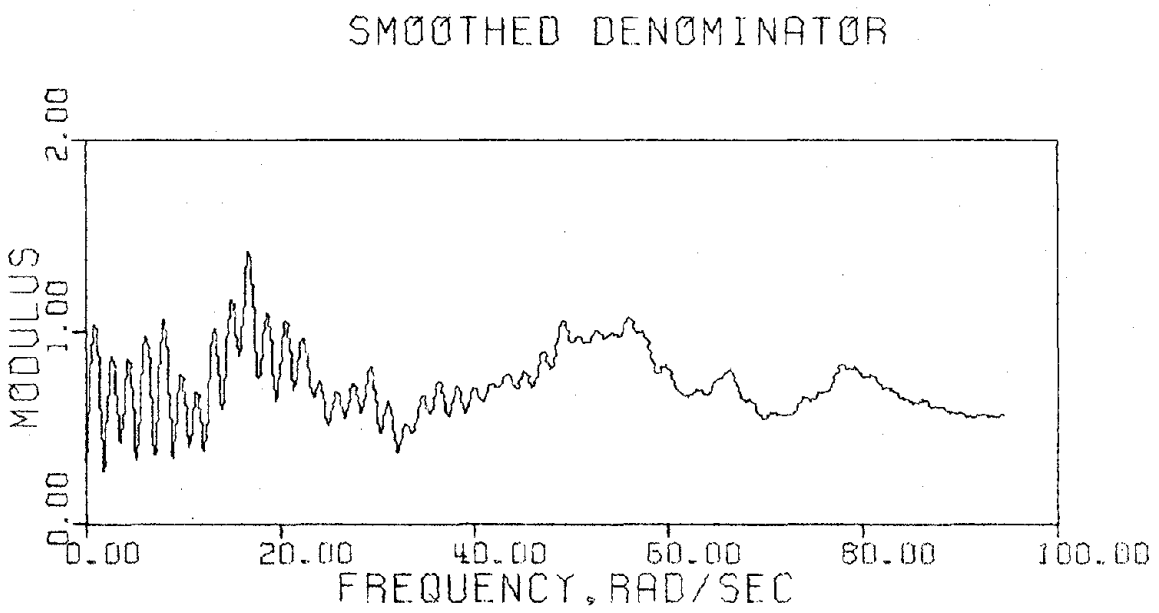

Fig. 5.4a Smoothed Numerator and Denominator for Body Waves at Ventura, Orion and Ventura Pair.

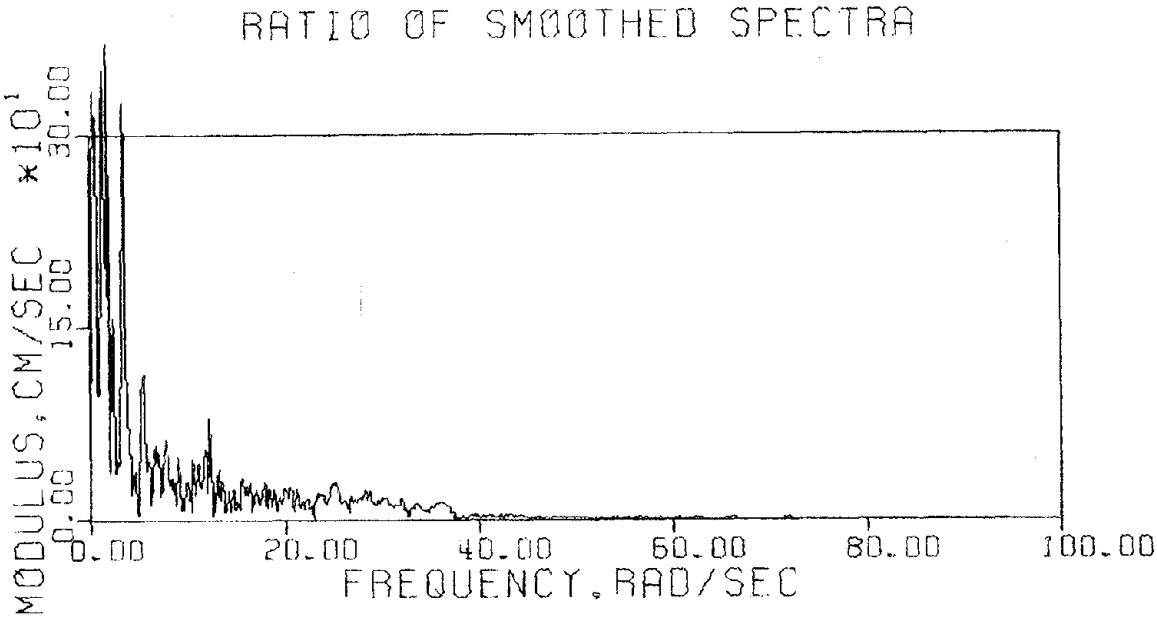

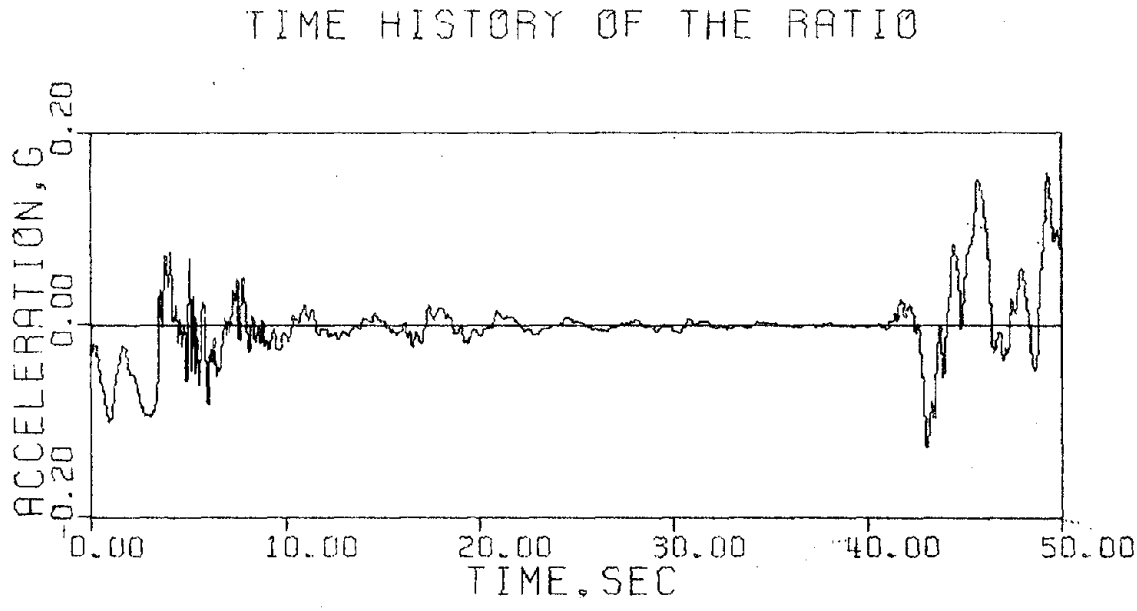

Fig. 5.4b Body Wave Spectrum and Its Inverse Transform at Ventura, Obtained from the Smoothed Numerator and Denominator

5.3 METHOD C: INTERPOLATION

Another method in treating the spurious peaks is by interpolation across the region of the peak. Once the location of the peaks are identified from the results, the values at those frequencies are simply removed. In place of the missing gaps, "straight lines" are interpolated across these gaps in the complex domain. This is done using the following equation,

$$G_i = \left(\frac{I_i - I_{first}}{I_{last} - I_{first}} \right) \left(G_{last} - G_{first} \right) + G_{first} \qquad \text{(Eq. 5.1)}$$

where the G's are the amplitudes, and the I's are freqencies. Fig. 5.5 illustrates this procedure. The results from this procedure are presented in Fig. 5.6 through 5.9 along with their inverse transform. The range of frequencies that were eliminated and interpolated are listed in Table 5.1. This same set of frequency ranges was used for each of the four spectra treated by this method.

FREQUENCY RANGES (RAD/SEC)	3.0-3.8	5.0-5.5	7.1-7.4	8.8-9.4	13.8-15.1
NUMBER OF DATA POINTS INVOLVED (ω =0.12272 RAD/SEC)	8	5	4	6	12

TABLE 5.1 Frequency Ranges For Which the Amplitudes were Interpolated

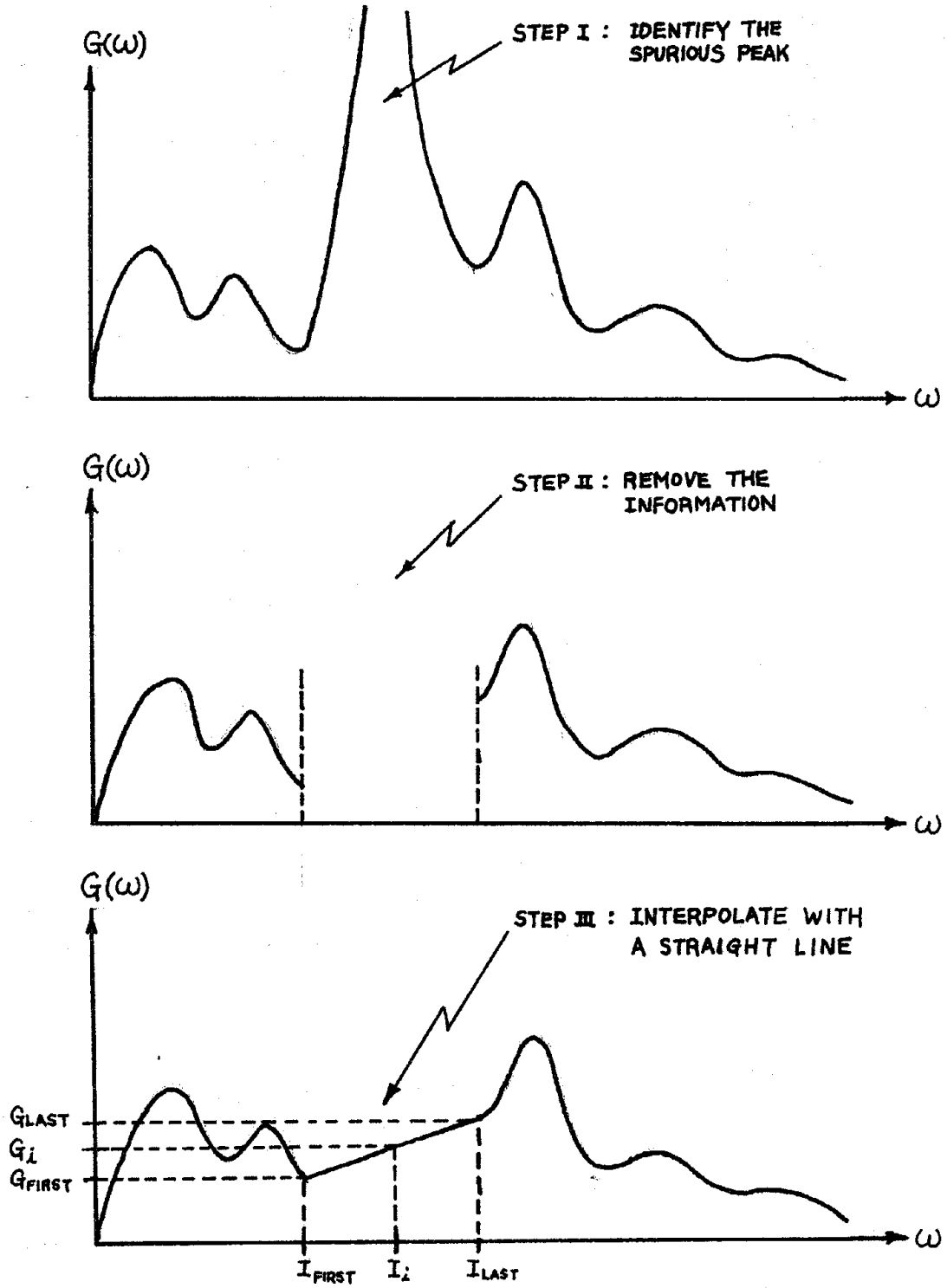

Fig. 5.5 Interpolation Procedure

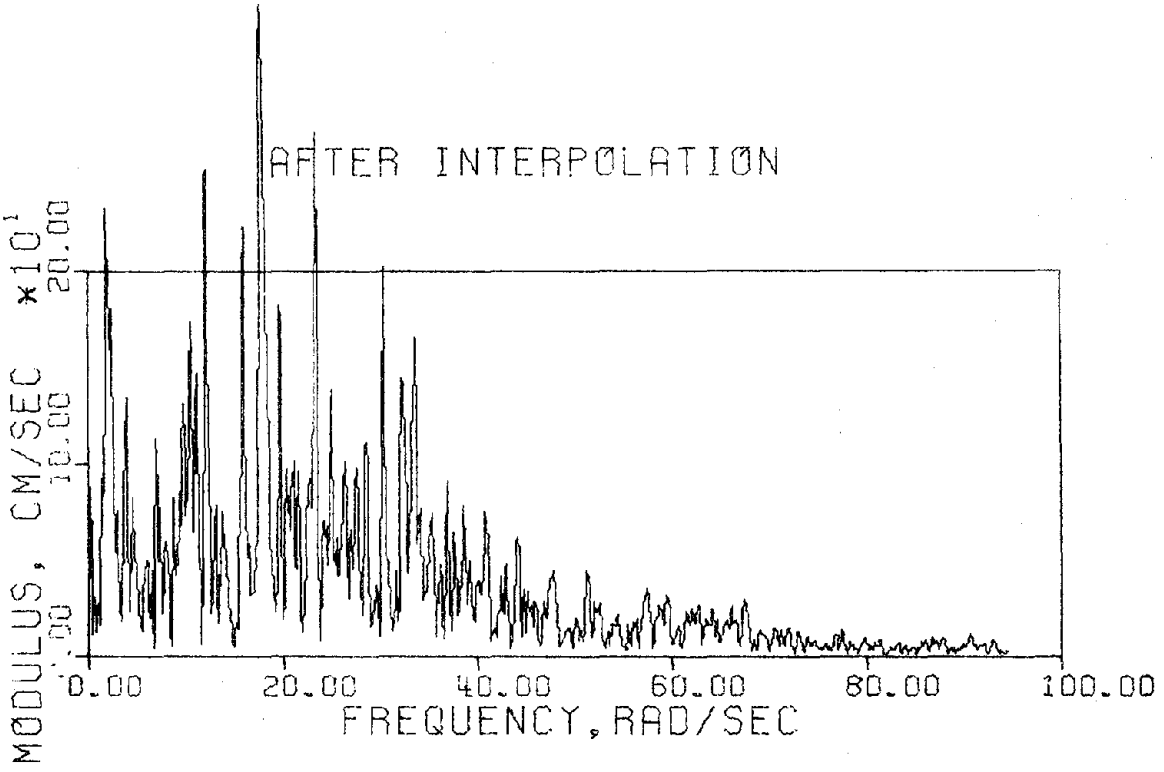

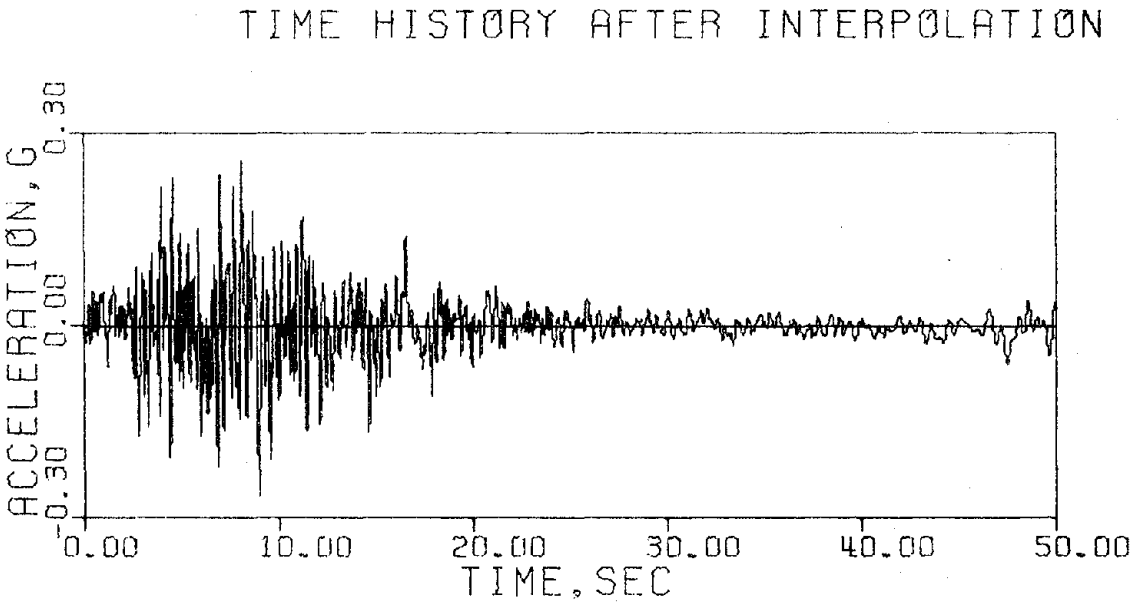

Fig. 5.6 Surface Wave Spectrum at Orion after Interpolation, Orion and Ventura Pair

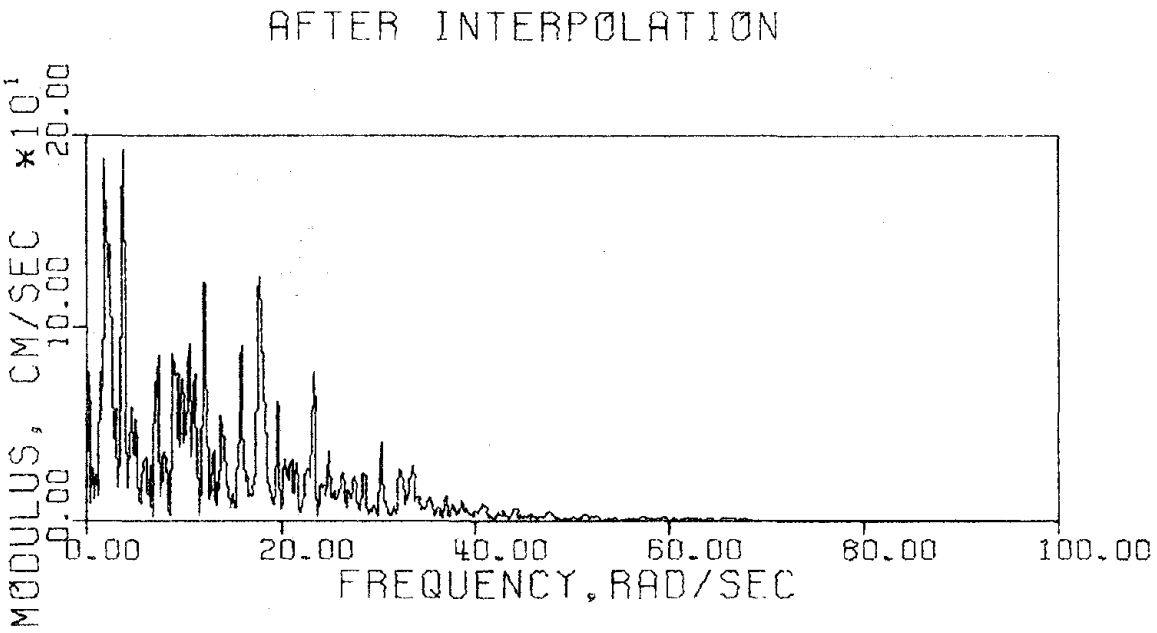

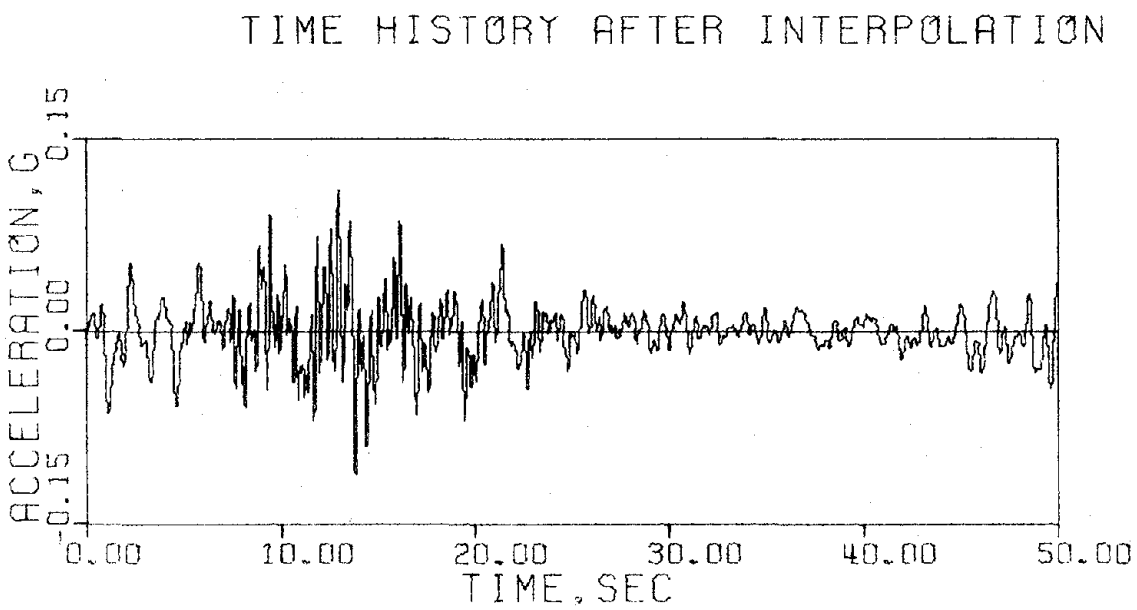

Fig. 5.7 Body Wave Spectrum at Orion after Interpolation, Orion and ventura Pair

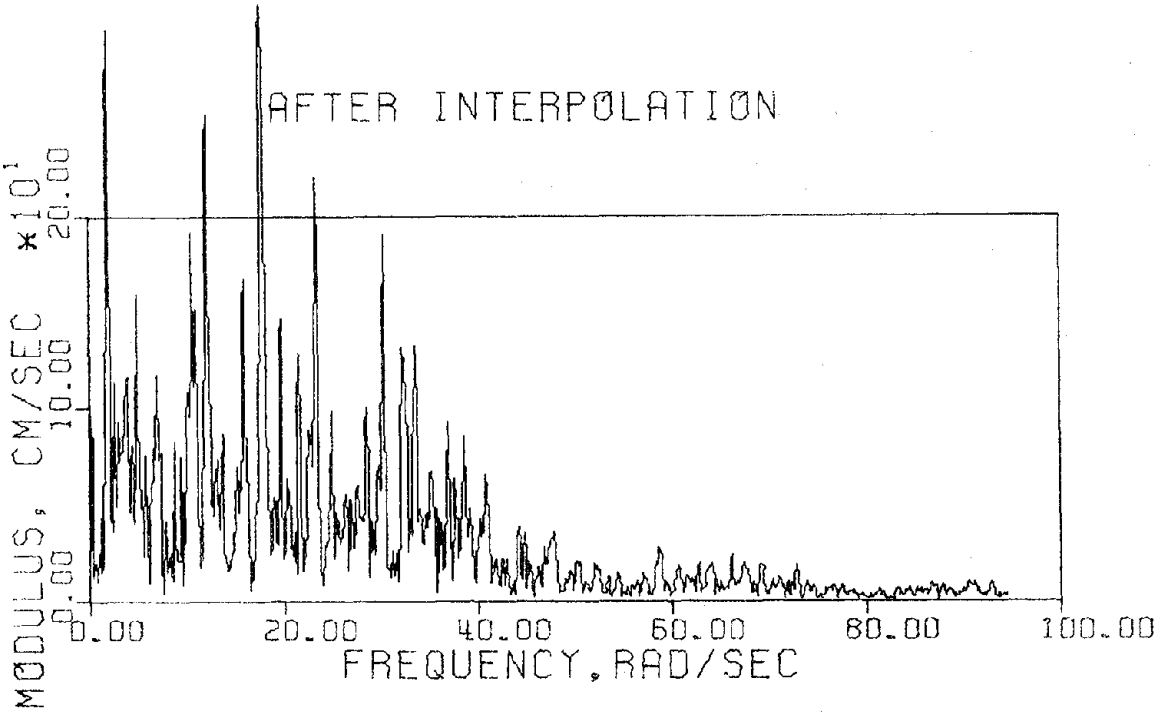

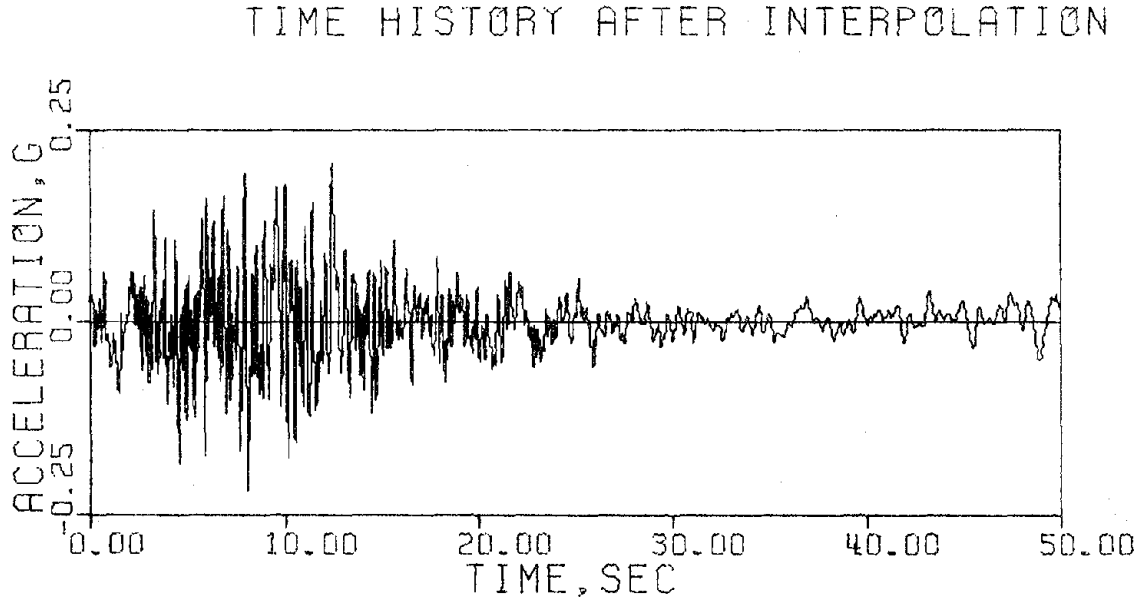

Fig. 5.8 Surface Wave Spectrum at Ventura after Interpolation, Orion and Ventura Pair

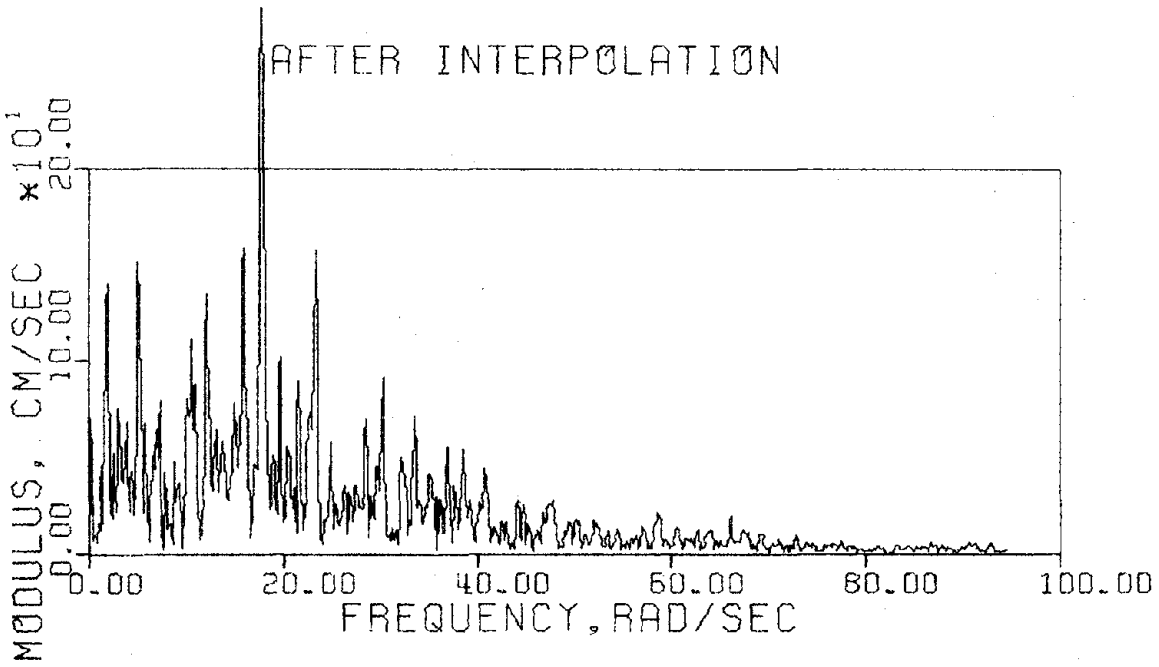

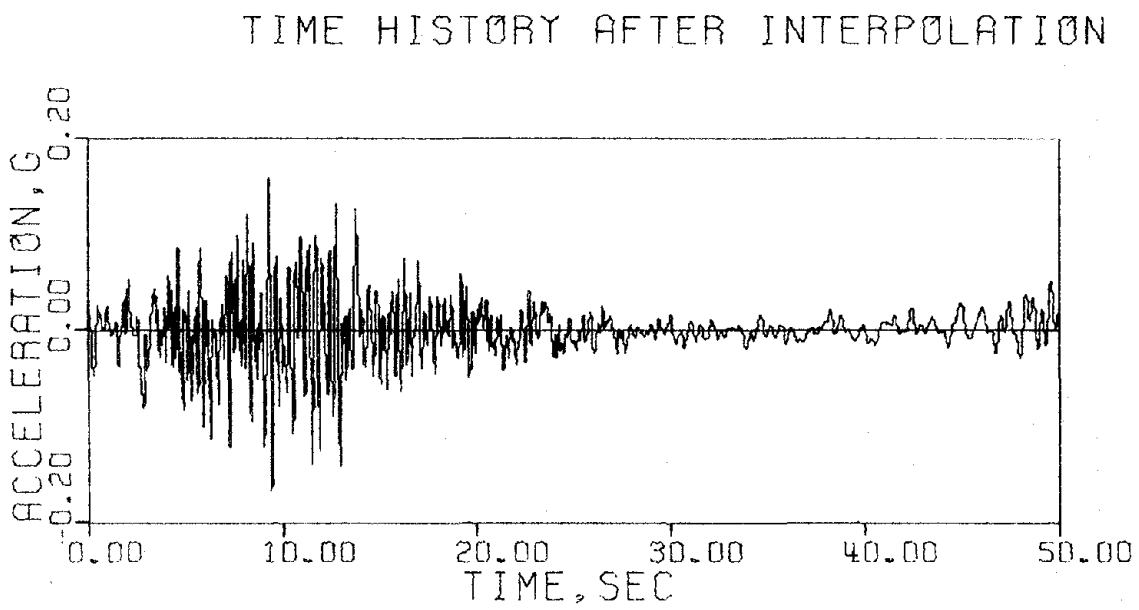

Fig. 5.9 Body Wave Spectrum at Ventura after Interpolation, Orion and Ventura Pair

5.4 METHOD D: MULTIPLE-STATION PROCEDURE

The fourth method of correcting spurious peaks is to calculate many sets of separated wave contents for a given station by pairing one particular station with a number of others. Since the chance of getting spurious peaks in all of these independent calculations at any particular frequency is not so great, therefore, a corrected spectrum of the separated body wave or surface wave can be constructed by replacing the unwanted sections of a particular separated spectrum with the same section obtained in any one of the other calculations where no spurious peaks exist in the section.

In this analysis, the records at Orion, Ventura, and Century Park East are used to obtain two independent body and surface wave components for Orion. Using the modulus of the two denominators of N-M as weighting factors, each pair of the independently calculated spectra for body wave and for surface wave at Orion can be combined to form a new spectrum which most likely will contain no spurious peak. In this thesis, the following procedure is incorporated. For every pair of points at a particular frequency, let us call them G_1 and G_2, where 1 and 2 refer to the two independent spectra, the final result for body and surface waves at every frequency point can be calculated by using the

equations* shown below,

$$G_{s_{final}} = \left(\frac{D_1}{D_1 + D_2}\right) G_{s1} + \left(\frac{D_2}{D_1 + D_2}\right) G_{s2}$$

$$G_{b_{final}} = \left(\frac{D_1}{D_1 + D_2}\right) G_{b1} + \left(\frac{D_2}{D_1 + D_2}\right) G_{b2} \qquad \text{(Eq. 5.2)}$$

where

D_x denote the modulus of the respective denominator at the particular frequency value of interest.

G_{xy} denote the complex values from the spectra at the same frequency point.

b denotes body wave component.

s denotes surface wave component

1 and 2 are the two independently calculated spectra. Fig. 5.10 to 5.13 illustrates the resulting body and surface wave spectra at Orion.

---

*See Appendix B, Program #2, Subroutine ADJUST.

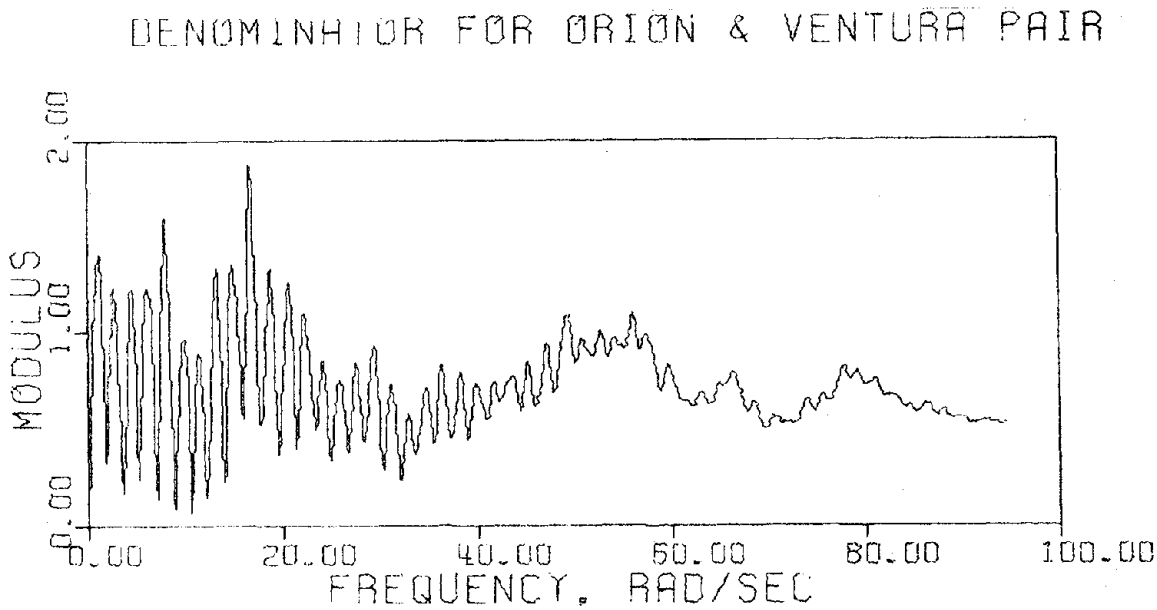

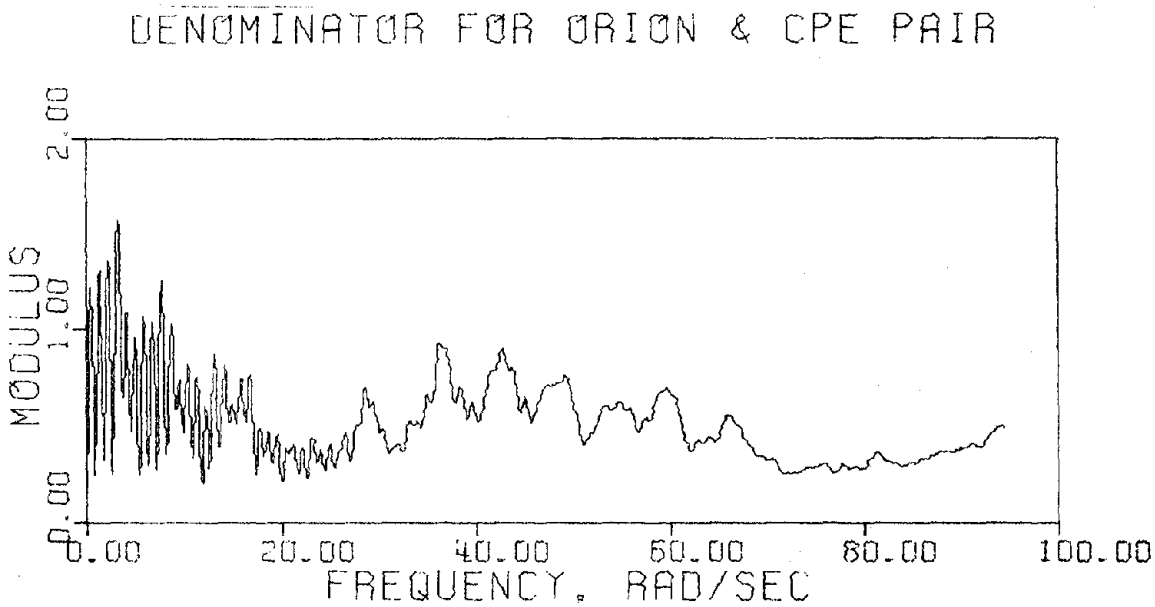

Fig. 5.10 The Denominators are used as Weighting Factors for Multiple-Station Procedure

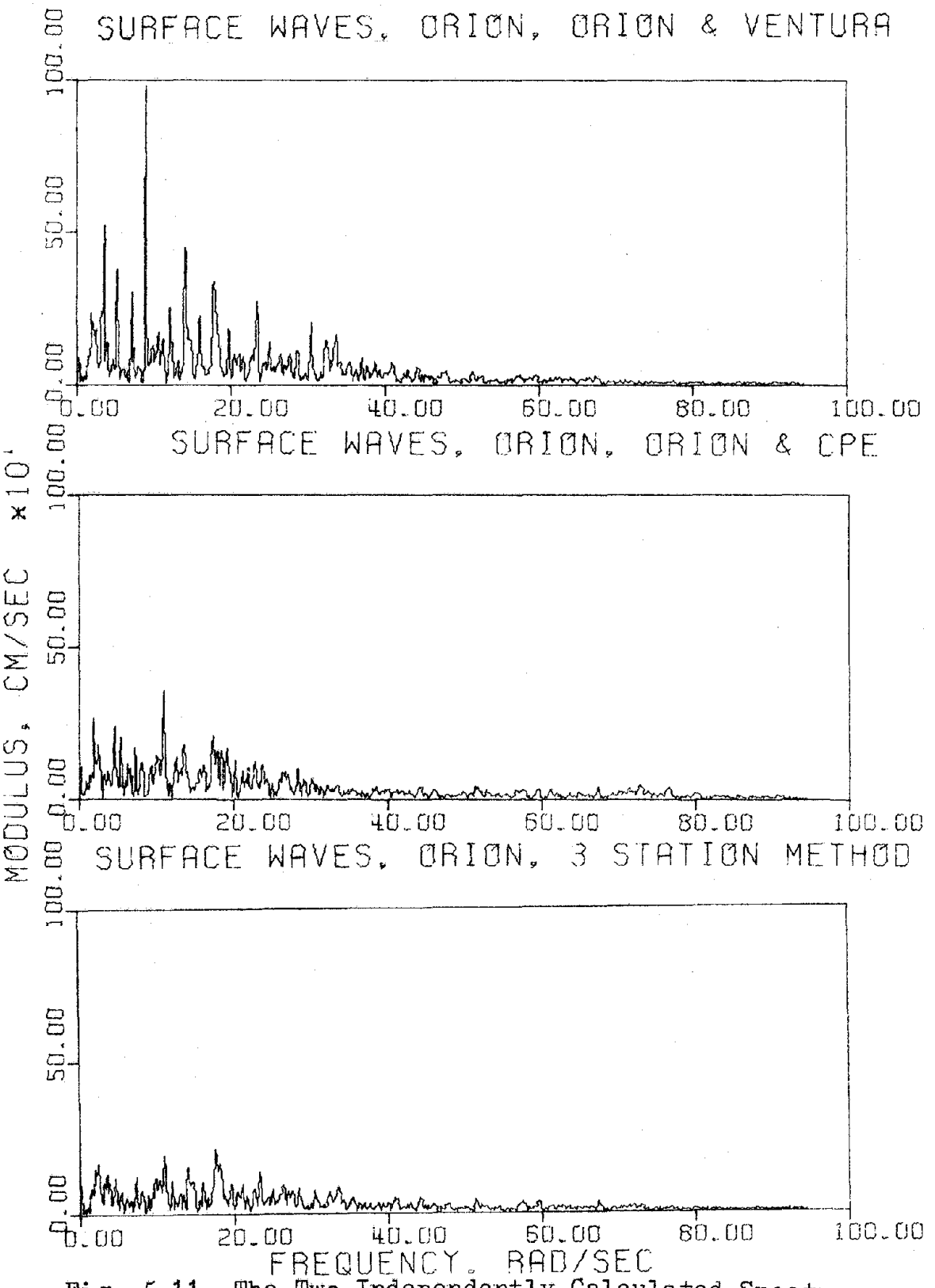

Fig. 5.11 The Two Independently Calculated Spectra for Surface Wave at Orion and The Combined Spectrum

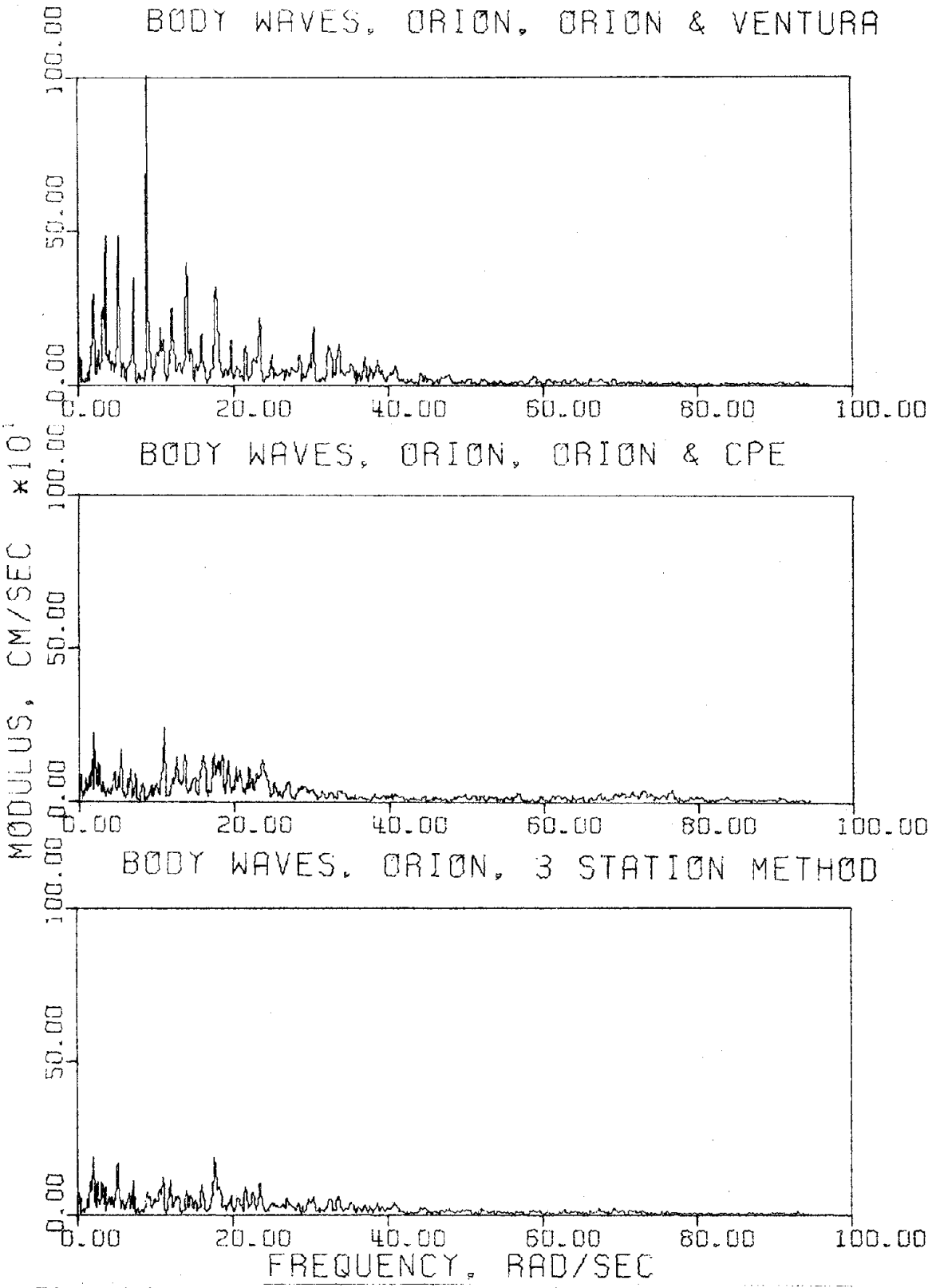

Fig. 5.12 The Two Independently Calculated Spectra for Body Wave at Orion and The Combined Spectra

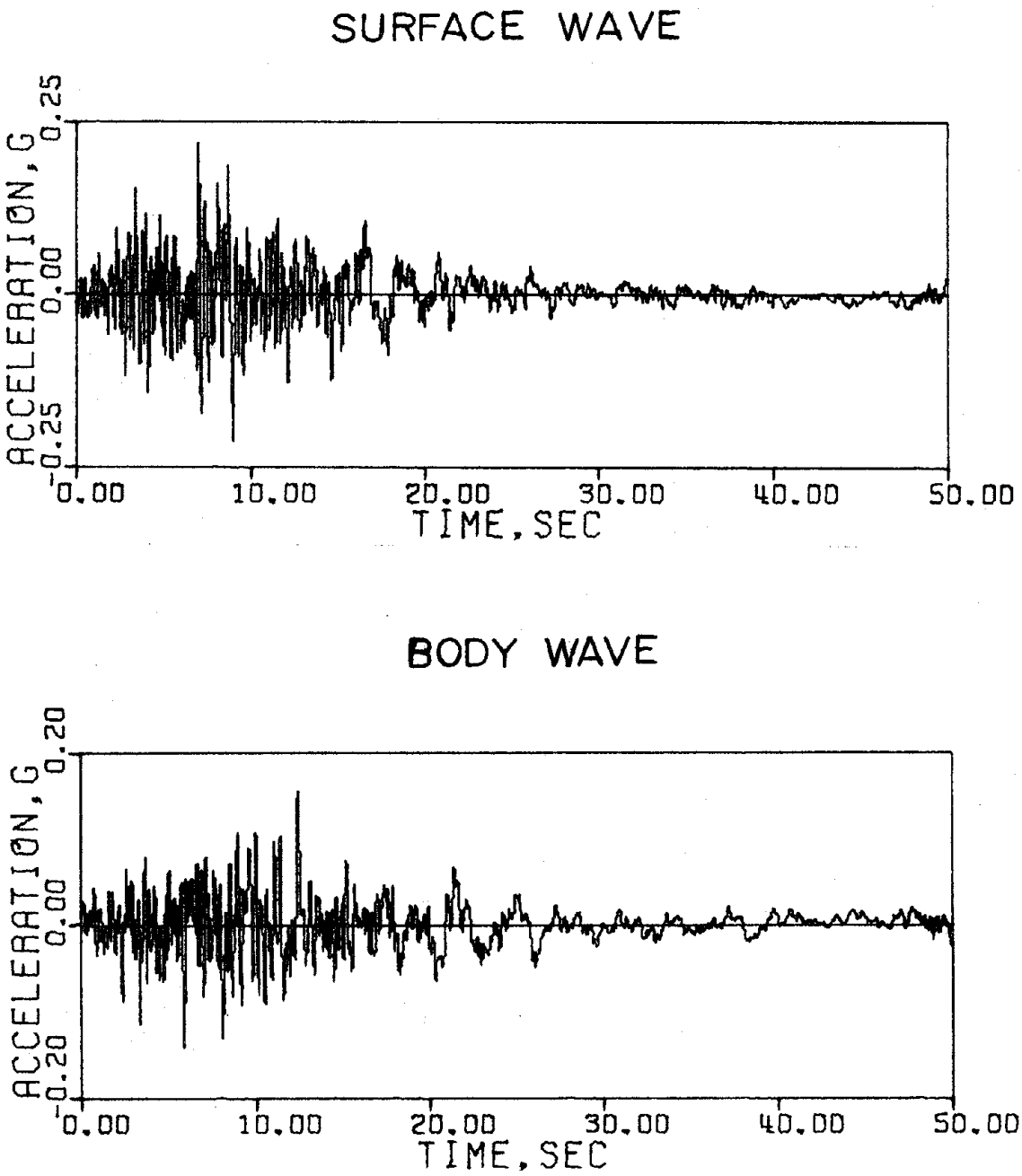

Fig. 5.13 Inverse Transform of the Combined Spectra of Surface Wave (top) and Body Wave (bottom) Components at Orion

5.5 DISCUSSION

Other than the first method, which was not analyzed, all of the three remaining methods seem to have given satisfactory body and surface wave spectra. Comparing the raw results for the separated body and surface wave spectra at Orion shown in Fig. 3.8b and 3.8e with those in this chapter, it can be noted that the improvements are quite significant. Note that the peak accelerations in the resulting time histories were significantly lowered to a level comparable to the peak acceleration of 0.25g recorded on the actual accelerogram at Orion (Caltech 1973).

However, the inverse transforms of the spectra obtained from the three methods did not compare too well. This is due to the fact that the inverse transforms are quite sensitive to the actual content of the Fourier spectra. The different corrections applied to the spectra can certainly affect the contents of these inverse transforms.

The inverse transform in Fig. 5.1b, 5.2b,5.3b and 5.4b contain some unwanted data at the ends. The author believes that they are caused by the aliasing effect (Otnes 1974) in the discrete Fourier transform operations. Since they do not directly affect the analysis intented in the thesis, therefore, no treatments are done to improve these inverse transforms.

CHAPTER 6

CONCLUSION

This thesis had the intention of doing preliminary testing of both a newly modified linear system model and a specific application of the model to the separation of body and surface waves. However, due to difficulties both in the construction of the surface wave transfer functions and the occurence of spurious peaks in the computed body and surface wave spectra, the problem became more complicated than was originally anticipated.

The primary problem which hampered this study was the appearance of the spurious peaks. Their domination of the calculated body and surface wave spectra made these spectra useless. Instead of doing research on the transfer functions of the separated ground motions, this thesis was diverted toward methods of eliminating the spurious peaks.

Three methods were examined in Chapter 5 for the elimination of the spurious peaks. Although they can only provide estimated corrections for the spectra of the separated body and surface waves, each of these methods served successfully to eliminate the spurious peaks from the calculated spectra of body and surface waves.

In addition to the above accomplishment, this thesis has also clarified the weaknesses of the system model, in particular the lack of realistic surface wave transfer functions. As was discussed in Sec. 3.2, due to this weakness the separated body and surface waves do not show the correct characteristics. Instead, the body and surface wave spectra are similar in shape. A typical illustration of this is shown in Fig. 5.13.

This thesis serves only as a preliminary evaluation of the newly proposed linear system model with its dependence on wave separation. Further work is needed to reconcile the model with strong earthquake data. The author recommends that the following studies be done:

(1) The establishment of good surface wave transfer functions, namely the W_s and X_s functions. Use of (2), (3) and (4) below can help.

(2) Suitable modeling of the various source related functions, E_s, E_b, R_s and R_b.

(3) An ideal model of the earth either simulated or based on field experiments should be created to serve as a test case to determine the correctness of the modeling technique for the linear system model.

(4) Middle field strong motion seismograms with clear separations of body and surface waves ought to be used to test the modeling of the linear system

using Eq. 2.1 and Eq. 2.6 for the analysis.

BIBLIOGRAPHY

1. Båth, Markus. Spectral Analysis in Geophysics, Elsevier Scientific Publishing Company, Amsterdam, The Netherlands, 1974.

2. Bendat, Julius S. and Allan G. Piersol. Random Data: Analysis and Measurement Procedures, Wiley-Interscience, New York, 1971.

3. Ben-Menahem, A. "Radiation of Seismic Body-waves from a Finite Moving Source in the Earth," J. Geophysical Research, Vol. 67, pp. 345-350, 1962.

4. Ben-Menahem, A. "Radiation of Seismic Surface-waves from Finite Moving Sources," Bull. Seis. Soc. Am., Vol. 51, pp. 401-435, 1961.

5. Brigham, E. Oran. The Fast Fourier Transform, Prentice-Hall Enc., Englewood Cliffs, New Jersey, 1974.

6. California Institute of Technology. "Strong Motion Earthquake Accelerograms, Digitized and Plotted Data," EERL72. Pasadena, California.

7. Carrivear, Arthur Rene. Strong Ground Motion from Strike-Slip Faulting, PhD. dissertation, Mech. and Struc. Dept., Univ. of Calif. Los Angeles, 1973.

8. Carriveau, Arthur Rene. Transfer Matrice for Layered Media with Normally Incident SH Waves, M.S. in Engineering, Mech. and Struc. Dept., Univ. of Calif. Los Angeles, March 1970.

9. Davison, Charles. A Manual of Seismology, Cambridge University Press, London, 1921.

10. Dobry, Ricardo, Robert V. Whitman, and Jose M. Roesset. "Soil Properties and The One-Dimensional Theory of Earthquake Amplification," Dept. of Civil Engineering, M.I.T., R71-18, May 1971.

11. Drake, Lawrence A, and A. K. Mal. "Love and Rayleigh Waves in the San Fernando Valley," Bull. Seis. Soc. Am., Vol. 62, No. 6, pp. 1673-1690, December 1972.

12. Duke, C. M. and A. K. Mal. "A Model for Analysis of Body and Surface Waves in Strong Ground Motion," Proc. U.S. Nat'l. Conf. on Earthquake Engr., EERI, pp. 17-24, 1975.

13. Duke, C. M. and P. J. Hradilek. "Spectral Analysis of Site Effects in the San Fernando Earthquake," Proc. of the Fifth World Conf. on Earthquake Engr., Rome, Italy, 1973, Vol. 1, Session 26, No. 77, Ministry of Public Works, Rome, Italy, 1973.

14. Duke, C. M., et al. "Subsurface Site Conditions and Geology in the San Fernando Earthquake Area," School of Engr. and Applied Science, Univ. of Calif., Los Angeles, UCLA-ENG-7206, December 1971.

15. Ewing, W. M., W. S. Jardetzky and F. Press. Elastic Waves in Layered Media, McGraw-Hill, New York, 1957.

16. Hanks, Thomas C. "Strong Ground Motion of the San Fernando, California, Earthquake: Ground Displacements," Bull. Seis. Soc. Am., Vol. 65, No. 1, pp. 193-225, February 1975.

17. Haskell, N. A. "Radiation Pattern of Rayleigh Waves from a Fault of Arbitrary Dip and Direction of Motion in a Homogeneous Medium," Bull. Seis. Soc. Am., Vol. 53, pp. 619-642, April 1963.

18. Haskell, N. A. "Crustal Reflection of Plane P- and SV-Waves," J. Geophysical Research, Vol. 67, pp. 4751-4767, 1962.

19. Haskell, N. A. "Crustal Reflection of Plane SH-Waves," J. Geophysical Research, Vol. 65, pp. 4147-4150, 1960.

20. Haskell, N. A. "The Dispersion of Surface Wave on Multilayered Media," Bull. Seis. Soc. Am., Vol. 43, pp. 17-34, 1953.

21. Heck, Nicholas Hunter. Earthquake, Princeton University Press, Princeton, 1936.

22. Hudson, D. E. and F. E. Udwadia. "Local Distribution of Strong Earthquake Ground Motions," Proc. Fifth World Conf. on Earthquake Engr., Vol. 1, pp. 691-700, 1964.

23. Johnsen, Keith. Subsurface Transfer Functions at Century City in the San Fernando Earthquake, M.S. in Engineering, Mech. and Struc. Dept., Univ. of Calif., Los Angeles, 1972.

24. Johnson, J. A. "Site and Source Effects on Ground Motion in Managua, Nicaragua," School of Engr. and Applied Science, Univ. of Calif., Los Angeles, UCLA-ENG-7536, May 1975.

25. Johnson, J. A., T. Yee, and C. M. Duke. "Preliminary Ground Motion Calculations and Site Effects at Banco Central," Managua, Nicaragua Earthquake of December 23, 1972, EERI Conf. Proc., Vol. 1, pp. 300-308, November 1973.

26. Kanai, K. "Semi-emperical Formula for the Seismic Characteristic of the Ground," Bull. of Earthquake Research Laboratory, Univ. of Tokyo, Vol. 35, pp. 309-325, June 1957.

27. Kurita, T. "Attenuation of Short-Period P-wave and Q in the Mantle," J. of Physics of the Earth, Vol. 16, pp. 61-78, 1968.

28. Lastrico, R. M. Effects of Site and Propagation Path on Recorded Strong Earthquake Motions, PhD. in Engineering, Mech. and Struc. Dept., Univ. of California, Los Angeles, 1970.

29. Mal. A. K. "Rayleigh Waves From a Moving Thrust Fault," Bull. Seis. Soc. Am., Vol. 62, No. 3, pp. 751-762, June 1972.

30. Matthiesen, R. B., C. M. Duke, D. J. Leeds and J. C. Fraser. "Site Characteristics of Southern California Strong Motion Earthquake Station, Part II," Dept. of Engineering, Univ. of Calif., Los Angeles, UCLA-ENG-64-15, February 1964.

31. McGillem, Clare D. and George R. Cooper. Continuous and Discrete Signal and System Analysis, Holt, Rinehart and Winston Inc., New York, 1974.

32. Murphy, F. R., N. L. Weaver, G. B. Lamers. "Effects of Local Geology on the Amplitude of Seismic Waves," Environmental Research Corporation, Alexandria, Virginia, NVO-1163-205, June 1970.

33. Otnes, Robert K. and Loren Enochson. Digital Time Series Analysis, John Wiley & Son, New York, 1972.

34. Roesset, Jose M. and Robert V. Whitman. "Theoretical Background for Amplification Studies," Dept. of Civil Engineering, M.I.T., Cambridge, Massachusetts, Research Report No. R69-15, March 1969.

35. Schnabel, P., H. Bolton Seed, and J. Lysmer. "Modification of Seismogragh Records for Effect of Local Soil Conditions," College of Engr., Univ. of Calif., Berkeley, Report No. EERC71-8, December 1971.

36. Seed, H. Bolton, I. M. Idriss and H. Dezfulian. "Relationships Between Soil Conditions and Building Damage in the Caracas Earthquake of July 29, 1967," College of Engr., Univ. of Calif., Berkeley, Report No. EERC70-2, February 1970.

37. Sines, George. Elasticity and Strength, A UCLA Engineering Syllabus, Univ. of Calif., Los Angeles, 1972.

38. Thomson, W. T. "Transmission of Elastic Waves Through a Stratified Solid medium," J. Appl. Phys., Vol. 21, pp. 89-93, 1950.

39. Trifunac, M. D. and A. G. Brady. "On the correlation of Seismic Intensity Scales with the Peaks of Recorded Strong Ground Motion," Bull. Seis. Soc. Am., Vol. 65 No. 1, pp. 139-162, February 1975.

40. White, J. E. Seismic Waves Radiation, Transmission and Attenuation, McGraw-Hill, New York, 1965.

41. USGS and NOAA. The San Fernando, California, Earthquake of February 9, 1971, Geological Survey Professional Paper 733, U. S. Govermnent Printing Office, Washington, 1971.

42. Whitman, Robert V. and others "Ground Motion Amplification Studies, Bursa, Turkey," Dept. of Civil Engr., M.I.T., Cambridge, Massachusetts, MIT-CE R74-58, September 1974.

APPENDIX A

GREEN'S FUNCTION SOLUTION FOR A DOUBLE COUPLE SOURCE IN FREQUENCY DOMAIN

In a infinite, homogenious, isotropic, elastic medium, the far field displacement motion due to a sudden dislocation source can be described by the following equation.

$$U_m(\xi,\omega)=U_i(o,\omega)T^m_{ij}n_j\Delta S \qquad \text{(Eq. A-1)}$$

where

U_m is the displacement in the m direction.

$[U_i(0,\omega)]$ is the discontinuity jump of the slip area.

T^m_{ij} is the traction vector for the m direction.

n_j is the normal vector of the slip plane.

S is the area of the fault.

i and j are the indices for the summation.

For a slip system described in Fig. A.1, the above equation of motion can be reduced to

$$U_m(\xi,\omega)=(D_1\Delta S)T^m_{13} \qquad \text{(Eq. A.2)}$$

by making the substitutions of $U_i(0,\omega)=\delta_{ij}D_1$ and $n_j=\delta_{j3}$. D_1 is themagnitude of the slip, δ_{ij} is the Kronecker delta.

The traction T^m_{13} described above can be expressed in terms of Green's function in the following manner,

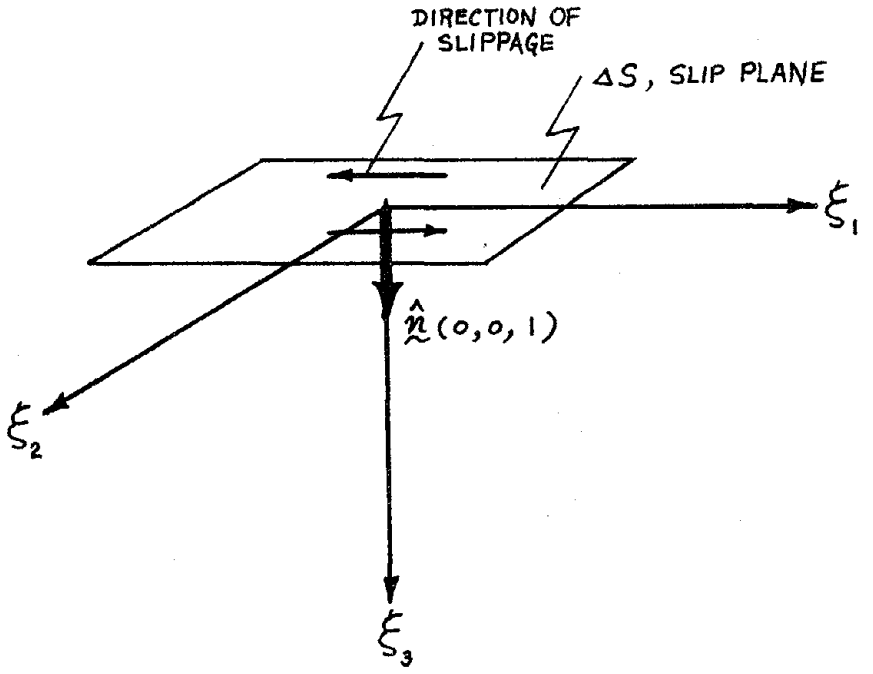

Fig. A.1 Sudden Slip on A Small Plane

$$T^{m}_{13}=\mu\left[\frac{\partial G_{3m}}{\partial \xi_1}+\frac{\partial G_{1m}}{\partial \xi_3}\right] \qquad \text{(Eq. A.3)}$$

where the Green's function can be written as a function of frequency shown below,

$$G_{ij}=\frac{1}{4\pi\rho\omega^2}\left[k_2^2\,\frac{e^{ik_2R}}{R}\,\delta_{ij}-\frac{\partial^2}{\partial\xi_i\,\partial\xi_j}\left(\frac{e^{ik_1R}-e^{ik_2R}}{R}\right)\right] \qquad \text{(Eq. A.4)}$$

where

$k_i = /c_i$.

is the density.

$_{ij}$ is the Kronecker delta.

Making use of Eq. A.3 and A.4, the far field displacement spectra described in Eq. A.2 can be expressed in the following forms.

$$U_1(\xi,\omega)=(\mu D_1\Delta S)\frac{1}{4\pi\rho\omega^2R}\left[(ik_2^3e^{ik_2R})\gamma_3+(ik_1^3e^{ik_1R}-ik_2^3e^{ik_2R})2\gamma_1^2\gamma_3\right]$$

$$U_2(\xi,\omega)=(\mu D_1\Delta S)\frac{1}{4\pi\rho\omega^2R}\left[(ik_1^3e^{ik_1R}-ik_2^3e^{ik_2R})\,2\gamma_1\gamma_2\gamma_3\right] \qquad \text{(Eq. A.5)}$$

$$U_3(\xi,\omega)=(\mu D_1\Delta S)\frac{1}{4\pi\rho\omega^2R}\left[(ik_2^3e^{ik_2R})\gamma_1+(ik_1^3e^{ik_1R}-ik_2^3e^{ik_2R})2\gamma_1\gamma_3^2\right]$$

where $\gamma_i=\delta_i/R$, the directional cosines.

It can be shown that the two terms in each of the above equations can be broken down into P-wave and S-wave parts. These components written in the form of indicial notations are given as follow.

CENSORED

For P-wave

$$U_i(\xi,\omega)=(\mu D_1 \Delta S)\left(\frac{1}{4\pi\rho\omega^2 R}\right)\left(i k_1^3 e^{i k_1 R}\right)\left(2\gamma_i \gamma_1 \gamma_3\right) \qquad \text{(Eq. A.6a)}$$

For S-wave

$$U_i(\xi,\omega)=(\mu D_1 \Delta S)\left(\frac{1}{4\pi\rho\omega^2 R}\right)\left(i k_2^3 e^{i k_2 R}\right)\left(\delta_{i1}\gamma_3 + \delta_{i3}\gamma_1 - 2\gamma_i \gamma_1 \gamma_3\right) \qquad \text{(Eq. A.6b)}$$

The above equations can both be interpreted in the following way. The first factor (D_1 S) is the seismic moment. The next two factors describe the geometric and exponential decay. They are both frequency dependent. And the last factor describes the radiation pattern.

In this thesis, the directionality factor for the S-wave response is used to describe the radiation patterns in the linear system analysis described in Cahpter 1. The equations of the following form are used to describe the surface wave and the body wave radiation patterns.

$$R_{si}(\theta,\phi,r)=A(\delta_{i1}\gamma_3+\delta_{i3}\gamma_1-2\gamma_i\gamma_1\gamma_3)$$
$$R_{bi}(\theta,\phi,r)=B(\delta_{i1}\gamma_3+\delta_{i3}\gamma_1-2\gamma_i\gamma_1\gamma_3) \qquad \text{(Eq. A.7)}$$

where $R_{si}(\theta,\phi,r)$ and $R_{bi}(\theta,\phi,r)$ are the components of the radiation pattern transfer functions for surface waves and body waves, respectively. And A and B are constants for amplitude adjustment.

For the simple reason that the investigations conducted in this thesis are quite preliminary, no rigorous effort is made in developing accurate functions

for the radiation patterns. The assumption of describing both surface wave and body wave radiation patterns the same way is quite sufficient for the scope of this research.

APPENDIX B

COMPUTER PROGRAMS

The listing of four major computer programs used in the thesis are included in this Appendix for reference. The main programs and their essential subroutines are listed below. Other required subroutines may be obtained from the UCLA Earthquake Laboratory.

1. Test Program For Separation of Body and Surface Waves

This program was used in the analysis done in Chapter 4. It generates a specified source function via Subroutine "GBS" and "SORCE1", calculate the total ground motion using the method discussed in Chapter 4, and then perform the separation with the specified parametric errors.

2. Multi-Station Body and Surface Wave Separation Program

This program was used in Chapter 5 both in providing untreated body and surface wave spectra for the use in the "smoothing scheme" and the "interpolation scheme", and also performing calculation to obtain the corrected spectra via "multiple-station scheme" by using Subroutine "ADJUST". Subroutine "MNPREP" prepares input data and denominator, M-N, and "SEPRAT" performs the separation. All other subroutines are general programs which can be obtained in the Earthquake Laboratory.

3. Division of Fourier Spectra

This program smoothed the numerator and the denominator of the complex Fourier spectra using Subroutine "CMOOTH", and calculates the ratio for the smoothing scheme described in Chapter 5.

4. Interpolation Program

The program perfroms the interpolation scheme described in Chapter 5.

PROGRAM #1

TEST PROGRAM FOR

SEPARATION OF BODY AND SURFACE WAVES

```
C     >>>>>TEST PROGRAM ON SURFACE & BODY WAVES SEPARATION<<<<<
C     AUG. 12, 1975  ARTIFICIAL SOURCE ANALYSIS.
      COMMON/SET1/QW1,VSW1,QD1,VSD1,R1,DS1,QW2,VSW2,QD2,VSD2,R2,DS2
      COMMON/SET2/A1(770),A2(770),A3(770),A4(770),A5(770)
     Z            ,B1(770),B2(770),B3(770),B4(770),B5(770)
      COMMON/SET3/                    CG1(770),CGE1(770),CGS1(770),
     1            CG2(770),CGB2(770),CGS2(770),OMEGA(770)
      COMMON/SET4/EG1,EG2,M,NDIM,NP2
      COMMON/SET5/XFIRST,XDELTA,ITYPE,IPLOT,HEIGHT,WIDTH,NLETRY,NLETRX
     1            ,IBUF(1024),YHEAD(6),XHEAD(6),TITLE1(20),TITLE2(20)
     2            ,TITLE3(20),TITLE4(20),TITLE5(20),NTLETR
      COMPLEX CX(770),                CNM(770),CNB(770),CMS(770)
     1        ,CMPLX,         CG1,CG2,CGB1,CGB2,CGS1,CGS2
      COMPLEX CX1(770),CX2(770),CMS$(770),CNB$(770)
C
      REAL W(770),D(770),A(770,5),B(770,5),DEMT5(6)
     1     ,$$$(770),R(770,5),C(770,5),CC(3850)
C
      REAL*8       W1(770),W2(770),D1(770),D2(770)
C
      INTEGER*4        IRENG(5),ISYMBL(5)
C
      DIMENSION TITLX1(20),TITLX2(20),TITLG1(20),TITLG2(20)
     1 ,EGB(5),EGS(5),DDS1(5),DDS2(5),DTIMEB(5),DTIMES(5)
C
      EQUIVALENCE(W1(1),CGB1(1)),(W2(1),CGB2(1)),(D1(1),CGS1(1))
     1           ,(D2(1),CGS2(1)),(W(1),CNM(1)),(D(1),CNM(132))
     2           ,(CX1(1),CG1(1)),(CX2(1),CG2(1)),(CX(1),      CMS(1))
     3                           ,(A(1),A1(1)),(B(1),B1(1))
     4           ,(C(1),CC(1))
C
C     SECTION 1 :  INITIALIZATIONS
C
      NAMELIST/INPUT/ITYPX1,ITYPX2,ITYPG1,ITYPG2,
     1               ICRDX1,ICRDX2,ICRDG1,ICRDG2
C     DEFINITION FOR "INPUT"
C          ITYP__ = DECK TYPE
C                 = 1 FOR 0.12272 RAD/SEC DECK (220 DECK)
C                 = 2 FOR 0.06136 RAD/SEC DECK (440 DECK)
C          ICRD__ = NUMBER OF CARDS TO INPUT FOR EACH DECK
      ITYPX1=1
      ITYPX2=1
      ITYPG1=1
      ITYPG2=1
```

Reproduced from best available copy.

```
      ICRDX1=220
      ICRDX2=220
      ICRDG1=220
      ICRDG2=220
      READ(5,INPUT)
C
C   CALCULATE NUMBER OF USABLE DATA POINTS FROM "INPUT"
      NPTS=MIN0(ICRDX1/ITYPX1,ICRDX2/ITYPX2,ICRDG1/ITYPG1,ICRDG2/ITYPG2)
     1  *7/2
      NP2=NPTS
      NPTS=NPTS-2
      WRITE(6,9999)NPTS
 9999 FORMAT('  NPTS =',I5)
      NDIM=NPTS
      M=5
      CALL $OMEGA(NPTS,OMEGA)
C   >>>>>CALCOMP PREPARATION<<<<<
      CALL PLOTS(IBUF,1024)
      CALL PLOT(0.0,-12.0,-3)
      CALL PLOT(0.0,+1.0,-3)
      HEIGHT=2.0
      WIDTH=5.0
      XFIRST=0.0
      XDELTA=20.0
      ITYPE=+1
      IPLOT=2
      NLETRY=7
      NLETRX=17
      NTLETR=35
C
C   SECTION 2 :  PREPARATION AND SOURCE GENERATION :
C
      READ(5,25) DIST1,X1DEEP,QW1,VSW1,QD1,VSD1
     1           ,DIST2,X2DEEP,QW2,VSW2,QD2,VSD2
   25 FORMAT(6F10.3)
      R1=SQRT((14.0-X1DEEP)**2+DIST1**2)-1.0
      R2=SQRT((14.0-X2DEEP)**2+DIST2**2)-1.0
      CALL SPREAD(NPTS,W1,R1,QW1,VSW1,1.0)
      CALL SPREAD(NPTS,W2,R2,QW2,VSW2,1.0)
      DO 201 I=1,NPTS
  201 W(I)=W1(I)/W2(I)
      DS1=DIST1-14.0
      DS2=DIST2-14.0
      CALL SPREAD(NPTS,D2,DS2,QD2,VSD2,0.5)
      CALL SPREAD(NPTS,D1,DS1,QD1,VSD1,0.5)
      DO 202 I=1,NPTS
  202 D(I)=D1(I)/D2(I)
```

```
      IDIM=1540
      IF(ITYPX1.EQ.1)CALL $FREAD(TITLX1,ICRDX1,IDIM,CX1 ,&999,&999)
      IF(ITYPX1.EQ.2)CALL $SREAD(TITLX1,ICRDX1,CX1 ,IDIM)
      IF(ITYPX2.EQ.1)CALL $FREAD(TITLX2,ICRDX2,IDIM,CX2 ,&999,&999)
      IF(ITYPX2.EQ.2)CALL $SREAD(TITLX2,ICRDX2,CX2 ,IDIM)
      DO 205 I=1,NPTS
  205 CX(I)=CX1(I)/CX2(I)
C   GENERATE G1, G2 ARTIFICIALLY
      IPLOTE=1                                                          C
C                                                                 0=ETOLPI
      IPLOTG=1                                                          C
C                                                                 0=GTOLPI
      CALL GBS(NPTS,CX1,CX2,W1,W2,D1,D2,IPLOTE,IPLOTG,A,B)
      DO 210 I=1,NPTS
  210 CNB(I)=CX(I)*W(I)
      DO 220 I=1,NPTS
  220 CMS(I)=CMPLX(D(I),0.0)
C
C   SECTION 3 :  COMPARE VARIOUS ERRORS IN SEPARATION
C
      ICNT=0
 1000 ICNT=ICNT+1
      READ(5,35,END=499)DDS1(ICNT),DDS2(ICNT),DTIMEB(ICNT),DTIMES(ICNT)
   35 FORMAT(4(10X,F10.2))
      RR1=SQRT((14.0-X1DEEP)**2+(DIST1+DDS1(ICNT))**2)-1.0
      RR2=SQRT((14.0-X2DEEP)**2+(DIST2+DDS2(ICNT))**2)-1.0
      DR1=RR1-R1
      DR2=RR2-R2
C   ADJUST FOR DISTANCE VARIATIONS ON CNB & CMS :
      IF(DDS1(ICNT).EQ.0.0 .AND. DDS2(ICNT).EQ.0.0) GO TO 305
      $1=EXP(-0.12272*((DR1/QW1/VSW1)-(DR2/QW2/VSW2))/2)
      $$$(1)=R1/R2*RR2/RR1
      DO 301 I=2,NPTS
  301 $$$(I)=$$$(I-1)*$1
      DO 302 I=1,NPTS
  302 CNB$(I)=CNB(I)*$$$(I)
      $1=EXP(-0.12272*((DDS1(ICNT)/QD1/VSD1)-(DDS2(ICNT)/QD2/VSD2))/2)
      $$$(1)=DS1/DS2*(DDS2(ICNT)+DS2)/(DDS1(ICNT)+DS1)
      DO 303 I=2,NPTS
  303 $$$(I)=$$$(I-1)*$1
      DO 304 I=1,NPTS
  304 CMS$(I)=CMS(I)*$$$(I)
      GO TO 310
  305 DO 306 I=1,NPTS
      CNB$(I)=CNB(I)
  306 CMS$(I)=CMS(I)
```

```
C   ADJUST FOR TIME VARIATION OF CNB & CMS
  310 IF(DTIMEB(ICNT).EQ.0.0) GO TO 311
      CALL TSHIFT(NPTS,CNB$,CNB$,OMEGA,DTIMEB(ICNT))
  311 IF(DTIMES(ICNT).EQ.0.0) GO TO 312
      CALL TSHIFT(NPTS,CMS$,CMS$,CMEGA,DTIMES(ICNT))
  312 CONTINUE
C
C   SECTION 4 :  RESULTS
C
      DO 405 I=1,NPTS
  405 CNM(I)=CNB$( I)-CMS$(I)
      CALL CONVR$(NDIM,M,NPTS,CNM,C,A,3,ICNT)
C   CHOOSE THE STATION TO ANALYZE, ISTN=?
      ISTN=1                                                            C
C                                                                 2=NTSI
      DO 410 I=1,NPTS
      CGB2(I)=(CG1(I)-CG2(I)*CMS$(I))/CNM(I)
  410 CGS2(I)=(CG2(I)*CNB$(I)-CG1(I))/CNM(I)
      IF(ISTN.EQ.1)GO TO 419
      CALL CONVR$(NDIM,M,NPTS,CGB2,A,B,3,ICNT)
      CALL CONVR$(NDIM,M,NPTS,CGS2,B,A,3,ICNT)
  419 IF(ISTN.EQ.2) GO TO 429
      DO 420 I=1,NPTS
      CGB1(I)=CNB$(I)*CGB2(I)
  420 CGS1(I)=CMS$(I)*CGS2(I)
      CALL CONVR$(NDIM,M,NPTS,CGB1,A,B,3,ICNT)
      CALL CONVR$(NDIM,M,NPTS,CGS1,B,A,3,ICNT)
  429 GO TO 1000
  499 ICNT=ICNT-1
C-----PLOT RESULTS :
      DATA ISYMBL/'1','2','3','4','5'/
      DATA DFMT5/'(1H ',',6F5','.1,1','01A1',')   ','    '/
      WRITE(6,40)
   40 FORMAT('-PLOT OF N - M')
      YFIRST=0.0
      YDELTA=15.0
      CALL CCPLT1(NP2 ,CC(001),OMEGA,PEAK,YDELTA,YFIRST,XDELTA,XFIRST
     1,ITYPE,IPLOT,YHEAD,NLETRY,XHEAD,NLETRX,HEIGHT,WIDTH,TITLE1,NTLETR)
C        )LBMYSI,1,STPN,1,Z,1+,TNCI,STMFD,0000.0,AGEMO,C,M,MIDN(ZILAD$ LLAC
      IBS=1                                                             C
C                                                                  0=SBI
      IF(IBS.EQ.0) GO TO 489
      WRITE(6,41)ISTN
   41 FORMAT('-BODY WAVES AT STATION ',I2)
```

```
C         )LBMYSI,1,STPN,1,Z,1+,TNCI,STMFD,0000.0,AGEMO,A,M,MIDN(ZILAD$ LLAC
      YFIRST=0.0
      YDELTA=0.4
      CALL CCPLT1(NP2 ,A2       ,OMEGA,PEAK,YDELTA,YFIRST,XDELTA,XFIRST
     1,ITYPE,IPLOT,YHEAD,NLETRY,XHEAD,NLETRX,HEIGHT,WIDTH,TITLE3,NTLETR)
      CALL CCPLT1(NP2 ,A3       ,OMEGA,PEAK,YDELTA,YFIRST,XDELTA,XFIRST
     1,ITYPE,IPLOT,YHEAD,NLETRY,XHEAD,NLETRX,HEIGHT,WIDTH,TITLE3,NTLETR)
      WRITE(6,42)ISTN
   42 FORMAT('-SURFACE WAVES AT STATION ',I2)
C         )LBMYSI,1,STPN,1,Z,1+,TNCI,STMFD,0000.0,AGEMO,B,M,MIDN(ZILAD$ LLAC
      CALL CCPLT1(NP2 ,B2       ,OMEGA,PEAK,YDELTA,YFIRST,XDELTA,XFIRST
     1,ITYPE,IPLOT,YHEAD,NLETRY,XHEAD,NLETRX,HEIGHT,WIDTH,TITLE4,NTLETR)
      CALL CCPLT1(NP2 ,B3       ,OMEGA,PEAK,YDELTA,YFIRST,XDELTA,XFIRST
     1,ITYPE,IPLOT,YHEAD,NLETRY,XHEAD,NLETRX,HEIGHT,WIDTH,TITLE4,NTLETR)
      CALL PLOT(5.0,0.0,999)
C    COMPARE ENERGY UNDER MODULI
  489 CALL $ENRGY(NDIM,ICNT,NPTS,A,EGB)
      CALL $ENRGY(NDIM,ICNT,NPTS,B,EGS)
C    CALCULATE % ERRORS VS THE SET #1
      DO 450 J=1,ICNT
      DO 450 I=1,NPTS
      A(I,ICNT-J+1)=(A(I,ICNT-J+1)-A(I,1))/A(I,1)
  450 B(I,ICNT-J+1)=(B(I,ICNT-J+1)-B(I,1))/B(I,1)
      WRITE(6,45)ISTN
   45 FORMAT('-% ERRORS FOR STATION ',I1,' ARE AS FOLLOW'/'    OMEGA   ',
     1 ' <',19('-'),'BODY WAVES',19('-'),'><',17('-'),'SURFACE WAVES',
     2 18('-'),'>')
      WRITE(6,46) (OMEGA(I),(A(I,J),J=1,5),(B(I,J),J=1,5),I=1,NPTS)
   46 FORMAT(1(1H ,0PF10.4,10(2PF10.2,'%')))
C
C    SECTION 5 :  PRINTOUT INFOS
C
C   -----PRINTOUT 4-----
      WRITE(6,30) (TITLG1(I),I=1,15),(TITLG2(I),I=1,15)
   30 FORMAT('1STATION 1 :',15A4/' STATION 2 :',15A4)
      WRITE(6,51) DIST1,DIST2
   51 FORMAT('0 EPICENTRAL DISTANCE OF 1 =',F10.3/'        "',9X,'"',5X,
     1 '"  2 =',F10.3)
      WRITE(6,52)R1,QW1,VSW1,DS1        ,QD1,VSD1,
     1           R2,QW2,VSW2,DS2        ,QD2,VSD2
   52 FORMAT('-',T16,'BODY WAVE',T39,'SURFACE WAVE'/'+',T11,21('_'),
     1 T34,22('_')/'  STATION  R(KM)',T21,'Q',4X,'VS(KM/S) DIST(KM)',
     2 2X,'Q',4X,'VS(KM/S)'/
     3                        '    1',4X,F7.3,1X,F7.1,1X,F6.2,2X,F7.3,1X,
     3 F7.1,1X,F6.2/ '     2',4X,F7.3,1X,F7.1,1X,F6.2,2X,F7.3,1X,
     4    F7.1,1X,F6.2///)
```

```
      WRITE(6,54) EG1,EG2,ISTN,EGB,ISTN,EGS
   54 FORMAT('-RELATIVE ENERGY ESTIMATES ARE :'/
     1  5X,'EG1=',F15.3/5X,'EG2=',F15.3/5X,'EGB',I1,3H'S=,5F15.3/
     2  5X,'EGS',I1,3H'S=,5F15.3)
      WRITE(6,55)
   55 FORMAT('-ERROR ANALYSES ARE AS FOLLOW :'/
     1          ' DDS1',6X,'DDS2',5X,'DTIMEB',4X,'DTIMES')
      WRITE(6,56)(DDS1(I),DDS2(I),DTIMEB(I),DTIMES(I),I=1,ICNT)
   56 FORMAT(1H ,4F10.5)
  999 STOP
      END



      BLOCK DATA
      COMMON/SET2/A1(770),A2(770),A3(770),A4(770),A5(770)
     Z            ,B1(770),B2(770),B3(770),B4(770),B5(770)
      COMMON/SET5/XFIRST,XDELTA,ITYPE,IPLOT,HEIGHT,WIDTH,NLETRY,NLETRX
     1            ,IBUF(1024),YHEAD(6),XHEAD(6),TITLE1(20),TITLE2(20)
     2            ,TITLE3(20),TITLE4(20),TITLE5(20),NTLETR
      DATA A1,A2,A3,A4,A5/3850*0.0/,B1,B2,B3,B4,B5/3850*0.0/
      DATA YHEAD/'MODU','LUS ',4*'    '/
      DATA XHEAD/'FREQ','UENC','Y,RA','D/SE','C   ','    '/
      DATA TITLE1/3*'    ','DEND','MINA','TOR,','N-M ',13*'    '/
      DATA TITLE2/3*'    ','TOTA','L GR','OUND',' MOT','ION ',12*'    '/
      DATA TITLE3/3*'    ','BODY',' WAV','E CO','MPON','ENTS',12*'    '/
      DATA TITLE4/3*'    ','SURF','ACE ','WAVE',' COM','PONE','NTS ',
     1 11*'    '/
      DATA TITLE5/3*'    ','SOUR','CE F','UNCT','ION ',13*'    '/
      END
```

```
      SUBROUTINE GBS(N,CX1,CX2,W1,W2,D1,D2,IPLOTE,IPLOTG,A,B)
      COMMON/SET1/QW1,VSW1,QD1,VSD1,R1,DS1,GW2,VSW2,QD2,VSD2,R2,DS2
      COMMON/SET2/A1(770),A2(770),A3(770),A4(770),A5(770)
     1            ,B1(770),B2(770),B3(770),B4(770),B5(770)
      COMMON/SET3/                    CG1(770),CGB1(770),CGS1(770),
     1             CG2(770),CGB2(770),CGS2(770),OMEGA(770)
      COMMON/SET4/EG1,EG2,M,NDIM,NP2
      COMMON/SET5/XFIRST,XDELTA,ITYPE,IPLOT,HEIGHT,WIDTH,NLETRY,NLETRX
     1            ,IBUF(1024),YHEAD(6),XHEAD(6),TITLE1(20),TITLE2(20)
     2            ,TITLE3(20),TITLE4(20),TITLE5(20),NTLETR
      COMPLEX          CG1,CGB1,CGS1,CG2,CGB2,CGS2
      COMPLEX CX1(N),CX2(N)
      COMPLEX CE(770)
      REAL*8 W1(N),W2(N),D1(N),D2(N)
      REAL A(770,5),B(770,5)
      DIMENSION TITLE(20),IRENG(5),DFMT3(6)
      CALL SORCE1(N,CE,OMEGA,A1,IPLOTE)
      DO 110 I=1,N
      CGB1(I)=CE(I)*W1(I)*CX1(I)
      CGB2(I)=CE(I)*W2(I)*CX2(I)
      CGS1(I)=CE(I)*D1(I)
      CGS2(I)=CE(I)*D2(I)
      CG1(I)=CGB1(I)+CGS1(I)
      CG2(I)=CGB2(I)+CGS2(I)
  110 CONTINUE
      IF(IPLOTG.NE.1)RETURN
      DATA IRENG/'G','B','S','?','?'/
      DATA DFMT3/4H(1H  , 4H,4F7 , 4H,3,1 ,4H01A1 ,4H)     , 4H     /
      CALL CONVR$(NDIM,M,N,CG1 ,A,B     ,3,1)
      CALL CONVR$(NDIM,M,N,CGB1,A,B     ,3,2)
      CALL CONVR$(NDIM,M,N,CGS1,A,B     ,3,3)
      CALL $ENRGY(NDIM,1,N,A1,EG1)
      WRITE(6,1)
    1 FORMAT('-ARTIFICIAL GROUND MOTION AT STATION 1 ')
C              )GNERI,1,N,1,XAMR,1+,3,3TMFD,0.0,AGEMO,A,3,MIDN(ZILAD$ LLAC
      YFIRST=0.0
      YDELTA=0.4
      CALL CCPLT1(NP2 ,A1      ,OMEGA,PEAK,YDELTA,YFIRST,XDELTA,XFIRST
     1,ITYPE,IPLOT,YHEAD,NLETRY,XHEAD,NLETRX,HEIGHT,WIDTH,TITLE2,NTLETR)
      CALL CCPLT1(NP2 ,A2      ,OMEGA,PEAK,YDELTA,YFIRST,XDELTA,XFIRST
     1,ITYPE,IPLOT,YHEAD,NLETRY,XHEAD,NLETRX,HEIGHT,WIDTH,TITLE3,NTLETR)
      CALL CCPLT1(NP2 ,A3      ,OMEGA,PEAK,YDELTA,YFIRST,XDELTA,XFIRST
     1,ITYPE,IPLOT,YHEAD,NLETRY,XHEAD,NLETRX,HEIGHT,WIDTH,TITLE4,NTLETR)
      CALL CONVR$(NDIM,M,N,CG2 ,B,A     ,3,1)
      CALL CONVR$(NDIM,M,N,CGB2,B,A     ,3,2)
      CALL CONVR$(NDIM,M,N,CGS2,B,A     ,3,3)
      CALL $ENRGY(NDIM,1,N,B1,EG2)
```

```
      WRITE(6,2)
    2 FORMAT('-ARTIFICIAL GROUND MOTION AT STATION 2 ')
C               )GNERI,1,N,1,XAMR,1+,3,3TMFD,0.0,AGEMO,B,3,MIDN(ZILAD$ LLAC
C           TSRIFX,ATLEDX,TSRIFY,ATLEDY,KAEP,AGEMO,      1B, 2PN(1TLPCC LLAC
C         )RTELTN,2ELTIT,HTDIW,THGIEH,XRTELN,DAEHX,YRTELN,DAEHY,TOLPI,EPYTI,1
C           TSRIFX,ATLEDX,TSRIFY,ATLEDY,KAEP,AGEMO,      2B, 2PN(1TLPCC LLAC
C         )RTELTN,3ELTIT,HTDIW,THGIEH,XRTELN,DAEHX,YRTELN,DAEHY,TOLPI,EPYTI,1
C           TSRIFX,ATLEDX,TSRIFY,ATLEDY,KAEP,AGEMO,      3B, 2PN(1TLPCC LLAC
C         )RTELTN,4ELTIT,HTDIW,THGIEH,XRTELN,DAEHX,YRTELN,DAEHY,TOLPI,EPYTI,1
      RETURN
      END



      SUBROUTINE SORCE1(N,CE,OMEGA,M1,IPLOTE)
      COMMON/SET4/EG1,EG2,M,NDIM,NP2
      COMMON/SET5/XFIRST,XDELTA,ITYPE,IPLOT,HEIGHT,WIDTH,NLETRY,NLETRX
     1            ,IBUF(1024),YHEAD(6),XHEAD(6),TITLE1(20),TITLE2(20)
     2            ,TITLE3(20),TITLE4(20),TITLE5(20),NTLETR
      COMPLEX CE(N),CEXP,CMPLX
      REAL OMEGA(N),DFMT1(6),M1(N)
      INTEGER ISYMBL(5)
      DO 100 I=1,N
  100 CE(I)=CEXP(CMPLX(-OMEGA(I)**2/0880.,-OMEGA(I)*1.00))
      IF(IPLOTE.NE.1)GO TO 10
      DATA ISYMBL(1)/'E'/
      DATA DFMT1/4H(1H ,4H,F12,4H.6,G,4H17.4,4H,101,4HA1) /
      CALL CONVR$(N,1,N,CE,M1,OMEGA,3,1)
      WRITE(6,1)
    1 FORMAT('0PLOT OF SOURCE FUNCTION #3 :')
C             )LBMYSI,1,N,1,XAMR,1+,1,1TMFD,0.0,AGEMO, 1M ,1, N (ZILAD$ LLAC
      YFIRST=0.0
      YDELTA=0.5
      CALL CCPLT1(NP2 ,M1      ,OMEGA,PEAK,YDELTA,YFIRST,XDELTA,XFIRST
     1,ITYPE,IPLOT,YHEAD,NLETRY,XHEAD,NLETRX,HEIGHT,WIDTH,TITLE5,NTLETR)
      RETURN
   10 WRITE(6,2)
    2 FORMAT('-NO SOURCE FUNCTION PLOT')
      RETURN
      END
```

PROGRAM #2

MULTI-STATION BODY AND SURFACE WAVE SEPARATION PROGRAM

```
C     MULTI-STATION BODY & SURFACE WAVES SEPATATION PROGRAM : (SEPT 23,1975)
C     FOR 3 STATIONS ONLY MOTION AT FIRST STATION IS OUTPUTTED
C     FOR 2 STATIOHS, BOTH STATIONS ARE CALCULATED.
      COMMON GS(2310),GB(2310),NM(1540),TRANS(2310),DUMMY(2310)
      COMMON/XTRA/INC,NDIM,MDIM,IPERF1
      COMPLEX*8 GS,GB,NM,TRANS,G(770),N(770),M(770) ,DUMMY
      COMPLEX*8 TOPB(1540),TOPS(1540)
      REAL*4      MOD(1540),T(770),S(2310),B(2310),SYMBOL(5)
      REAL*4 BLANKS(20)
      EQUIVALENCE (NM(1),MOD(1)),(TRANS(1),N(1)),(TRANS(771),M(1))
     1            ,(DUMMY(1),S(1)),(DUMMY(1156),B(1))
     1            ,(DUMMY(1541),G(1))
      EQUIVALENCE (GS(1),TOPS(1)),(GB(1),TOPB(1))
C     >>>>>INITIALIZATION<<<<<
      DATA BLANK/'     '/,BLANKS/20*'     '/
      NDIM=770
C     +++MDIM=NUMBER OF STATIONS - 1
      MDIM=2
      MDIM=1
      MDIM1=MDIM+1
      NDIM$=2048
      NPTS=770
      NDIMM2=NDIM*2
      NCD=NDIMM2/7
      NPTS2=NPTS*2
      PEAKB=200.
      PEAKS=200.
      INC=5
      INC=1
      INC=2
C     IPERF1 PUNCHES OUT NUMERATORS AND DENOMINATORS
C     IPERF2 PUNCHES OUT RESULTS
C     IPERF3 PUNCHES OUT THE ADJUSTED RESULTS FROM 3-STATION METHOD
      IPERF1=1
      IPERF1=0
      IPERF2=1
      IPERF2=0
      IPERF3=1
      IPERF3=0
      IF(IPERF1.NE.0 .OR. IPERF2.NE.0 .OR. IPERF3.NE.0)INC=1
      CALL MNPREP(NPTS,NM)
      CALL SEPRAT(NPTS,NM,TOPS,TOPB,GS,GB)
```

```
C     >>>>>SEPARATION<<<<<
      DO 100 ICOUNT=1,MDIM
      LOC    =NDIM*(ICOUNT-1)+1
      CALL PREP1(NPTS,NM(LOC))
      CALL SEP1(NPTS,TOPS(LOC),TOPB(LOC))
      IF(IPERF1.EQ.0) GOTO101
      IF(MDIM.GT.1)GOTO102
      DATA TS1/'TS1'/,TB1/'TB1'/,TS2/'TS2'/,TB2/'TB2'/,TNM/'N-M'/
C     PUNCH OUT FOR MAJOR STATION
      BLANKS(2)=TS2
      CALL $FPERF(BLANKS,NCD,TOPS(LOC),NPTS2)
      BLANKS(2)=TB2
      CALL $FPERF(BLANKS,NCD,TOPB(LOC),NPTS2)
  102 CONTINUE
      BLANKS(2)=TNM
      CALL $FPERF(BLANKS,NCD,NM   (LOC),NPTS2)
      IF(MDIM.GT.1)GOTO101
C     PUNCH OUT FOR MINOR STATION
      BLANKS(2)=TS1
      CALL $FPERF(BLANKS,NCD,GS(NDIM+1),NPTS2)
      BLANKS(2)=TB1
      CALL $FPERF(BLANKS,NCD,GB(NDIM+1),NPTS2)
  101 CONTINUE
C     SMOOTH NM(LOC),TOPS(LOC),AND TOPB(LOC) HERE
      CALL SEP2(NPTS,NM(LOC),TOPS(LOC),TOPB(LOC),GS(LOC),GB(LOC))
  100 CONTINUE
      IF(MDIM.GT.1)CALL ADJUST(NPTS)
      DATA TGS1/'GS1'/,TGS2/'GS2'/,TGB1/'GB1'/,TGB2/'GB2'/
      IF(IPERF2.EQ.0)GOTO199
      BLANKS(2)=TGS2
      CALL $FPERF(BLANKS,NCD,GS(1),NPTS2)
      BLANKS(2)=TGS1
      CALL $FPERF(BLANKS,NCD,GS(NDIM+1),NPTS2)
      BLANKS(2)=TGB2
      CALL $FPERF(BLANKS,NCD,GB(1),NPTS2)
      BLANKS(2)=TGB1
      CALL $FPERF(BLANKS,NCD,GB(NDIM+1),NPTS2)
      BLANKS(2)=BLANK
  199 CONTINUE
      IF(IPERF3.EQ.0)GOTO198
      DATA TADJS/'ADJS'/,TADJB/'ADJB'/
      BLANKS(2)=TADJS
      CALL $FPERF(BLANKS,NCD,GS(NDIMM2+1),NPTS2)
      BLANKS(2)=TADJB
      CALL $FPERF(BLANKS,NCD,GB(NDIMM2+1),NPTS2)
  198 CONTINUE
```

```
      ASSIGN 201 TO IWHERE
      DO 200 J=1,MDIM1
      IF(J.EQ.MDIM1 .AND. J.GT.1) ASSIGN 210 TO IWHERE
      NJ=NDIM*(J-1)
      L1=NJ+1
      L2=NJ+NPTS
      DO 210 I=L1,L2,INC
      S(I)=CABS(GS(I))
      B(I)=CABS(GB(I))
      GO TO IWHERE,(210,201)
  201 MOD(I)=CABS(NM(I))
  210 CONTINUE
  200 CONTINUE
      DATA SYMBOL/'1','2','*','?','?'/
      DO 300 I=1,NPTS,INC
  300 T(I)=I
      CALL $DALI$(NDIM,MDIM,MOD,T,0.000,MDIM,+1,RMAX,1,NPTS,INC,SYMBOL)
      CALL $DALI$(NDIM,MDIM1,S,T,PEAKS,MDIM1,+1,RMAX,1,NPTS,INC,SYMBOL)
      CALL $DALI$(NDIM,MDIM1,B,T,PEAKB,MDIM1,+1,RMAX,1,NPTS,INC,SYMBOL)
C   INVERSE F. T. VIA "TRANS"
      STOP
      END
```

```
      SUBROUTINE SEPRAT(NPTS,NM,TOPS,TOPB,GS2,GB2)
      COMMON DUMMY1(6160),N(770),M(770),G1(770),DUMMY2(1540),G2(770)
      COMMON/XTRA/INC,NDIM,MDIM,IPERF1
      COMPLEX*8 N,M,NM(NPTS),GB2(NPTS),DUMMY1,DUMMY2,GS2(NPTS),G1,G2
      COMPLEX*8 ONE,TWO
      COMPLEX*8 TOPB(NPTS),TOPS(NPTS)
      COMPLEX GB1(770),GS1(770)
      REAL*4 TITLE(20)
      EQUIVALENCE(DUMMY1(771),GS1(1)),(DUMMY1(3081),GB1(1))
      CALL $FREAD(TITLE,220,1540,G2,&999,&999)
      WRITE(6,11) TITLE
   11 FORMAT(1H0,20A4)
      RETURN
      ENTRY SEP1(NPTS,TOPS,TOPB)
      CALL $FREAD(TITLE,220,1540,G1,&999,&999)
      WRITE(6,11) TITLE
      DO 110 I=1,NPTS,INC
      ONE=G1(I)
      TWO=G2(I)
      TOPB(I)=(ONE-M(I)*TWO)
      TOPS(I)=(N(I)*TWO-ONE)
  110 CONTINUE
      IF(IPERF1.EQ.0 .OR. MDIM.GT.1)RETURN
      DO120I=1,NPTS,INC
  120 DUMMY1(I+NDIM)=TOPB(I)*N(I)
      NM4=NDIM*4
      DO130I=1,NPTS,INC
  130 DUMMY1(I+NM4)=TOPS(I)*M(I)
      RETURN
      ENTRY SEP2(NPTS,NM,TOPS,TOPB,GS2,GB2)
      DO 210 I=1,NPTS,INC
      GB2(I)=TOPB(I)/NM(I)
      GS2(I)=TOPS(I)/NM(I)
  210 CONTINUE
      IF(MDIM.GT.1)RETURN
      DO 220I=1,NPTS,INC
      GB1(I)=N(I)*GB2(I)
      GS1(I)=M(I)*GS2(I)
  220 CONTINUE
      RETURN
  999 STOP
      END
```

```
      SUBROUTINE MNPREP(NPTS,NM)
      COMMON DUMMY1(770),XB2(770),XS2(770),DUMMY2(770),DUMMY3(770),
     1 DUMMY4(770),DUMMY5(1540),NS(770),MS(770),DUMMY6(770),DUMMY7(2310)
      COMMON/XTRA/INC,NDIM,MDIM,IPERF1
      COMPLEX*8 XB2,XS2,NS,MS,XB1(770),XS1(770),XB(770),XS(770),
     1 N(770),M(770),DUMMY1,DUMMY2,DUMMY3,DUMMY4,DUMMY5,DUMMY6,DUMMY7
      COMPLEX*8 NM(NPTS)
      COMPLEX CMPLX
      REAL*4 WB2(770),WS2(770),WB1(770),WS1(770),WB(770),WS(770)
      REAL*4 TITLE(20)
      EQUIVALENCE (DUMMY3(1),WB2(1)),(DUMMY4(1),WS2(1))
     1            ,(XB1(1),XB(1),N(1),NS(1)),(XS1(1),XS(1),M(1),MS(1))
     2            ,(DUMMY7(1),WB1(1),WB(1)),(DUMMY7(771),WS1(1),WS(1))
C    >>>>>SECTION 1<<<<< (PREPARE DATA FOR THE STATION OF INTEREST-STATION #2)
      READ(5,12) VB,VS
   12 FORMAT(2(10X,F10.3))
      WRITE(6,22)VB,VS
   22 FORMAT('0VB=',F10.4,' KM/SEC',5X,'VS=',F10.4,' KM/SEC')
      READ(5,11)DIST2,HLAYR2,QB2,QS2
   11 FORMAT(4F10.3)
      WRITE(6,21)DIST2,HLAYR2,QB2,QS2
   21 FORMAT('0DIST = ',F10.4,' KM, H LAYER = ',F10.4,' KM, QB = ',
     1 F10.4,', QS = ',F10.4)
      HSORCE=13.0
      CALL $FREAD(TITLE,220,1540,XB2,&999,&999)
      WRITE(6,13)TITLE
C    PREPARE XS2, WB2, WS2 HERE IF ANY
   13 FORMAT(1H0,20A4)
      R2=SQRT(DIST2**2+(HSORCE-HLAYR2)**2)
      RETURN
      ENTRY PREP1(NPTS,NM)
      READ(5,11) DIST1,HLAYR1,QB1,QS1
      WRITE(6,21)DIST1,HLAYR1,QB1,QS1
      R1=SQRT(DIST1**2+(HSORCE-HLAYR1)**2)
C    >>>>>SECTION 2<<<<< (WB) :
      CALL SRATIO(NPTS,WB,R1,QB1,VB ,R2,QB2,VB ,1.0)
C    >>>>>SECTION 3<<<<< (XB) :
      CALL $FREAD(TITLE,220,1540,XB1,&999,&999)
      WRITE(6,13) TITLE
      DO 310 J=1,NPTS,INC
  310 XB(J)=XB1(J)/XB2(J)
C    >>>>>SECTION 4<<<<< (WS) :
      CALL SRATIO(NPTS,WS,DIST1,QS1,VS ,DIST2,QS2,VS ,0.5)
C    >>>>>SECTION 5<<<<< (XS) :
      CONTINUE
```

```
C     >>>>>SECTION 6<<<<< (N,M,) :
      DO 610 I=1,NPTS,INC
  610 M(I)=CMPLX(WS(I),0,0)
      DO 620 I=1,NPTS,INC
  620 N(I)=WB(I)*XB(I)
C     >>>>>SECTION 7<<<<< (TIME SHIFT ON M & N) :
      TDLAYS=(DIST1-DIST2)/VS
      TDLAYB=(R1-R2)/VB
      CALL TSHIFT(NPTS,0,0,TDLAYS,M,MS)
      CALL TSHIFT(NPTS,0,0,TDLAYB,N,NS)
      WRITE(6,71) TDLAYS,TDLAYB
   71 FORMAT('-DELAY TIME FOR SURFACE WAVE IS ',F10.4/
     1        ' DELAY TIME FOR   BODY   WAVE IS ',F10.4)
C     >>>>>SECTION 8<<<<< (N-M) :
      DO 800 I=1,NPTS,INC
  800 NM(I)=NS(I)-MS(I)
      RETURN
  999 STOP
      END
```

```
      SUBROUTINE ADJUST(NPTS)
      COMMON GS(770,2),GS$(770),GB(770,2),GB$(770),NM(770,2),DUMMY(4620)
      COMPLEX*8 GS,GS$,GB,GB$,NM,DUMMY
      COMMON/XTRA/INC,NDIM,MDIM,IPERF1
      DO 100 I=1,NPTS,INC
      PART1=CABS(NM(I,1))
      PART2=CABS(NM(I,2))
      X=PART1+PART2
      PART1=PART1/X
      PART2=PART2/X
      GS$(I)=PART1*GS(I,1)+PART2*GS(I,2)
      GB$(I)=PART1*GB(I,1)+PART2*GB(I,2)
  100 CONTINUE
      RETURN
      END
```

PROGRAM #3

DIVISION OF FOURIER SPECTRA

```
C     +++++DIVISION OF FOURIER SPECTRA+++++
      COMPLEX*8 C1(772),C2(772),C1S(2048),C2S(772)
      REAL*4 TITLE(20),X(772),CABS,T(772),SYMBOL(5),S(1544)
      DIMENSION IBUF(1024),TITL1(20),TITL2(20),TITL3(20)
     1          ,YHEAD1(6),YHEAD2(6),XHEAD(6),ACC(2048),TIME(2002),
     2           YHEADT(6),XHEADT(6),TITLT(20)
 1000 CONTINUE
      NCT=220
      NDIM=772
      NDIM2=1544
      NPTS=770
      NSMTH=2
      IWTS=3
      ICHK=0
      ICCOMP=0
      ICCOMP=1
      IDALI=1
      IDALI=0
      IINVRS=0
      IINVRS=1
      IF(NSMTH/2*2 .NE. NSMTH) ICHK=1
      CALL $FREAD(TITLE,NCT,NDIM2,C1,&999,&990)
      WRITE(6,9)
    9 FORMAT(1H-)
      WRITE(6,1) TITLE
      CALL $FREAD(TITLE,NCT,NDIM2,C2,&999,&990)
      WRITE(6,1) TITLE
    1 FORMAT(1H ,20A4)
      DO 100 I=1,4
      C1(I)=(0.0,0.0)
  100 CONTINUE
  110 IF(NSMTH.EQ.0) GO TO 120
      CALL CMOOTH(NPTS,C1,C1S,IWTS,1,1.0)
      CALL CMOOTH(NPTS,C2,C2S,IWTS,1,1.0)
      NSMTH=NSMTH-1
      IF(NSMTH.EQ.0) GOTO120
      CALL CMOOTH(NPTS,C1S,C1,IWTS,1,1.0)
      CALL CMOOTH(NPTS,C2S,C2,IWTS,1,1.0)
      NSMTH=NSMTH-1
      GOTO110
  120 IF(ICHK.EQ.1) GOTO140
```

```
      DO130 I=1,NPTS
      C1S(I)=C1(I)
  130 C2S(I)=C2(I)
  140 DO 145 I=1,NPTS
      S(I)=CABS(C1S(I))
  145 S(I+NDIM)=CABS(C2S(I))
      DO150 I=1,NPTS
  150 C1S(I)=C1S(I)/C2S(I)
      DO160 I=1,NPTS
      X(I)=CABS(C1S(I))
  160 CONTINUE
      CALL $OMEGA(NPTS,T)
      DATA SYMBOL/'1','2','3','4','5'/
      IF(IDALI.EQ.0)GOTO200
      NP=200
      INC=1
      P1=500.0
      P2=5.0
      P3=200.0
      CALL $DALI$(NDIM,1,S(1),T, P1    ,1,+1,RMAX,1,NP,INC,SYMBOL)
      CALL $DALI$(NDIM,1,S(NDIM+1),T,P2     ,1,+1,RMAX,1,NP,INC,SYMBOL)
      CALL $DALI$(NDIM,1,X,T,P3     ,1,+1,RMAX,1,NPTS,1,SYMBOL)
  200 IF(ICCOMP.EQ.0)GO TO 800
      CALL PLOTS(IBUF,1024)
      CALL PLOT(0.0,-12.0,-3)
      CALL PLOT(0.0,1.0,-3)
      NTLETR=40
      NLTRY1=14
      NLTRY2=7
      NLTRX=17
      DATA YHEAD1/'MODU','LUS,','CM/S','EC  ',2*'    '/
      DATA YHEAD2/'MODU','LUS ',4*'    '/
      DATA XHEAD/'FREQ','UENC','Y,RA','D/SE','C   ','    '/
      DATA TITL1/2*'    ','SMOO','THED',' NUM','ERAT','OR  ',13*'    '/
      DATA TITL2/2*'    ','SMOO','THED',' DEN','OMIN','ATOR',13*'    '/
      DATA TITL3/'    ','RATI','O OF',' SMO','OTHE','D SP','ECTR',
     1           'A   ',12*'    '/
```

```
      PEAK=0.0
      HEIGHT=2.0
      WIDTH=5.0
      ITYPE=+1
      IPLOT=+2
      XFIRST=0.0
      XDELTA=20.0
      YFIRST=0.0
      YDLTA1=100.0
      YDLTA2=1.0
      YDLTA3=150.0
      CALL CCPLT1(NDIM,S(      1),T,PEAK,YDLTA1,YFIRST,XDELTA,XFIRST,
     1 ITYPE,IPLOT,YHEAD1,NLTRY1,XHEAD,NLTRX,HEIGHT,WIDTH,TITL1,NTLETR)
      CALL CCPLT1(NDIM,S(NDIM+1),T,PEAK,YDLTA2,YFIRST,XDELTA,XFIRST,
     1 ITYPE,IPLOT,YHEAD2,NLTRY2,XHEAD,NLTRX,HEIGHT,WIDTH,TITL2,NTLETR)
      CALL CCPLT1(NDIM,X         ,T,PEAK,YDLTA3,YFIRST,XDELTA,XFIRST,
     1 ITYPE,IPLOT,YHEAD1,NLTRY1,XHEAD,NLTRX,HEIGHT,WIDTH,TITL3,NTLETR)
  800 IF (IINVRS.EQ.0)  GO TO 900
      CALL $INVRS(C1S,ACC)
      TIME(1)=0.0
      DO 850 I=2,2000
  850 TIME(I)=TIME(I-1)+0.025
      PEAK=0.0
      IF (IDALI.EQ.1)  CALL $DALI$ (2000,1,ACC,TIME,PEAK,1,-1,
     1     RMAX,1,2000,INC,SYMBOL)
      ITYPE=-1
      IPLOT=-2
      YDELTA=0.0
      YFIRST=0.0
      XDELTA=10.0
      XFIRST=0.0
      NLTRYT=14
      NLTRXT=8
      IF (ICCOMP.EQ.1) CALL CCPLT1 (2002,ACC,TIME,PEAK,YDELTA,YFIRST,
     1     XDELTA,XFIRST,ITYPE,IPLOT,YHEADT,NLTRYT,XHEADT,NLTRXT,
     2     HEIGHT,WIDTH,TITLT,NTLETR)
      DATA YHEADT/'ACCE','LERA','TION',',G  ','    ','    '/
      DATA XHEADT/'TIME',',SEC',4*'    '/
      DATA TITLT/'    ','TIME',' HIS','TORY',' OF ','THE ','RATI',
     1  '0   ',12*'    '/
  900 GOTO1000
  990 IF(ICCOMP.EQ.1)CALL PLOT(5.0,0.0,999)
      WRITE(6,8)
    8 FORMAT(//' >>>>>END<<<<<')
  999 STOP
      END
```

```
      SUBROUTINE CMOOTH(N,XR,XS,I,IND,SCALE)
      COMPLEX XR(N),XS(N),S,TP(10),TC(10),XRKM,XRKP,CONJG
      REAL F(10)
  131 FORMAT(1H1,'*************HUEVADA*************          I =',I8,
     1          '          IND =',I8///////)
      IF(I.LT.1 .OR. I.GT.10) GO TO 13
      IF(IND.EQ.2) GO TO 15
      IF(IND.NE.1) GO TO 13
      K = I + 1
      A = K**2
      FP = 1./K
      DO 10 J=1,I
      K = K - 1
   10 F(J) = K/A
      GO TO 21
   15 K = I
      A = 3*2**I - 2
      FP = 2**I/A
      DO 20 J=1,I
      K = K - 1
   20 F(J) = 2**K/A
   21 N2 = 2*N
      I2 = 2*I
      JZ = N - I2
      DO 30 J=1,I
      S =(0.,0.)
      DO 40 K=1,I
      KM = J - K
      IF(KM.LE.0) XRKM = CONJG(XR(2-KM))
      IF(KM.GT.0) XRKM = XR(KM)
   40 S = S + F(K)*(XRKM + XR(J+K))
   30 TC(J) = S + FP*XR(J)
      DO 50 JJ=I,JZ,I
      JI = JJ - I
      DO 60 L=1,I
      J = JJ + L
      S =(0.,0.)
      DO 70 K=1,I
   70 S = S + F(K)*(XR(J-K) + XR(J+K))
   60 TP(L) = S + FP*XR(J)
      DO 50 K=1,I
      XS(JI+K) = TC(K)
   50 TC(K) = TP(K)
      JI = JI + I
      JJ = JI + I
      KM = I
```

```
 69 DO 75 L=1,KM                                                    AMOR 430
    J = JJ + L                                                      AMOR 440
    S =(0.,0.)
    DO 80 K=1,I                                                     AMOR 460
    KP = J + K                                                      AMOR 470
    IF(KP.GT.N) XRKP = CONJG(XR(N2-KP))
    IF(KP.LE.N) XRKP = XR(KP)
 80 S = S + F(K)*(XR(J-K) + XRKP)
 75 TP(L) = S + FP*XR(J)                                            AMOR 500
    DO 85 K=1,I                                                     AMOR 510
    XS(JI+K) = TC(K)                                                AMOR 520
 85 TC(K) = TP(K)                                                   AMOR 530
    JI = JI + I                                                     AMOR 540
    IF(J.EQ.N) GO TO 88                                             AMOR 550
    KM = N - J                                                      AMOR 560
    JJ = J                                                          AMOR 570
    GO TO 69                                                        AMOR 580
 88 DO 90 K=1,KM                                                    AMOR 590
 90 XS(JI+K) = TC(K)                                                AMOR 600
    IF(SCALE.EQ.0.) RETURN
    S1 = 0.
    S2 = 0.
    DO 91 J=1,N
    S1 = S1 + CABS(XR(J))
 91 S2 = S2 + CABS(XS(J))
    FAC = SCALE*S1/S2
    WRITE(6,101) FAC
101 FORMAT(' FAC = ',F10.4)
    DO 92 J=1,N
 92 XS(J) = FAC*XS(J)
    RETURN                                                          AMOR 610
 13 WRITE(6,131) I,IND                                              AMOR 620
    STOP                                                            AMOR 630
    END                                                             AMOR 640
```

PROGRAM #4

INTERPOLATION PROGRAM

```
C     INTERPOLATION PROGRAM FOR AVOIDING SPURIOUS PEAKS
        COMPLEX*8 CX(2048 ),CLEFT(20),CRIGHT(20),CSLOPE
      REAL*4 TITLE(20),OMBAD(20),CMGOOD(20),ID(42),XMOD(772),OMEGA(772)
     1       ,SYMBOL(5)  ,YHEADT(6),XHEADT(6)
     1,TIME(2002),ACC(2048),TITL1(20),TITL2(20),TITLT(20)
      DIMENSION IBUF(1024),YHEAD(6),XHEAD(6)
      NAMELIST/INFO/NSECTN
      DATA SYMBOL/5*'?'/,ASTR/'*'/
      NCT=220
      NPTS=770
      NDIM=NPTS*2
      NINC=1
      IDALI=1                                                           C
      IDALI=0                                                           C
      ICCOMP=0                                                          C
      ICCOMP=1                                                          C
      IINVRS=0                                                          C
      IINVRS=1                                                          C
      IF(ICCOMP.EQ.0)GOTO101
      CALL PLOTS(IBUF,1024)
      CALL PLOT(0.0,-12.0,-3)
      CALL PLOT(0.0,1.0,-3)
      WIDTH=5.0
      HEIGHT=2.0
      XFIRST=0.0
      XDELTA=20.0
      ITYPE=+1
      IPLOT=2
      NLETRY=15
      NLETRX=17
      NTLETR=40
      DATA YHEAD/'MODU','LUS,',' CM/','SEC ',2*'    '/
      DATA XHEAD/'FREQ','UENC','Y,RA','D/SE','C   ','    '/
  101 CONTINUE
      DATA TITL1/'    ','BEFO','RE I','NTER','POLA','TION',14*'    '/
      DATA TITL2/'    ',' AFT','ER I','NTER','POLA','TION',14*'    '/
      DATA TITLT/'    ','TIME',' HIS','TORY',' AFT','ER I','NTER',
     1           'POLA','TION',11*'    '/
      DATA YHEADT/'ACCE','LERA','TION',',G  ',2*'    '/
      DATA XHEADT/'TIME',',SEC',4*'    '/
      IPLOT1=1                                                          C
      IPLOT1=0                                                          C
      PEAK=200.0
      CALL $OMEGA(NPTS,OMEGA)
 1000 CALL $FREAD(TITLE,NCT,NDIM,CX,&999,&900)
      SYMBOL(1)=ASTR
```

```
      IF(IPLOT1.EQ.0)GOTO111
      DO 110 I=1,NPTS
  110 XMOD(I)=CABS(CX(I))
      WRITE(6,15)TITLE
   15 FORMAT('1UNTREATED RECORD :   ',20A4//)
      YFIRST=0.0
      YDELTA=0.0
      IF(ICCOMP.EQ.1)CALL CCPLT1(NPTS+2,XMOD,OMEGA,PEAK,YDELTA,YFIRST,
     1 XDELTA,XFIRST,ITYPE,IPLOT,YHEAD,NLETRY,XHEAD,NLETRX,
     2 HEIGHT,WIDTH,TITL1,NTLETR)
      IF(IDALI.EQ.1)CALL $DALI$(NPTS,1,XMOD,OMEGA,PEAK,1,+1,RMAX,1,NPTS,
     1                          NINC,SYMBOL)
  111 CONTINUE
    OMBAD(I)=BEGINNINGS OF BAD RECORDS  ;  OMGOOD(I)=BEGINNINGS OF GOOD RECORDS
      READ(5,INFO)
      WRITE(6,INFO)
      WRITE(6,11)TITLE
   11 FORMAT('1REGIONS TO BE ADJUSTED BY INTERPOLATION FOR '/5X,20A4/
     1          ' ARE'/6X,'FROM(RAD/SEC)',3X,'TO(RAD/SEC)'//)
      IF(NSECTN.LT.1)GOTO900
      DO 120 NSEC=1,NSECTN
      READ(5,12)          OMBAD(NSEC),OMGOOD(NSEC)
   12 FORMAT((2(10X,F10.0)))
      WRITE(6,13)OMBAD(NSEC),OMGOOD(NSEC)
   13 FORMAT(1H ,5X,F10.4,5X,F10.4)
  120 CONTINUE
      NSEC=NSEC-1
      NIDS=NSEC*2+2
      ID(1)=1
      DO 130 I=1,NSEC
      ID(I*2)=INT(OMBAD(I)/0.12272  )+1
  130 ID(I*2+1)=INT(OMGOOD(I)/0.12272  )+1+1
      ID(NIDS)=NPTS
C    NWT+1 POINTS (2.4 RAD/SEC) LEFT AND RIGHT OF THE BAD REGION ARE USED AS
C    ADJUSTMENT FACTORS :
      WRITE(6,21)
   21 FORMAT('-NUMBER OF GOOD POINTS USED AT LEFT (1) AND RIGHT (2) ENDS
     1 FOR OBTAINING AVERAGE END VALUES FOR INTERPOLATION'/
     2' AND NUMBER OF POINTS RECREATED BY INTERPOLATION (3) ARE AS FOLLO
     3WS : '/1HC,12X,'(1)',12X,'(2)',12X,'(3)')
      DATA CLEFT/20*(0.0,0.0)/,CRIGHT/20*(0.0,0.0)/
```

```
C    NWT+1 = NUMBER OF WEIGHTS USED ON EACH SIDE FOR INTERPOLATION
      NWT=0
      DO200 J=1,NSEC
      J2=J*2
      JL=ID(J2)
      JR=ID(J2+1)
      IDL=JL-NWT
      J2S1=J2-1
      IF(IDL.LT.ID(J2S1)) IDL=ID(J2S1)
      IDR=JR+NWT
      IF(IDR.GT.ID(J2+2)) IDR=ID(J2+2)
      DO 210 I=IDL,JL
  210 CLEFT(J)=CX(I)+CLEFT(J)
      NLEFT=JL-IDL+1
      CLEFT(J)=CLEFT(J)/NLEFT
      DO 220 I=JR,IDR
  220 CRIGHT(J)=CRIGHT(J)+CX(I)
      NRIGHT=IDR-JR+1
      CRIGHT(J)=CRIGHT(J)/NRIGHT
      NSPACE=JR-JL
      CSLOPE=CRIGHT(J)-CLEFT(J)
      JLP1=JL+1
      JRS1=JR-1
      DO 230 I=JLP1,JRS1
  230 CX(I)=CLEFT(J)+CSLOPE*(I-JL)/NSPACE
      WRITE(6,22) NLEFT,NRIGHT,NSPACE
   22 FORMAT(1H ,10X,I5,10X,I5,10X,I5)
  200 CONTINUE
      WRITE(6,31)TITLE
   31 FORMAT(' RECORD AFTER INTERPOLATION :   ',20A4//)
      DO 310 I=1,NPTS
  310 XMOD(I)=CABS(CX(I))
      YFIRST=0.0
      YDELTA=100.0
      IF(IDALI.EQ.1)CALL $DALI$(NPTS,1,XMOD,OMEGA,PEAK,1,+1,RMAX,1,NPTS,
     1                          NINC,SYMBOL)
      XDELTA=20.0
      ITYPE=+1
      IPLOT=+2
      IF(ICCOMP.EQ.1)CALL CCPLT1(NPTS+2,XMOD,OMEGA,PEAK,YDELTA,YFIRST,
     1 XDELTA,XFIRST,ITYPE,IPLOT,YHEAD,NLETRY,XHEAD,NLETRX,
     2 HEIGHT,WIDTH,TITL2,NTLETR)
```

```
      IF(IINVRS.EQ.0)GOTO800
      CALL $INVRS(CX,ACC)
      TIME(1)=0.0
      DO750I=2,2000
  750 TIME(I)=TIME(I-1)+0.025
      PEAK=0.0
      IF(IDALI.EQ.1)CALL $DALI$(2000,1,ACC,TIME,PEAK,1,-1,RMAX,1,2000,
     1 NINC,SYMBOL)
      ITYPE=-1
      IPLOT=-2
      YDELTA=0.0
      YFIRST=0.0
      XDELTA=10.0
      XFIRST=0.0
      NLTRYT=14
      NLTRXT=8
      IF(ICCOM P.EQ.1)CALL CCPLT1(2002,ACC,TIME,PEAK,YDELTA,YFIRST,
     1 XDELTA,XFIRST,ITYPE,IPLOT,YHEADT,NLTRYT,XHEADT,NLTRXT,HEIGHT,
     2 WIDTH,TITLT,NTLETR)
  800 CONTINUE
      GOTO1000
  900 IF(ICCOMP.EQ.1)CALL PLOT(10.0,0.0,999)
  999 STOP
      END
```